Dynamic Analysis of Upper Limbs Movement of Breast Cancer Patients

António José Pereira Guerra

MASTER THESIS

Supervisor UP: Hélder P. Oliveira: PhD, FEUP / DEI

Supervisor INESC TEC: João P. Monteiro: INESC TEC

Mestrado Integrado em Bioengenharia

September, 2015

Aos meus avôs, António, António, Ana e Maria do Carmo

Resumo

O cancro da mama é o principal tipo de cancro em mulheres, possuindo uma elevada taxa de sobrevivência. No entanto, os tratamentos habituais (radioterapia ou remoção cirúrgica dos nódulos linfáticos da axila, por exemplo) tendem a levar a uma diminuição da qualidade de vida da paciente, já que pode conduzir à diminuição da funcionalidade dos membros superiores.

Para diminuir o impacto destes problemas na qualidade de vida da paciente, tal como para prevenir futuras complicações, é importante uma detecção prematura de lesões. Esta detecção é tradicionalmente realizada por métodos subjectivos, desde a medição de volume, medição de ângulos ou inquéritos. Com este trabalho pretende-se a criação de um método objectivo - contrariando a prática habitual - que permita realizar uma análise mais correcta da condição física da paciente e os problemas associados ao membro superior. Para tal, procedeu-se à selecção de um conjunto de exercícios a realizar pela paciente, tendo-se adquirido dados RGB-D e *Skeleton Tracking* durante os mesmos.

Os dados adquiridos foram processados de forma a obter-se melhores características dos mesmos. Assim, para os dados provenientes do *Skeleton*, foram avaliados os impactos de cinco diferentes filtros e comparados com um *ground truth* marcado manualmente. Após esta avaliação, o melhor filtro foi aplicado a todos os dados adquiridos. Já no que respeita aos dados RGB-D, estes permitem estimar o volume do braço da paciente, sendo feita uma segmentação desta zona. Para esta segmentação foram testadas três metodologias que foram comparadas com um *ground truth* marcado manualmente. O método de segmentação com melhores resultados foi o usado para a segmentação do braço para o cálculo do volume. Em seguida, e usando dados RGB-D segmentados para a zona pretendida, é construída uma nuvem de pontos onde, aplicando-se um algoritmo de *convex hull*, é possível estimar o volume.

Por último, foram usados algoritmos de classificação supervisionados com vista a construir um modelo de classificação. Os paciente adquiridos foram divididos em classes consoante a sua condição. Foi avaliado a presença de dor, rigidez, força, linfedema e a funcionalidade. Devido ao número elevado de características extraídas, foi necessário proceder à selecção das mesmas, tendo-se usado três métodos para minimizar o conjunto de características testadas. Os resultados obtidos foram bastante promissores para a classificação de pacientes após cancro da mama, sendo melhores do que os presentes na literatura.

Abstract

Breast cancer is the leading cause of cancer in women, with a high rate of survival. However, common treatment procedures, such as radiation therapy or surgical removal of the axillary lymphatic nodes, lead to a decrease in patients' quality of life due to impairments in upper limb function.

Premature detection of these types of problems is vital to decrease the impact in UBF and further complications. Nevertheless, detection is currently performed using subjective methods, either using volume and angle measurements or inquiries. The present work aims to create an objective method to perform this evaluation and provide a more accurate analysis of upper limb impairments. For that, a number of exercises were selected and, using Microsoft Kinect, RGB-D and skeleton tracking data was acquired.

Data acquired was then processed to ensure better feature extraction. To accomplish it, a filter selection was performed by comparing the results of five different filters with a marked ground truth, being the selected filter applied in skeleton tracking data. RGB-D data allows the computation of volume measurements. However, this requires that the arm is segmented, therefore, three methods of segmentation were compared with a marked ground truth, and the method with the best results was used for arm segmentation. Volume calculation was then performed, using point cloud information created by the segmented RGB-D data and convex hull algorithm.

Lastly, supervised classification algorithms were used to construct a prediction model for characterized patient condition. Acquired patients were divided in classes according to her condition. Were evaluated the presence of pain, stiffness, weakness, lymphedema and functionality. Due to the high number of extracted features, three methods of feature selection were used to minify the set of features tested. Results obtained in this work were very promising for breast cancer patients' classification, and are better than those presented in the literature.

Agradecimentos

Tal como a palavra "amor", a palavra "obrigado" é muitas vezes usada em vão e sem significado. É casual, cada vez mais normal. Agradece-se à pessoa que nos segura a porta. Agradece-se a um elogio à roupa. Não que a palavra não se adeque, mas sim depois é complicado (ia escrever lixado, mas acho que tal não deve entrar numa tese... no mínimo escreveria f*****, à moda do Porto, que é o que agora sinto. Foi o LaTeXque pôs os *, não eu) escrever coisas como estas. Porque não é o "obrigado" habitual. É um agradecimento muito mais sentido que apenas um agradecimento à pessoa que disse "santinho" depois de espirrarmos. Por isso, na falta de melhor palavra, este obrigado, o que agora sinto, será, durante este texto, representado por *alpercata*.

Começo por *alpercatar* ao professor Hélder, sempre incansável mesmo quando cansado e farto, com o qual aprendi qual o país com maior percentagem de mulheres professoras do 1º ciclo. Entre outras coisas, menos importantes mas que até acabaram por dar jeito. *Alpercata* também ao João, que muita paciência teve para me aturar, ao Dr. André e ao Enf. Sérgio que sempre se mostraram disponíveis para ajudar no que fosse preciso.

Alpercatar a uma lista findável de pessoas, que tentarei recordar de memória (segue-se uma longa enumeração... se achas que estás nesta lista, procura o teu nome. Se não, passa à frente): à Ana (e a toda a "sua" música, que me "emprestou" para ouvir sem nunca pedir de volta), à catarina, à Maria, à Liliana, ao Miguel, ao João Costa, ao Rui, ao Dinis, ao Ricardo e ao Yvan (que já não vejo há muito tempo, mas que sem eles não chegaria aqui), ao João Andrade, à Cláudia, à Sara, à Bárbara, ao Pedro, à Bruna, ao Frederico, à Jessica D., ao Marco, à Sílvia, sem nenhuma ordem especial sem ser aquela que a memória me permitiu.

Uns quantos *alpercatamentos* mais particulares: ao Duarte, companheiro de batalha e de noitadas nestes últimos tempos, que tanto aturou e sempre se mostrou disponível para aturar mais. Se há pessoas que têm bom coração és tu e a...

Inês, a quem muito *alpercato*. Por me teres aturado quase noite sim, noite sim. Por fazeres um trabalho que talvez nem eu faria. E por muito mais que te terei a *alpercatar* e que tu o sabes.

À Ana, que gosta de ser tratada por Helena, por me ter feito companhia, mesmo com um interregno, nos últimos 17 anos e pouco. Mesmo distante, não esquecida.

Um *alpercatamento* muito grande à minha *piquena* Jessica, com a qual troquei de lugar: ela foi para a serra, eu fui para o mar (rimou porque quis, não foi ao calhas...). *Alpercato* por tudo o que fizeste (mesmo quando tinhas problemas no telemóvel), por me perceberes e por me apoiares. Sabes o quanto gosto de ti, e se não o sabes é porque és cega e surda, visto que já o escrevi e disse imensas vezes. E muitas vezes o continuarei a dizer e a escrever, se assim o deixares.

Chegam agora os *alpercatamentos* mais sentidos e que não serão esquecidos. Porque é de (quase) engenheiro para engenheiros (excepto dois, que até esta altura ainda não acabaram... fraquitos, mas que lá chegarão), segue-se em tópicos:

- Ao Hugo, pela tua piada sem a ter. Por te demonstrares sempre presente, e por te lembrares quando necessário de mim.

- Ao Jorge, por deixares-me ser teu irmão mais velho e tu meu. Aprendi muito contigo, talvez mais do que possas pensar. Aprendi que os homens não são feitos de células, mas de raça. Aprendi o que é a amizade.

- Ao João, que me fez companhia durante os cinco anos mais importantes da minha vida. O Nuno disse para escrever no meio disto "pelas boémias". As boémias que mais recordo contigo foram noitadas a fazer trabalhos, e no meio tu a veres vídeos enquanto eu desesperava. Podia ser mau sinal, pois não são as verdadeiras boémias que me recordo primeiramente e te *alpercato*. Não o é. Pois, mesmo tendo imensas recordações de boémias que se dizem a sério, recordo-me primeiro dos trabalhos que contigo fiz e o quão me diverti, mesmo quando a diversão parecia a última coisa possível. Poderia *alpercatar-te* muito mais, mas sei que te cansarias a ler e corrigir o texto.

- Ao Daniel. Aos telefonemas quase extasiantes. Às conversas infindáveis. A ti, principalmente. À pessoa que és e sempre demonstraste ser. Por seres a pessoa que me ouvia quando precisava. Por seres verdadeiramente um amigo. Por me aturares quando te peço mil e uma coisas. Por seres o tipo que nunca disse que não ou, quando o disse, sempre tentou de uma forma subtil (alguém vai levar esta frase para outros sentidos... vai pô ******* João. Criança, pá). Por seres um tipo fixe, o mais fixe que há, mesmo que o encubras com uma armadura rígida.

A vocês os 4, há algo que vos quero dizer mais que a todos os outros: costuma-se dizer que na universidade é que se fazem os verdadeiros amigos, aqueles para a vida. Se há pessoas com quem quero e acho que comprovarei isso, é com vocês. Um *alpercato* não chegará, nem dois, por tudo o que me deram e fizeram. Espero que tenha feito 1/100 do que fizeram por mim. Já seria muito (e esta porcaria de fazer coisas cansa também... não vamos exagerar).

Vamos agora aos suspeitos do costume. À minha irmã, que fez de irmão e irmã em casa quando não estava. Se não souberes o quanto gosto de ti, não perguntes que eu não te consigo dizer.

Ao meu pai, por tudo o que me ensinaste, por toda a paciência que tiveste, por nunca duvidares de mim. Por me deixares sonhar e ser convencido, por me agarrares quando precisava, por me dares a mão quando ela era preciso.

À minha mãe, a quem não sei como *alpercatar*. Nunca saberei, nem nunca saberei o que fizeste por mim, de tão grande que foi. Por queres sempre que te telefone, por me receberes sempre. Por vezes não era o filho pródigo, mas quase. Não há muito mais que eu possa escrever... *alpercato* por tudo.

Por último, a quatro pessoas que me marcaram, marcam e marcarão todos os dias e para o resto da minha vida, mesmo quando não cá estiverem. Ao meu avô António, por me ter dado uma boina em pequeno, por me ter ensinado a cavar a terra, pelas histórias que contas, por me teres segurado quando ia a entrar na lareira. Por me teres dado a honra de ser nomeado como tu. Por, ainda agora, seres a pessoa que mais admiro. Ao meu avô António, também por me teres permitido levar o teu nome comigo, pelo Guerra, por me trazeres o jornal todos os dias, por seres um exemplo de vida, por me teres dado as cores azuis e brancas. Foi por ti que tanto sofri no início, mas também foi assim que aprendi mais sobre quem sou. À minha avó Ana, por te preocupares, por quereres sempre ensinar e por eu nunca te dar razão. Pelas tuas lágrimas. Por ainda hoje me chamares António José. À minha avó Maria do Carmo, por me teres dado de comer dia sim dia sim, por te preocupares comigo, por me educares.

A estes últimos *alpercato* as coisas pequenas, estas e outras que não citei, essa sim uma lista infindável. As grandes acho que não precisam de tal, porque se precisassem nunca as fariam. Por serem ensinamentos de vida diários, por me fazerem um homem melhor todos os dias. Por me fazerem homem, ou o mais perto disso que algum dia chegarei.

A todos estes que citei, um muito *alpercato*. Nunca os conseguirei retribuir. Ficam as palavras e os gestos...

António Guerra

"There's a science to walking through windows."

Matt Berninger

Contents

List of Figures

List of Tables

List of Abbreviations

2D	Two-dimensional
3D	Three-dimensional
CAD	Computer Aided Design
CAML	Computer Aided Measurement Laser
CGI	Computer-generated imagery
cm	Centimetres
CT	Computed Tomography
DASH	Disability of Arm, Shoulder and Hand
DEXA	Dual-energy X-ray absorptiometry
DNA	Deoxyribonucleic acid
EIS	Electrical Impedance Spectrograph
EORTC QLQ BR23	European Organization for Research and Treatment of Cancer Quality of Life Questionnaire - Breast Cancer Module
FACT-B	Functional Assessment of Cancer Therapy-Breast
g	grams
Hz	Hertz
ICG	Indocyanine green
IR	Infrared
KAPS	Kwan's Arm Problem Scale
m	meters
MRI	Magnetic resonance imaging
NIRF	Near-Infrared Fluorescence
PMVS	Patch-based Multi-view Stereo
PSFS	Patient-Specific Functional Scale
QOL	Quality of Life
ROM	Range of Motion
SPECT	Single-Photon Emission Computed Tomography
TOF	Time-of-Flight
UEFI	Upper Extremity Functional Index
ULDQ	Upper Limb Disability Questionnaires
ULM	Upper Limb Movement
UBF	Upper Body Function

WHO	World Health Organization

Chapter 1

Introduction

1.1 Context

Breast cancer is the leading cause of cancer in women, with an estimated 1.383.500 new cases in 2010 [1], and an estimated 60.290 new cases in 2015 only in the USA [2]. Nevertheless, mortality rate is equal to 27% or less in developed regions [3], due to effective therapies and medical procedures, as well as prompt diagnosis. Since survival rates are so high, it is important to understand the Quality of Life (QOL) of women after breast cancer surgery, and the impacts of the treatment in these parameters.

Problems related to Breast Cancer are often associated with surgical procedures and post-surgical treatment, some of which can lead to several Upper Body Function (UBF) problems. However, these do not have a defined healing process, leading to lower QOL and difficulty in accomplishing daily activities. Concerns with the QOL of breast cancer patients have been growing, with several studies trying to address this problem and showing that it can be affected by several clinical problems related to breast cancer surgery, and also by psychological problems such as depression, anxiety and problems with body image [4].

On the other hand, UBF assessment is usually performed by subjective self-reports. Even though self-reports have shown good results, these are limited and can present deceiving results. Also, the commonly used self-reports only assess UBF or QOL. This leads to a limited understanding of patients' condition.

An important factor that causes impairments in UBF and lower QOL is the presence of lymphedema. This is common in women after breast cancer surgery where the removal of the axillary lymph node system is needed. Lymphedema can be related with pain and restricted shoulder mobility. These problems have high correlation with decreased QOL in breast cancer patients, impacting their daily activities [5]. Still, a more premature diagnostic of such conditions allows a better management of the problems, leading to improvements in upper limb functionality and, thence, patients' QOL.

1.2 Motivation

Breast cancer has a high survival rate, nonetheless, survivors from the disease can experience long-term sequelae from treatment, including possible presence of lymphedema or lower range of motion (ROM). Assessment of UBF and QOL of these patients are usually performed separately by subjective methods, which can be inaccurate and very time consuming. Although objective methods have been proposed, their use is reduced, mainly due to the associated costs.

Also, an early diagnosis can be difficult to perform by traditional methods. Studies showed that subjective self-reports are more sensitive and can lead to a more premature detection of reduced UBF [6]. Nevertheless, these can be inaccurate. Therefore, there is currently a demand for an objective method that can assess UBF and QOL. This method needs to be accurate, low-cost, able to produce results in quickly, reproducible and capable of performing early diagnosis of upper-limb impairments.

Furthermore, an early diagnosis of low UBF allows a better managing of patients' condition, as well as an improvement in QOL for breast cancer patients, enabling the creation of a more accurate physiotherapy plan and enhancing success in the rehabilitation process.

1.3 Objectives

The main purpose of this study is to improve existing methodology, initially developed by Moreira [7], to assess breast cancer patients' UBF using Microsoft Kinect, an equipment capable of producing 3D images of its surroundings, and, using a more diverse and complete set of exercises, understand which are best for UBF evaluation. For that purpose, several methodologies of signal and image processing were tested to understand which are the most robust for the problem in question.

Microsoft Kinect provided RGB and depth data as well as a skeleton tracking algorithm and, with this, patients' movements will be extracted and several features will be computed to assess UBF, presence of lymphedema, pain, weakness or stiffness and functionality level.

Collected data will be processed to allow its use in the development of a serious game to help improving the rehabilitation mechanism and reduce the risk of lymphedema. This work was performed with the support of medical staff, more specifically Dr. André Magalhães and nurse Sérgio Magalhães from Hospital S. João.

1.4 Contributions

This work had the following main contributions:

- Improvement of the application proposed by Moreira [7] to collect medical data from post-surgery breast cancer patients. This data was collected using Microsoft Kinect and consists of RGB images, depth frames and skeleton's joints positions over time.

- Creation of a database with collected data, composed by diverse exercises and movements, which can be further used in other works in the area.
- Improvement of the methodology proposed by Moreira [7] for arm segmentation and volume calculation using the data from Kinect.
- Creation of a new methodology for feature extraction using Skeleton Tracking data, involving the selection of filters and features, with the latter being dependent on the exercises performed.
- Select exercises that allows patient condition's characterization.
- Extract features that can characterize patient movement during the exercise.
- Associate all gathered measurements to assess, for instance, pain, morbid stiffness or weakness in post-surgery breast cancer patients.
- Creation of a classified models to patient condition from select features.

Publications Related to the thesis

The work related with this thesis resulted in the following publication:

- António Guerra, Hélder P. Oliveira, João P. Monteiro. Evaluation of upper limbs movements after surgery in breast cancer patients. In Proceedings of the 1^{st} Doctoral Congress in Enginnering, Porto, Portugal, 11^{th}-12^{th} June, 2015.
- André T. Magalhães, Sérgio Magalhães, António Guerra, Edgar Costa, Hélder P. Oliveira, José Luís Fougo. An objective tool to detect lack of mobility of the arm and shoulder and the presence of lymphedema after breast cancer treatment. In Proceedings of the 6^{th} International Meeting of Oncoplastic and Reconstructive Breast Surgery, Nottingham, United Kingdom, 21^{st} – 23^{rd} September, 2015

1.5 Document Structure

Following this section, this document is composed by seven more chapters. Chapter 2 presents an introduction to the breast and breast cancer problem. In chapter 3, the literature review of subjective methods for volume and UBF assessment and also human tracking systems are analysed. Also, some insights of RGB-D cameras are provided. Chapter 4 describes the creation of the application; with the characterization of the acquired database being done in Chapter 5. All tested methods for feature extraction are explained in Chapter 6, as well as the obtained results. Classification models and results of these are expounded in Chapter 7. Lastly, Chapter 8 is composed by a conclusion to the presented research.

Chapter 2

Breast Cancer

2.1 Cancer

Cancer is characterized by an abnormal and unregulated cell growth, due to an unregulated cell cycle [8]. Normally, cell cycle is regulated by Deoxyribonucleic acid (DNA) and consists mainly in three phases: growth, division and death. The regulation of those phases is mainly performed by two gene categories: oncogenes, which promote cell growth and reproduction, and tumour suppressor genes, which inhibits cell division and survival. If an over-expression of an oncogene or an under-expression of tumour suppressor genes occur, and the regulatory mechanisms do not prevent the perpetuation of this error, the cell starts to replicate without control [9]. This replication can lead to two different types of tumour: benign, which is not cancer and is not dangerous to health; and malignant (considered cancer) [10].

Cancers can be classified by the origin of the tumour. This can be inferred by cell resemblance and the classification varies between carcinoma (from epithelial cells, present in breast, prostate or lungs), sarcoma (from connective tissue, as bones, cartilage or fat), lymphoma and leukaemia (hematopoietic cells, this is, blood cells), germ cell tumour (from pluripotent cells present in testicle or ovary) and blastoma (from embryonic tissue or immature cells) [8].

The majority of cancer cases (90-95%) are related with environmental factors, as tobacco, obesity, infections or radiation. Of these, tobacco is the leading cause of death, with 22% [11] of cancer deaths. In addition to environmental factors, 5-10% result of inherited genetics. BRCA1 and BRAC2 are two of the known genes that can lead to cancer, in this case breast, ovarian or pancreatic cancer [12].

The treatment for cancer differs according to different factors, as type, location and grade of cancer. The treatment includes surgery, chemotherapy, radiation, hormonal, target therapy and palliative care and can be composed by one or more treatment options. In some cases, due to the condition of the cancer or the person's health and wishes, the treatment can be not curative, but only expand lifespan to the person with cancer.

2.2 Breast Anatomy and Physiology

The breast is an organ that exists in women and its located in the upper region of the torso. This organ is responsible for producing milk, having 15-20 glandular lobes which are composed of about 40 terminal duct lobular units to that purpose [13]. The breast usually has the shape of a cone, but it can have variations in both shape, volume, size or location. Those variations occur among women but also in the same woman, since the size and shape of the breast are influenced by hormonal changes [13]. Breast anatomy is present in Figure 2.1.

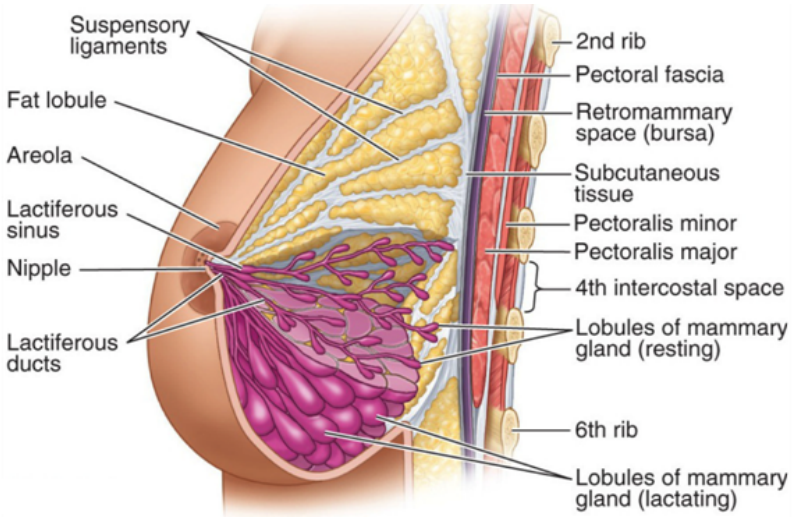

Figure 2.1: Breast Anatomy from Medial View (From [14])

Furthermore, the breast is linked to the lymphatic system, with 75% of lymph from the organ going to axillary lymph nodes and 25% to parasternal lymph nodes (Figure 2.2) [15]. These are important to oncology, since breast cancer can suffer metasteses and these are dispersed by the lymphatic system that works through a complex network which connects several organs and tissues that can be implicated in the process [13].

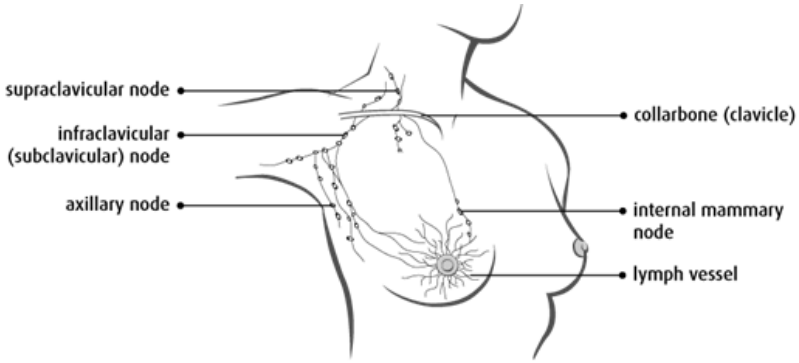

Figure 2.2: Breast Lymphatic System (From [16])

The lymphatic system can be divided in two main structures: lymph vessels and lymph nodes. The lymph vessels are responsible for carrying the lymph towards the heart, with waste products

and immune system cells. Lymph nodes are a major site for immune cells, acting as a filter for foreign particles and cancer cells [13].

2.3 Breast Cancer and Treatments

Breast cancer is the leading cause of cancer in women, with anan estimated number of 1.383.500 new cases and 458.400 estimated deaths worldwide in 2010 [1]. This type of cancer commonly develops in cells from the lining of milk ducts, known as ductal carcinomas, or in lobules that supply the ducts with milk, known as lobular carcinomas. However, the number of sub-types of cancers currently known is 18, like inflammatory or angiosarcoma [1]. Breast cancer can also be divided in non-invasive or invasive. Non-invasive (also known as carcinoma *in situ*), is when the cancer remains in the region of origin. Contrariwise, the cancer is categorized as invasive when the cells invade the surrounding tissue.

The symptoms of breast cancer are numerous, however the first symptom is usually a lump in the breast. This can be found by palpation, a method responsible for the detection of more than 80% of breast cancer cases [17]. Other symptoms are alteration in skin colour or texture, or changes in the nipple. Despite being an important method for the detection of breast cancer, the lump method is not very effective, since only 20% of the lumps are really cancerous [18].

Breast cancer is classified according to several factors, influencing the prognosis and treatment. As explained above, it can be classified by its histological appearance and *in situ* or invasive. Grading is another factor and consists in comparing cancer cells and normal breast cells by differentiation and organization in the milk ducts. Cancer cells, unlike normal cells, become disorganized due to uncontrolled division. Another factor is stage, which is based in the TNM[1] [19] system, a measure dependent of tumour's size, if the cancer has spread to lymph nodes and whether the tumour has metastasized.

In addition to these factors, the treatment depends on the location of the tumour and the woman's health and age. Furthermore, the treatment tries to be as uninvasive as possible, attempting to get an aesthetic solution, allowing the patient to have the best QOL possible. Treatment usually consists in surgery, followed by possible chemotherapy or radiotherapy.

Surgical removal can be total or partial. The removal of the entire or part of the breast is known as mastectomy and can be of five types [20]:

- Simple mastectomy: The entire breast tissue is removed as well as the nipple, areola and, in certain cases, the sentinel lymph node (first node of axillary lymph node), performed usually to women with large areas of carcinoma *in situ* (Figure 2.3a).

- Radical mastectomy: This procedure involves removing the entire breast, the axillary lymph nodes and pectoralis muscles. This surgery is performed only in severe cases as metastases in to the pectoralis muscles, since can be disfiguring.

[1] **T** describes the size of the original (primary) tumor and whether it has invaded nearby tissue; **N** describes nearby (regional) lymph nodes that are involved; **M** describes distant metastasis (spread of cancer from one part of the body to another).

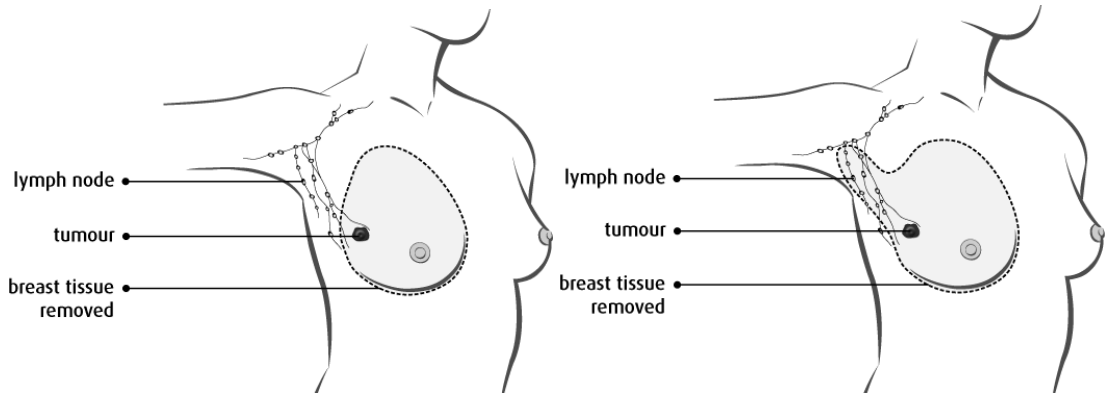

(a) Simple Mastectomy Procedure (b) Modified Radical Mastectomy Procedure

Figure 2.3: Common Mastectomies Procedures in Breast Cancer Patients (From [21])

- Modified radical mastectomy: The entire breast tissue is removed along with all the axillary content. In this type of mastectomy, the pectoral muscles are spared (Figure 2.3b).

- Skin-sparing mastectomy: This type of surgery consists in removing breast tissue through an incision made around the areola. This type of procedure allows the reconstruction of the breast.

- Nipple-sparing/subcutaneous mastectomy: Breast tissue is removed but the nipple-areola complex is preserved. This procedure is recently used for tumours outside the subareolar position.

In recent times the use of lumpectomy is growing. This technique consists in the removal of only the lump affected with cancer, and is used in patients with a single tumour, smaller than 4 centimetres (cm) [22] (Figure 2.4). This technique allows the preservation of the essential breast, which can be a positive factor, since patients who experienced a mastectomy fell less attractive, less sexually desirable and ashamed of their body with impacts in the rehabilitation process [23, 24].

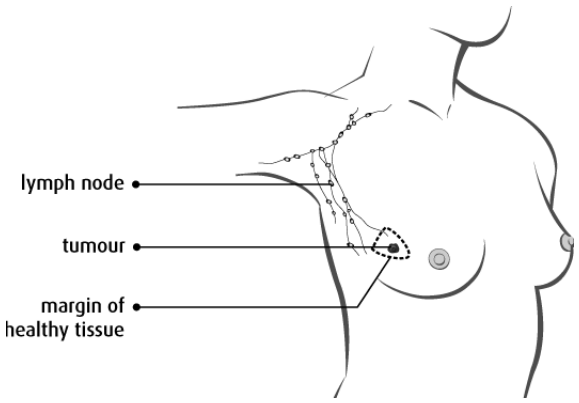

Figure 2.4: Breast-conserving Surgery Procedure (From [21])

The removal of the axillary lymph nodes is common in some methods of mastectomy, in order to allow understanding whether the cancer has spread. This can lead to lymphedema (Chapter 2.4). Although new techniques as sentinel lymph node dissection have been used to test the spread, between 20-40% of women have axillary metastasis, which leads to the removal of this complex [25]. With that said, the appearance of lymphedema in women with breast cancer is common.

2.3.1 Survival Rate

Survival rate of breast cancer patients is related with the stage of cancer. The percentage of women survived breast cancer for respective stage in England is in Table 2.1.

Table 2.1: Survival Rate from Breast Cancer in England (From [26])

Stage	**> 5 Years**	**> 10 Years**
1	90%	85%
2	70%	60%
3	50%	40%
4	13%	10%

These numbers resemble the data from developed countries. However, as explained above, the survival from this type of cancer has problems to the patients, since there are physical and physiological damages to the survivals. So, recovery and improvement of QOL are an important factor in survivals of breast cancer and to assess their rehabilitation.

2.4 Lymphedema

Lymphedema is a medical condition that results from disequilibrium between the microvascular filtration rate of the capillaries and venules and that of the lymphatic drainage system [27]. These results in fluid retention which usually leads to localized tissue swelling.

So, lymphedema is the result of *low output failure* (a reduction of lymphatic transport). This phenomenon can be divided in two generic types: primary lymphedema, caused by a congenital lymphatic dysplasia (intrinsic fault of lymphatic vessels [27]), or secondary lymphedema, usually due to operative procedures such as dissection or irradiation [28]. This can be also triggered by obesity, this being the most prevalent form of lymphedema [29]. There are four types of lymphedema, as can be seen in Table 2.2.

Lymphedema in upper limbs usually manifests as swelling, although patients with this alteration can also suffer from numbness, tightness and tenderness. This commonly leads to pain or reduced mobility in the shoulder and is customarily detected by the patients [30]. Also, recent studies show that some self-reported symptoms can indicate the presence of lymphedema more prematurely than traditional methods [31]. Lymphedema is usually considered as an incurable, progressive, disfiguring, and disabling disorder that is difficult to treat [32].

Table 2.2: Lymphedema stages according Flodi Staging System (adapted from [27])

Clinical Stage	Pathology	Symptoms
0	Focal fibrosclerotic tissue alteration	Latency: no symptons
1	High protein edema; Focal fibrosclerotic; Tissue alterations	Reversible: pitting edema; Elevation reduces swelling; Possibly "congestion pain
2	Extensive fibrosclerosis; Proliferation of adipose tissue	Spontaneously irreversible: hard swelling that does not respond to elevation
3	Extensive fibrosclerosis; proliferation of adipose tissue	Elephantiasis: similar to stage II with a degree of severity involving invalidism

Approaches to treatment can be divided in two: conservative (non-operative) or operative methods, depending on the stage and other factors. Non-operative methods can be combined with physical therapy, that can consist in a skin care with light manual massage, followed by exercises as basic range of motion of the extremities. It can also be made as intermittent pneumatic compression, drug therapy (as diuretics, benzopyrones or antoimicrobials) or massage alone. Operative treatment can consist in microsurgical procedures, like reconstructive methods and derivative methods, liposuction or lymph node transplantation. These methods can be used in parallel to get a better rehabilitation. However, as explained, these approaches do not lead to a full recovery.

2.4.1 Lymphedema Incidence in Breast Cancer Patients

As previous mentioned, the removal of the axillary lymph node is a common method in breast cancer, since allows infer if the cancer has spread. These patients have an increased risk of developing secondary lymphedema, which is even higher when radiation therapy is performed. Studies showed that between 25% and 28% of women treated for breast cancer develop secondary lymphedema. However, this number can range from 6.7% to 62.5% [33], depending on the study in question. The reasons that lead to lymphedema are unknown, but recent studies found a possible link between breast cancer-related lymphedema and certain genes [34]. It was also found that patients with primary lymphedema have higher risks to develop secondary lymphedema [35].

This can conduct to physical problems as well as psychological problems, since women with lymphedema have higher risks of depression and anxiety, with a poorer adjustment to their illness, having problems in domestic and relationship environments [36] as an unsatisfactory appearance of themselves [37]. Motivational problems may take origin in those cases, as previously explained. Therefore, a correct assessment of lymphedema state and treatment to use are very important factors in recuperation of breast cancer surgery.

Likewise, an early detection of lymphedema allows a correct assumption of therapy methods, reducing the risk of chronic lymphedema development [38]. Because of this, methods that allow measurement of upper-limb volume are an effective and important aspect in correctly diagnosing lymphedema.

2.5 Post-surgery physical exercise

Physical exercise to rehabilitation proposes in chronic diseases has been proven by several authors, to lead to a improvement in QOL and reducing all-cause mortality [39].

Studies of exercise importance in rehabilitation of breast cancer patients have been performed with evidences that suggest that exercise is an effective intervention to improve QOL, cardiorespiratory fitness and physical function in breast cancer survivors [39].

However, a gold standard exercise plan is hard to design, since the studies use different exercise regimes due to the lack of consensus on the optimal exercise prescription. This leads to dubious conclusions regarding the best exercise plan, as McNeely *et al.* [39] showed, since it is hard to compare results, requiring a broader and more complete study.

Also, an important factor to consider is pre-diagnosis exercise, with the International Agency for Research on Cancer of the World Health Organization (WHO) showing a link between physical exercise and lower risk of breast cancer [40].

2.5.1 Exercise in breast cancer survivors with lymphedema

Physical therapists, surgeons, and other health professionals have warned these women to avoid vigorous, repetitive, or excessive upper body exercise, believing that such types of exercises might actually induce lymphedema [41, 42]. However, this notion as been contradicted by studies, as Harris *et al.* [42] as well as McKenzie *et al.* [43] concluded that lymphedema is not related with exercise.

Furthermore, some experts believe that supervised exercise program can lead the decrease of stresses cause by lymphedema. This belief is supported by Schmitz *et al.* [44] study, where it was found that exercise group had lower incidence of lymphedema flare-ups (14% in the exercise group versus 29% in the control group). However, more research is needed to understand the benefits of exercise in lymphedema patients.

These results are supported by the National Lymphedema Network, referring that "is very important for individuals with lymphedema to be physically fit and maintain a healthy weight" [45]. This association refers that exercise plan depends upon the severity and cause of lymphedema and other co-existing medical conditions. One type of exercise important for lymphedema treatment is Lymphedema Remedial Exercise, used when reduction of size of a limb is necessary, and consists in active, repetitive, non-resistive motion of the involved body part [45]. Other type of exercises recommended to lymphedema patients are Flexibility or Stretching exercises, Resistance or Weight-Lifting exercises and Aerobic Conditioning or Cardiopulmonary exercises.

Chapter 3

Literature Review

3.1 Methods for Volume Assessment

Detection of lymphedema can be performed by medical history and physical examination, or through tonometry (applying pressure for one minute on a region where edema fluid is known to accumulate) [46]. However, this type of diagnosis can only be done in advanced stages of the disease, since that in early stages the detection of edema is very difficult [47]. Since an early detection of lymphedema is a very important factor in the minoritization of the problem, these methods are not very effective.

Currently, the methodologies focus in limb volume assessment, which in ideal conditions are performed with comparison between pre and post surgery limb volume. However, these conditions are not typically used, because volume of the limb before surgery is not usually measured. Consequently, bilateral comparison is performed to assess the presence of edema [48]. Nevertheless, some authors defend that, since difference between arms occur in healthy women, this measure is imprecise [30].

3.1.1 Subjective Methods for Volume Assessment

The method for detection of lymphedema must be efficient, easy to use, non-invasive, inexpensive, hygienic, reliable and adaptable to any part of the body that could be affected by lymphedema [27]. This criteria leads to assessment of measuring/detection lymphedema not having a golden standard [31], despite some studies considering Water Displacement the most complete in this criteria [30, 37]). Traditional methodologies will be described bellow.

- Water Displacement: This procedure is relatively inexpensive and is considered the gold standard of upper limb volume measure. As can be seen in Figure 3.1, this procedure consists in immersing the limb into a container with water (at 20 to 32^{o}C [49]) and the volume that is displaced of water represents the volume of the limb.

  Water displacement has several problems. First, it is hard to be precise in the performance of this procedure, since patients usually have difficulties due to low mobility of the arm.

In addition, the definition of the exact point to perform comparison is very hard to do, something also related with lower mobility in upper limbs and other factors [49].

Figure 3.1: Example of Water Displacement Method (From [27])

Additionally, Water Displacement is time consuming, not portable, unhygienic [37] and messy [30]. Furthermore, it often has a broad standard deviation (up to 25 mL) [50] and also does not allow perception of the limb shape, which can be a important factor in lymphedema assumption.

- Circumferential Measurement: Circumferential measurement is an indirect method. It is done using a flexible measuring-tape to measure the limb circumference in different points (Figure 3.2). After that, using mathematic formulas [51], the volume is estimated. The accuracy of this method is highly related to the number of measurements (studies recommend a distance of less than 4 cm between measures [52]) and knowledge of the health professional. The correlation between this method and Water Displacement is described by several authors [31, 52], however there are authors that disagree with this conclusion [37].

  This method can be also affected by compression of soft tissues due to tension in the tape, leading to underestimation of circumference, wrapping the tape in an incorrect angle around the limb or inaccurate spacing between measurements. Also, the use of old tape can lead to incorrect results [30]. Studies also found that this method can overestimate volume by more than 100 mL [37].

  However, when performed correctly, this method can be very accurate, allowing the perception of limb shape and limb circumference in key points [27]. Also, this method takes a long time to operate, despite being possible to use it at home.

Figure 3.2: Exemplification of Circumferential Measurement Method Procedure (From [53])

- Perometer: This method is similar to circumferential measurement, but performed by a device that scans the limb with infrared (IR) light and assesses limb volume. The device has two emitting diodes on adjacent sides and rows of corresponding sensors on the opposite two sides. The movement of the frame along the limb allows the automatic calculation of the volume from a large number of vertical and horizontal diameter measurements at 3.1 mm interval [30]. This method can be compared with the circumferential measurement, showing more accuracy, being more reliable, more convenient and providing highly reproducible measurements of upper limb volume, with each measurement taking only a few seconds [54]. In addition, this method allows detecting the localizations of anomalies with lower standard deviation (8.9 mL) [27].

  Considering that, this method is seen as the more accurate of limb volume measurement and can become the gold standard [30], despite some authors referring that is not used widely [49].

  This technique shows a difficulty in measuring the full length of the arm due to the necessary abduction of the limb and an incorrect estimation of hand measurement. Also, it has higher costs than the two previous methods mentioned and the size of the equipment does not allow its transportation. The dispositive also has problems in measurement of dynamic events or occlusion, which lead to the creation of a 3D-Led-scanner system. Withal, this equipment is even more expensive and it was not tested properly to conclude its efficiency [30].

- Tonometry: As previous explained, tonometry consists in applied pressure to a region where edema fluid is known to accumulate, resulting in a depression in the tissues where edema is present. This can be performed manually or using an instrument called tonometer, but is a procedure with a high degree of subjectivity and the instrument is unstable and heavy [55].

  However, tests to create an electronic device have been conducted. This device shows similar results to manual tonometry, but is expensive. Furthermore, both manual tonometry and electronic tonometry are very inaccurate, mainly in lower stages of lymphedema [30, 55].

- Bioelectric Impedance: Impedance can be described as the measure of the opposition that a circuit presents to a current when a voltage is applied. In humans, bioimpedance is the opposition of the flow of an electrical current through the body, and is inversely related to the volume of conductive material in the region [27]. In this method, electrodes are attached to the skin in the region of interest and measure the impedance at a range of frequencies of a small current, allowing to calculate the total body water (usually at 50 kHz) and extracellular water (usually at 0 kHz), assuming that extracellular and intracellular fluids act as a network of resistors with the cell membranes behaving as an imperfect capacitor [30]. After that, the values are normalized with the contralateral limb.

  This procedure is not as exact as traditional techniques, nevertheless, its operating time is lower. Despite that, it entails higher costs and is not generally used. Products present in market are Lymphometer and Electrical Impedance Spectrograph (EIS) [31].

3.1.1.1 Summary

A summary of the characteristics of the mentioned methods is present in Table 3.1.

Table 3.1: Comparison of most significant subjective methods for volume assessment. Adapted from [56]

Method	**Time to operate**	**Portable**	**Cost**	**Hygienic**	**Complexity**	**Accuracy**	**Local Measures & Shaped**
Water Displacement	Low	No	Low	No	Medium	High	No
Circumferential Measurement	High	Yes	Low	Yes	Low	Medium	Yes
Perometer	Medium	No	Medium	Yes	High	High	Yes
Tonometry	Low	Yes	Low	Yes	Low	Low	No
Bioelectric Impedance	Medium	No	High	Yes	High	Medium	No

3.1.2 Imaging Techniques

Imaging techniques to assess the presence and stage of lymphedema and also upper limb volume are frequently used. This allows for the detection of lymphatic disruption before signs of lymphedema become visible. In this chapter, the several techniques used are explored.

- Lymphoscintigraphy: Is a special type of nuclear medicine imaging [57] that identifies the lymph drainage basin, determines the number of sentinel nodes, differentiates sentinel nodes from subsequent nodes, locates the sentinel node in an unexpected location, and marks the sentinel node over the skin for biopsy [58]. This technique uses small amounts of radioactive material and is non invasive with the exception of intravenous injections (usually for contrast).

This is the traditional standard-of-care in imaging detection of lymphedema, however it has limited clinical use, due to its radioactive tracer that can restrict its "point-of-care", poor spatial resolution and long integration time [27].

- Near-Infrared Fluorescence Imaging: Near-Infrared Fluorescence (NIRF) Imaging is a technique that allows *in vivo* imaging of lymphatic system in humans. This allows the visualization of the lymphatics directly of contractile lymphatic propulsion and can be used for diagnosing early lymphedema and assessing lymphatic function and its response to lymphedema therapy [59].

  To perform that method, it is necessary to administrate a green dye, called indocyanine green (ICG), in intradermal regions. This allows the visualization of detail lymphatic capillaries and dipper vessel, and the demonstration of lymphatic flow through quantification of the velocity and frequency of contractile events [27].

  The mentioned technique shows significant differences in lymphatic vasculature's architecture between patients with and without lymphedema, as well frequency of lymphatic vessels [60]. However, this has not been approved in the United States and due to the use of low-energy photons its use is limited to lymphatic vessels until 3 to 4 cm below the skin surface [27].

- Computed Tomography: It can determine the area of the limb in any level, showing good results in volume measurement, showing also subcutaneous compartment and alteration of this volume. Furthermore, it can be quantified the density of the tissue [30].

  Computed Tomography (CT) is also capable of monitoring the effect of treatment, and when lymphedema exists, it can detect skin and subcutaneous compartment thickening [61]. Nevertheless the radiation is a drawback for repeated use of CT [30].

- Single-Photon Emission Computed Tomography: The use of a gamma camera to visualize the gamma-emmitting radionuclide that is injected in to the patient allows the perception of lymphatic vessels and its morphologic abnormalities. This can be visualized by CT, enabling the perception of the anatomic extension of backflow more accurately than lymphoscintigraphy [27]. Even so, there are still studies trying to understand the use of this technique to guide radiation therapy to specific lymph nodes [62].

- Magnetic Resonance Imaging: This technique results of a progress in lymphoscintigraphy, in which a gradolinium-base contrast agent is injected subcutaneously in the patient and magnetic resonance imaging (MRI) is used to assert lymphatic capillaries and any abnormally in its constitution. Also, MRI shows irregular blurring in areas of dermal backflow [27]. Regardless, this technique is usually neglected compared with CT, due to small difference between two methods and CT radiation being cheaper and more readily available.

- Ultrasound: Although ultrasound use is uncommon in lymphedema assessment, some authors tested this capacity [61], essentially as a complementary tool. It can be used to

determine skin, cutaneous, epifascial and subfascial thickeness [47]. This practice also showed inconclusive results in volume difference, leading to little use in the detection of lymphedema [30].

High frequency ultrasound (20 MHz) reveals characteristic patterns of cutaneous fluid location in various types of edema, with a distinctively uniform pattern in lymphedema [47].

- Dual-energy X-ray absorptiometry: Dual-energy projection methods have been used for measurements of bone and soft-tissue composition in vivo [63]. It uses a tissue-specific mode with attenuation of X-Ray related with the density, thickness and chemical structure of the material in question [64]. Although it is more accurate than traditional methods, Dual-energy X-ray absorptiometry (DEXA) has problems due to the radiation used.

3.1.2.1 Summary

A summary of the characteristics of this methods is presented in Table 3.2.

Table 3.2: Main imaging techniques to volume and lymphedema assessment (Adapted from [56])

Method	**Time to operate**	**Cost**	**Complexity**	**Accuracy**	**Radiation Problems**
Lymphoscintigraphy	Medium	Medium	Medium	Medium	Medium
NIRF	High	High	Medium	High	Medium
CT	Low	Medium	Medium	Medium	Medium
SPECT	Low	High	Medium	High	Medium
MRI	High	High	High	High	High
Ultrasound	Medium	Medium	Medium	Low	Nonexistent
DEXA	Low	High	High	High	High

3.1.3 Objective Methods

An objective and fast method to measure lymphedema has been pursued, since methods already mentioned are subjective due to the need of human perception to work. The development of 3D technology and its possibility to be used in several assessments has been used in lymphedema detection.

An example is Computer Aided Measurement Laser (CAML), propose by Trombetta *et al.* [65] in 2012. For that, the authors used 3D IR laser scanning for limb analysis and data collection of its shape, size and appearance, and computer aided design (CAD) system, to create a model through the data collected, as circumferential and limb volume measurements.

The IR laser scanning used was Polhemus FastSCAN^{TM}. This equipment was tested in 2007 by McKinnon *et al.* [66] for volume measurement. For comparison and results validation, the previously mentioned water displacement method (Chapter 3.1.1) was used. FastSCAN combines laser scanning with 3D special orientation. The results showed that this device is precise in volume

measurement and results are reproducible. So, FastSCAN can be used in a clinical environment for lymphedema assessment. Figure 3.3 shows FastSCAN in use.

Figure 3.3: Use of FastSCAN^{TM} for Volume Assessment (From [67])

Results from CAML are similar, since the authors concluded that the errors between the system and circumferential measurements are minimal and acceptable.

Other systems can be found in literature, with Insignia^{TM} laser scanning system [68] being the most interesting, showing to be suitable for volume assessment.

3.1.4 Summary

There are several methods of volume assessment of the upper limb, with some authors considering water displacement as the gold standard. However, there is not a consensus in therms of that the gold standard measurement is, due to difficulties in performing a correct assessment using water displacement in patients with upper limb problems. There are other methods as circumferential measurement or bioelectric impedance, but all of these have problems in a correct assessment of upper limb volume.

In order to counter these problems, some technologies to objectively estimate volume of the upper limb as been propose. Polhemus FastSCAN^{TM} has been the most used, showing good results. However, these technologies are very expensive and are quite difficult to be handled by non-professionals. Imaging techniques also show these problems.

Therefore, there is the need for a more objective method to assess upper limb volume, using a technique that allows monitorization at home, while also being low-cost and easy to handle.

3.2 Human Tracking Systems

Human movement tracking is a very important aspect to analyse change in the human body's pose, needing a well developed motion-sensor technology to perform that task. Human motion tracking is divided in three main fields: non-visual tracking, visual tracking and robot-aided tracking [69]. Robot-aided tracking will not be considered in this essay, given that it does not have the necessary characteristics, due to its high associated cost, to the fact that is it not portable and to the need of a professional to help in its used.

Also, since this essay's focus in Upper Limb Movement (ULM) and Shape, the research focused in papers and devices to this part of the human body. A broader and complete research for all human body can be found in Zhou *et al.* [69].

3.2.1 Tracking Based in Sensors

For tracking human actions, sensors used in these systems adhere to the human body in order to collect movement information. They can be used as a simple method to situations where "line-of-sight" can be a problem, since they are not affected by that [69].

In the case of Upper Limb, this type of sensors has been used to help rehabilitation. Salazar *et al.* [70] developed a three-accelerometer system that records the arm movements and was successful in transmitting the data acquired to a remote computer. Moreover, they successfully processed the acquired data, mainly filtering from artefacts, and plotted it, allowing visualizing significant differences in the plots generated from a stroke patient and a person with no pathologies.

Also Zhang *et al.* [71] used two three-axis acceleration sensors to obtain upper limb movement information. Results showed that these sensors can be used to calculate the movement of the arm and its endpoint. There are also products in the market with this type of sensors. One example found is SaeboFlex, a portable dispositive to help in upper limb rehabilitation. However, due to its limitations in functionality, the use of non-visual tracking systems is limited to specific activities and disease. Also, sensors do not have constant reliability like other systems and are more likely to come apart.

3.2.2 Vision-Based Systems

The used of vision-based human motion capture can be divided in three groups with respective to its function: surveillance applications, control applications and analysis applications [72]. Surveillance applications consist in monitoring a large number of people, and are not relevant to this study. Nevertheless, control applications (applications that estimated motion or pose) and analysis applications (orthopaedic analysis or athletes' performance analysis) are relevant for this study, since ULM analysis can be of these two types.

There are plenty of publications on human motion capture and analysis (Moeslund *et al.* [72] found 352 papers between 2000 and 2006), and can be divided in three groups: Marker-based, Marker-free visual base (2D Markerless and 3D Markerless human motion tracking system) and

Combinatorial Tracking [69]. This last will not be taken into consideration since it results from a combination of the other two, which will be described.

3.2.2.1 Marker-based human tracking systems

Visual marker base tracking is a technique where sensors are applied to track human movements. The sensors are usually used in articulated structures, since all of this can have an unpredictable movement [69].

The first work in this field was from Johansson in 1973, using his Moving Light Display, capable of tracking trajectories due to small reflective markers attached to human joints. After that, different techniques and procedures were tested. Furthermore, the commercialization of these systems is increasingly common. The use of optical systems to capture human gestures and motion has been growing. One type of this is the use of markers attached on the body of the subject and a set of various cameras. After the detection of the markers, an image processing program combines the 2D data and calculates the 3D position. These systems have some problems with the procession when a marker is hidden [73]. The use in animation movies and Computer-generated imagery (CGI) potentiated this field, due to its accuracy when performed in controlled conditions. Also, the commercialization of this type of technology is increasingly common. Examples of this are VICON [74], consider a golden standard [69], and Codamition [75].

In addition to full body tracking, a specialization occurs to analyze some movements and body parts. Schmidt *et al.* [76] developed a procedure for unconstrained wrist and elbow motions. Figure 3.4a shows the disposition of the markers. Also, this system uses 5 cameras to pick the localization of the markers, as can be seen in Figure 3.4b.

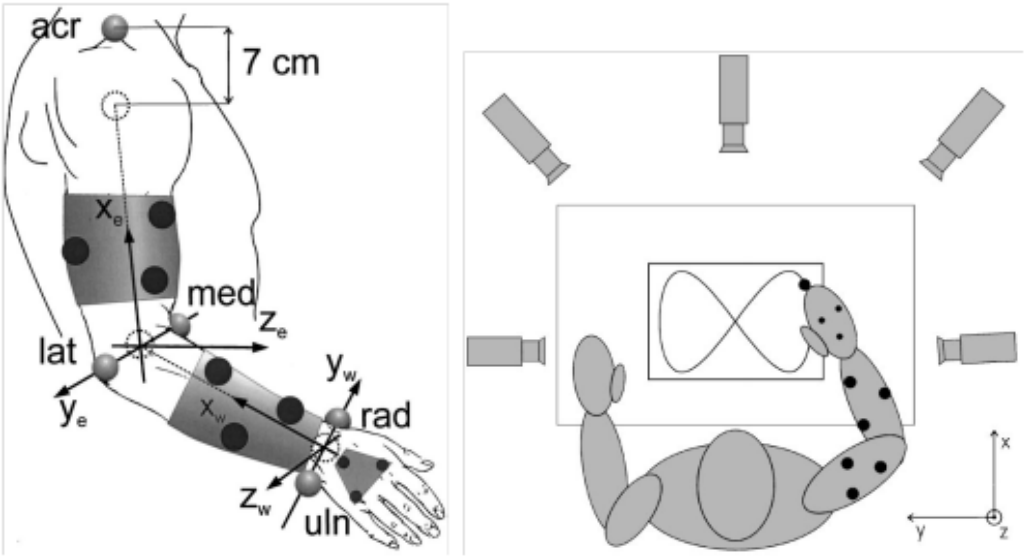

(a) Markers Position in the Upper Limb (b) Propose System from Schmidt *et al.*

Figure 3.4: Markers and Camera Position in Schmidt *et al.* system (From [76])

Tao *et al.* [77] also used markers to performer a similar experience, but only with three markers.

Notwithstanding, the results obtained by Schmidt *et al.* have several problems, since sensors reveal some difficulties, due to its need to performed some corrections in the results due to the influence of skin-movement artefacts on join angles. This system has also some inconvenients, since patients with complications in upper limb can have some difficulties setting the sensors. Likewise, the system requires a lot of calibration and professional intervention, making it expensive and very complex.

The Rutgers Arm II, described in Burdea *et al.* [78], is a system that has similar principles, but, instead of markers, uses IR LEDs and a low-cost IR tracking system to test ROM of the arm. This system, due to LEDs markers, can use less cameras, however the difficulties surrounding them are similar to Schmidt *et al.*

3.2.2.2 2D Markerless human tracking system

Use of 2D motion tracking is common when the only concern is the human movement and other aspects are irrelevant. This approach can be performed using shape models or, in other words, matching generated object models with acquired image data [69].

Several studies can be found in literature. Leung *et al.* [79] applied a 2D ribbon model to gather information on a moving human. For that, first it was extracted human outline from an image sequence using 2D ribbon model. After that, interprets if the outline belongs to a part of a body or to background.

Also, Ju *et al.* [80] performed a study of human motion using 2D markerless technology. It is assumed that a person can be represented by a set of planar patches connected (so-called cardboard person mode). To better results, the model constrain the parametrized image motion to articulated motion. This allows the description of the movement.

However, the use of this technique in ULM has not been explored, with little literature in this area published. This can be explained by the lower features extracted by this when compared with 3D Tracking Systems which, despite having a more elaborated processing system, is rewarding when extracting the movement of only one subject.

Hooi *et al.* [81], nonetheless, explored 2D technology to estimate automatic human pose and recover limp position and orientations without body markers. For that, the upper limb orientation is obtained using Radon transform.

Also, they used a foreground detection using brightness difference between the background image and the current image in pixel-wise basis. After that, a detection of limbs and head was performed. The results are showed in Figure 3.5.

This work showed that the segmentation of the upper limb detection is well performed, however, due to clothing, some part is disregarded. Also, some pose results showed ambiguities due to singularities and error in background clutter. So, future work in this topic includes improvement on human pose estimation [81]. Furthermore, this work presents limitations in volume measure-

(a) RGB image (b) Result Image after Segmentation

Figure 3.5: Results from Hooi *et al.* - Segmentation of Upper Limb and Head (From [81])

ment, an important factor to a correct evaluation of Upper Limb Performance. Also, they have restriction due to their viewing angle.

3.2.2.3 3D Markerless human tracking system

The use of 3D technology to track human movement has been used in alternative to 2D and its constraints. This can be divided in three main areas: model-based tracking, modelling human movements allowing the minimization of problems since future movements can be predicted, regardless of self-occlusion; feature-based tracking, using 2D and 3D features; and camera configuration, using a single or multiple camera distribution [69].

The use of a multi-view system consists in the reconstruction of a complete 3D object model from images taken by cameras in different points of view. Comparisons between different algorithms were performed to evaluate the currently best [82]. This review showed that PMVS (Patch-based Multi-view Stereo) [83] were the most successful approach to solve this problem.

PMVS utilizes multiple images and, due to a calibration matrices, reconstruct objects in 3D model, like the human body. First it starts with a sparse set of corresponding features, which are then expanded to the nearest projected pixels, forming 3D rectangular patches. After that, the algorithm iterates between three functions: matching, expansion and filtering. Results can be found in Figure 3.6.

This technique can be used in Upper Limb detection, however requires the use of well calibrated cameras and turn table positions, which demands professional help to operate, is very time

Figure 3.6: Reconstruction of different objects and human face using PMVS system. Small differences can be found in figure a) (Adapted from [83])

consuming and is very expensive.

Other method similar is described in Lam *et al.* [84], but with less cameras, which leads to reduced costs. The applied technique presented similar results to PMVS, although it requires a defined framework to be performed to be correct applied. However, calibration needs and help from professional still exists.

Caillette *et al.* [85] also performs 3D Human Body Tracking. For that voxels were used and classified from statistics on distance to the background in 2D models and, after process, is applied a 3D reconstruction process. After that, body reconstruction is performed using automatic blobs. Figure 3.7 show the obtained results.

Results have some problems in a correct assessment of human body shape, due to the use of blobs.

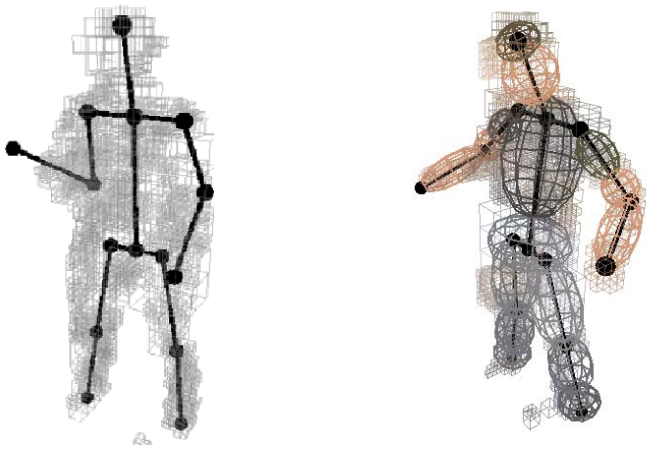

(a) Model fitting on the voxels using only volume information

(b) Automatic blobs reconfiguration to 3D reconstruction

Figure 3.7: Detection of human movement using voxels and blobs (Adapted from [85])

3D Markerless Upper Limb Tracking Systems

The application of multi-view system in upper limb reconstruction has been studied. Gonçalves *et al.* [86] calculated the arm movement without any constraints in its behaviour. For that, the arm was modelled as two truncated cones connected with spherical joints. A recursive estimator was used to predict the appearance of the arm on the image.

This work only needs a camera and displayed good results in correctly detecting the arm movement. Nonetheless, this method needs models of the head, neck and shoulder region for an exact estimation of hand movement. Also, a dark background is needed for it to be performed.

The assessment of posture and joint movements of the upper limbs of patients after mastectomy is also tested by Haddad *et al.* [87] using two non-invasive software's (authors of the study do not mention the used software).

Öhberg *et al.* [88] performed a study in subjects with lymphedema secondary to breast cancer, using volumetric data from a 3D-camera and compared with Water Displacement and Circumferential Measurement (Chapter 3.1). The results showed a tendency for 3D-camera to overestimate the volume in comparison of the Water Displacement, but this overestimation was insignificant. So, this method is a viable method for measuring arm volume.

3.2.3 Summary

The use of motion tracking systems to assess upper limb volume has been made, with good results in the estimation of volume. Öhberg *et al.* [88] showed good results in volume estimation using a 3D-camera when compared with traditional methods. However, authors do not refer associated costs with this method.

Other types of human tracking systems can be important to assess upper limb movement, such as 2D markerless or sensor based tracking systems, however they present handicaps, since volume estimation can not be made.

So, to perform a correct evaluation of upper limb movement and collect the relevant measures, a 3D approach is the most complete. However, traditional 3D techniques can reveal some problems, such as associated costs or need of calibration.

3.3 RGB-D Cameras

A relatively easy way to collect 3D image data is using RGB-D cameras. RGB-D cameras are novel sensing systems that capture RGB images along with per-pixel depth information, relying in either structured light patterns combined with stereo sensing or time-of-flight laser sensing to generate depth estimates that can be associated with RGB pixels [89].

This technology has existed for some years, with the first technology being developed by PrimeSense [90]. Swiss Ranger and PMD Tech products have been in the market, however with associated costs close to 10000 $.

However, RGB-D sensors can cost about 200 $, due to licenses for commercially use. Examples of this are the Microsoft Kinect and Asus Xtion PRO Live sensors. Properties of the diverse sensors can be found in Table 3.3.

Table 3.3: Comparison of characteristics of different sensors (Adapted from [91, 92])

Sensor	Max. Range	Resolution	Field of View in Degrees	Weight	Price (approximate)
Microsoft Kinect	10 m	640 x 480	57.8 x 43.3	440 g	200 $
Asus Xtion PRO Live	3.5 m	640 x 480	58 x 45	-[1]	200 $
SwissRanger 4000	8 m	176 x 144	69 x 56	470 g	10000 $
PMD CamCube 3.0	7 m	200 x 200	40 x 40	1438 g	10000 $

As seen in Table 3.3, both the Microsoft Kinect and Asus Xtion PRO Live show better properties and price when compared with other sensors. Between these two, Resolution and Field of View are similar, with the only difference being that the Microsoft Kinect has better range than the Asus. This can be relevant in medical environment, since is not as restrictive.

3.3.1 Microsoft Kinect

Microsoft Kinect (Figure 3.8) is a RGB-D sensor, created by Microsoft, providing synchronized colour and depth image [93]. The hardware of this dispositive consists in a normal RGD camera, a depth sensor and a four-microphone array and software allows the development of several applications due to is various tools.

[1] Weight value is not present in the literature

Figure 3.8: Microsoft Kinect Constitution (From [94])

As can be seen in Figure 3.8, Microsoft Kinect has three components to collecting images: an IR projector, an IR sensor/camera and a colour camera. The depth sensor is due to IR projector that casts an IR speckle dot pattern to 3-D scene and due to IR camera, which captures the reflected IR speckles [93].

RGD camera delivers the three basic colour component of the video. Usually, the camera is used at 30 frames/second, offering a resolution of 640x480 pixels with an 8-bit per channel. However, Microsoft Kinect also has the option to produce images with resolution of 1280x1024 pixels, but only at 10 frames/second.

The depth sensor consists of an IR laser projector and an IR camera that create a depth map. The sensor has a practical range of 0.8 m-3.5 m, with a resolution of 640x480 pixels and a frame rate of 30 frames/second.

Also important in Microsoft Kinect is the software used to collect data. There are several software's, but the main are OpenNI [95], Microsoft Kinect SDK [96] and OpenKinect (LibFreeNect) [97].

OpenKinect is an open source library, however, due to non-skeleton tracking, is not as used as the other two. OpenNI and Microsoft Kinect SDK are functionally comparable, although with a few differences. OpenNI requires a predefined calibration pose to skeletal tracking, which can be difficult to perform in patients with difficulties, which Microsoft SDK does not need.

However, the number of false positives in Microsoft Kinect SDK is more common than OpenNI. Moreover, Microsoft Kinect SDK has the ability to track only 10 joints in case the lower body is not visible [93].

OpenNI focus is hand detection and hand-skeletal tracking whereas Microsoft SDK realizes simple gesture recognition. A summary of these characteristics is presented in Table 3.4.

Several articles have done performance evaluation of Microsoft Kinect. Smisek *et al.* [98] did a comparison with three different cameras. The results show that the Microsoft Kinect has superior accuracy than that of a Time-of-Flight (TOF) camera and close to a medium-resolution stereo camera, with lower associated costs. Khoshelham *et al.* [99] measured the accuracy and resolution of depth measurement of Microsoft Kinect, showing that the error increases when the distance increases, raging between a few millimetres at close range to about 4 cm.

Table 3.4: Comparation between Microsoft Kinect software (Addapted from [93])

	Open NI	**Microsoft SDK**
Camera Calibration	Yes	Yes
Automatic Body Calibration	No	Yes
Number of Joints	15	20
Seated Skeleton	No	Yes
Body gesture recognition	Yes	Yes
Hand gesture analysis	Yes	Yes
3-D scanning	Yes	Yes
Motor control	Yes	Yes
Number of False Positives	Lower	Higher

Furthermore, skeletal tracking algorithm of Microsoft Kinect has also been tested. Dutta [100] tested this feature and concluded that Microsoft Kinect is able to capture 3D coordinates with an error smaller than 1 cm. Obdrzalek *et al.* [101] tested the joint location, however in this study the subject was performing a set of exercises and compared with the data generated by a marker-base motion capture system. It was found that Microsoft Kinect is a low-cost alternative to these systems, however current algorithm frequently fails due to occlusions, not distinguishing depth (an example is the limb close to the body) or clutter (recognition of other objects in the scene as joint).

3.3.1.1 Microsoft Kinect for Upper Limb Assessment

Microsoft Kinect is used to perceive human pose, behaviour or posture. For instance, Dutta [100] uses Microsoft Kinect to record posture and movement in the workplace. Also, an interesting example of the capacities of Microsoft Kinect is the article of Tong *et al.* [102] that use several Kinect's to a complete 3D body scanning and reconstruction. Another interesting application of Microsoft Kinect as performed by Zeng *et al.* [103], where an estimation of human body shape with clothing was performed. This showed that Microsoft Kinect applications are several and diversified, and all these techniques can be crossed and used in parallel when necessary.

Regarding upper limb movement, Pastor *et al.* [104] uses the capacities of the Microsoft Kinect to help in the rehabilitation of stroke patients. So, with skeleton tracking algorithm, the points from the joints are obtained. After that, a serious game would score the exercises performed by the patients taking into account the points and the expected pattern. This can be performed at home, since Microsoft Kinect is relatively inexpensive when compared with all the other methods, and improve rehabilitation.

Chang *et al.* [105] tried a similar approach, but for people with cerebral palsy. However, while Pastor *et al.* performed his test in several patients due to complexity of the disease, Chang *et al.* only performed in two patients. Nonetheless, this study showed a lower enthusiasm when the patients did not have feedback results of the exercise performed and when this feedback existed the results were much better and patients were a lot more motivated in the recuperation.

Kurillo *et al.* [106] performed a study to evaluate the ROM of upper limb extremity. This is an imperative factor in breast cancer patients, since it is an important measurement in UBF and to assess its full recovery. Using the skeleton tracking data from Microsoft Kinect, the team showed that the results from Microsoft Kinect are sufficiently accurate and robust to perform this type of evaluation in medical environment.

Lu *et al.* [56] uses Microsoft Kinect system to perform Volume Measurement in patients with lymphedema, only taking a few minutes to acquire the necessary images. This use allows the detection of local swelling sites as well as high accuracy and low cost in lymphedema detection. Also, this system allows reproduction of these results at home. However, the system requires a manual selection of the region to be measured. For that, the device needs to be approximately at 80 cm of distance. After that, all the data is analysed and redundant images are eliminated. Lastly, the images go through a filtering process and surface reconstruction. Result from a patient with lymphedema is presented in Figure 3.9.

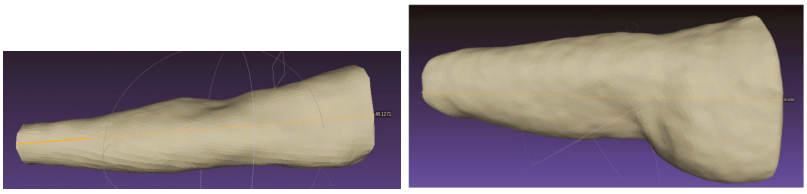

(a) Patient without Lymphedema (b) Patient with Lymphedema

Figure 3.9: Results of upper limb reconstruction from a patient with and without lymphedema (From [56])

This was compared with results from perometry method. Using different views, they verified the accuracy of the procedure. Results showed that the method is robust. However, the need to select manually the length of the arm can be a difficulty.

The authors also tested if the system was capable of detecting small and localize swelling. For this, they used a pen in the arm. Results are showed in Figure 3.10.

(a) Upper Limb Reconstruction Model (b) Upper Limb Photo with Pen

Figure 3.10: Comparison between model reconstruct using Lu *et al.* methodology and image taken by a camera (From [56])

As it can be seen, the system is able to shape the pen and also an increase in volume calculated, showing good results.

Lastly, Moreira [7] used Microsoft Kinect also to study Upper Limb Volume, ROM and other features to evaluate aesthetics and lymphedema presence. Furthermore, using self-reports, the data

was validated. However, the work only used one type of exercise to ROM evaluation. Also, the work was limited to a not-diversified database, which can harm the results obtained. Precision on the detection of lymphedema was also a problem.

3.3.2 Summary

RGB-D sensors can substitute traditional methods to track human movement. Some sensors can be found in literature, with Microsoft Kinect demonstrating improved properties when compared with the remaining.

The use of Microsoft Kinect to Upper Limb Evaluation has been performed by several authors. Kurillo *et al.* and Lu *et al.* showed good results in measuring ROM and volume. However, this studies do not have a complementary approach and are constrained to one measurement.

Moreira has a more integrated approach, but the results are not as good. So, there is a need to a more integrated approach that allows a more complete evaluation of UBF and corrected extracted features with QOL parameters.

3.4 Methods for UBF Evaluation

The evaluation of UBF, although related with lymphedema detection and measurement, is not limited to its presence. Impairments in the movement and limitation in daily activities are an important factor in breast cancer patients an a important measurement in the QOL. This can not be related with lymphedema, as Engel *et al.* [107] showed that patients without lymphedema can have lower UBF and Upper Limb Motion, with a consequent reduction QOL. This is usually related with ROM, however other features are important to assess UBF.

The methods to evaluate UBF can be divided in subjective and objective. Subjective methods are the most used, since they have low costs and favourable results. Furthermore, subjective methods can assess more features than traditional objective methods. However, subjective methods can be deceived and the results are less reproducible between patients.

3.4.1 Subjective Methods for UBF Assessment

Although only measurements to volume assessment have been presented, there is evidence that suggests that subjective assessment of UBF can detect lymphedema more prematurely and is more sensitive to the development of lymphedema [6]. Also, unlike previous measurements, subjective assessment through patient self-report allows functional but also psychosocial aspects to be taken into account [108].

This can be proven since studies showed that indicators as QOL, psychological morbidity, depression or anxiety can have impact in women who have lymphedema after breast cancer [109, 110]. Similarly, it is important to understand the impact of lymphedema in QOL of patients [48]. In addition, rehabilitation professionals can use this information to construct a better plan for recuperation of the patient [111].

There are several self-report questioners that can be performed to assess UBF. Disability of Arm, Shoulder and Hand (DASH) [112] (Appendix A) is the most used inquiry, with some studies referring that it is used about 46% of the times [46]. Still, this was not designed for breast cancer patients, and it is not even validated for this population [113]. This report consists of 30 questions that assess pain, weakness, numbness and functionality, and can be an optional module that is related with work and sports [32]. Studies found that DASH shows better results in breast cancer population, even when compared with inquiries design to this condition [46].

Other self-report that is used in breast cancer patients is Kwan's Arm Problem Scale (KAPS). This report was created to assess cancer in upper limb, and consists in 13 items divided in 2 scales. The first consists in problems in upper extremity function, pain, stiffness and swelling. Second is a subscale that rates impairment in activities of daily living. This scale has been shown to be convergent and exhibits discriminant validity in breast cancer survivors [114]. However, this report does not take into account psychometric properties. Other self-report targeted to breast cancer are Upper Limb Disability Questionnaires (ULDQ) and 10 Questions by Wingate (Wingate in Table 3.1). These are not as commonly used, so they will not be described, however their characteristics present in Table 3.1.

Also used in breast cancer patients is Upper Extremity Functional Index (UEFI), which allows the evaluation of upper-limb functional status in several activities through 20 items. This test has validation to breast cancer women, however, it was not designed to this group [115].

Patient-Specific Functional Scale (PSFS) is also used in this group of patients. This test was developed to understand the effect of a treatment in the patient, using for that 5 daily life activities they are unable to perform or at which they are having difficulty. This can be very important to assess QOL of patient after treatment [116].

Besides all these questionnaires, Functional Assessment of Cancer Therapy-Breast (FACT-B+4) is also used in patients with breast cancer. This self-report is part of FACT inquiries that are targeted to cancer patients and allows evaluating QOL of the patients in several levels. B+4 is a subscale that is focused in upper extremity. This can be used to design rehabilitation therapies [117].

It is important to notice that some of these inquiries are not validated to breast cancer patients, and results must take account of that [46].

Also, it is important to understand the importance of factors such as demographic characteristics, time since surgery, comorbidity, fatigue, depression and weight [118], considering that those factors influence QOL and some inquires do not take this into account.

Furthermore, there are some subjective measurements that can be very important to a correct assessment of UBF that usually are not taken into account in traditional self-reports. Measures such as patient experiences, symptomatology and functional limitations and also phychological, social, spiritual and physical aspects, can have a great impact in treatment and assessment of patient recuperation. This are usually classified as PRO [46] measures and were identified 10 of this in a recent review [119]. Although these are more reliable and exact self-reports are challenging to construct, since they have to adjust to every patient to a correct assessment. An example is the

already mentioned FACT-B+4, though there are others as the European Organization for Research and Treatment of Cancer Quality of Life Questionnaire - Breast Cancer Module (EORTC QLQ BR23) or BREAST-Q [120].

3.4.1.1 Summary

Self-reports mentioned are summed in Table 3.5.

Table 3.5: Main self-reports to UBF Evaluation (Adapted from [120])

Self-report scale	**Construct of Measure**	**Description**	**Clinical Interpretation**	**Validated in Breast Cancer Population**	**Comments**
DASH	Pain-related upper extremity disability	30 questions relating to symptoms (5 items) and functional tasks (25 items). Work and sports specific optional modules (4 items each).	0-100, a higher score reflects greater upper extremity disability	No	Although is not validate, DASH is used with great results in breast cancer patients
KAPS	Upper extremity problems (symptoms) and function	13 items consisting of 2 scales. Problem subscale (8 items) rating problems with upper extremity/shoulder function, pain, stiffness and swelling; ADL subscale (5 items) rating impairment of ADL	8-40, problem subscale; 5-25, ADL subscale. Higher scores reflect increased difficulty	Yes	Created specifically to women with breast cancer
ULDQ	Not Reported	80 items organized into 6 categories: symptom severity in the past 2 week; problem/symptom frequency in the past 2 week; current activity limitation; time relating to interference with normative work in the past 2 week; time with specified problems with work or daily activity performance in the past 2 week; and interference with weekly social, sports, or recreational activities in the last 2 week	Not Reported	Yes	Created specifically to women with breast cancer
Wingate	Functional status of women status postmastectomy over time	10 questions, each relating to degree of difficulty performing specified upper extremity tasks with the affected extremity	0-40, where lower scores are indicative of greater upper limb function	Yes	Created specifically to women with breast cancer
UEFI	Upper extremity function	20 items, 5-point scale (0-4)	Higher score corresponds to higher function	Yes	Validated against FACT-B
PSFS	Clinical measure of function	3 items; 11-point scale (0-10)	Higher score corresponds to higher function	Yes	Validated against FACT-B and UEFI
FACT-B+4	Upper extremity impairment	4 items with arm subscale; 5-point scale (0-4)	Higher score correspond to better QOL, less impairment	Yes	-

3.4.2 Objective Methods for UBF Assessment

Although subjective methods have good results in UBF evaluation, they can be deceived. So objective methods have been studied, including tests of flexibility, strength and endurance. The most common method is goniometry [121], used to assess ROM in all planes. After that, comparisons between limbs are performed, allowing the evaluation of abduction, flexion, extension, internal rotation and external rotation.

Endurance tests are usually performed using isometric and maximal performance of a set of tasks/exercises using the repetition maximum method, with each stage taking one minute and in each iteration exists an increment on speed of movement or weight held [122]. Other tests can be found in literature, as Box and Block or Nine-hole Peg Test. However, objective methods are not usually used, since they have limited use to specify function, unlike subjective methods. Also, objective methods can not be validated to breast cancer patients.

3.4.3 Summary

UBF assessment is usually performed by subjective tests that measure psychological, social and physical function, allowing understandment QOL of the patient. However, and even if these tests can be very important to UBF assessment, they can have false results due to partiality in results and to the fact that they are not reproducible. Nevertheless, objective methods are very limited, since they usually only measure limited features, and can be operator-dependent and time-consuming. Also, these methods are not validated to breast cancer patients, which can lead to false results.

So, it is of the utmost importance to create a method that can be objective but also can cover high number of features, leading to a better and efficient evaluation of UBF in breast cancer patients.

3.5 Conclusion

Traditional methods for volume estimation are subjective, and have a high number of sources of errors, with the most common being water displacement and circumferential measurements. These methods have problems, such as low accuracy, being time consuming or even impractical in clinical environment. Objective methods to perform volume estimation have been proposed, however these methods are expensive and usually dependent on an expert user.

Furthermore, patient condition is not fully defined by the presence of lymphedema. Pain, weakness, stiffness and functionality can be evaluated using self-report questionnaires, a method that can be reliable. However, this method is also subjective, and response can vary from patient to patient. Evaluation of upper-limb movement can also be performed using goniometry, which is an objective measurement with limitations in its accuracy. Therefore, nowadays, there is no objective measurement available that can fully characterize patient condition.

Human motion tracking systems can be a possibility to create a system that allows this characterization. This is due to the possibility of representing human movement in real time. There is

a wide range of possibilities, however none of them was created to assess UBF in breast cancer patients. RGB-D cameras have the necessary properties to perform this assessment, since they can be used for volume estimation and for tracking patients' movement, allowing the creation of applications in this area.

Chapter 4

Protocols for Acquisitions of Upper-Body Function

Patients' condition and UBF were assessed with objective methods using an RGB-D sensor. For that purpose, initially, it was important to select the sensor to be used for data acquisition. After that, a group of exercises was selected with the help of medical staff, and only then were the acquisitions performed. In order to do these acquisitions, protocols were defined and the space where the acquisitions were performed was also analysed.

4.1 Technology Selection

As explained in Chapter 3.3, RGB-D data is an easy way to collect 3D data, an important tool in this work. Of the RGB-D cameras in the market, Microsoft Kinect (Section 3.3.1) sensor is the most adequate one for medical acquisitions, due to its low cost and technical properties such as range and resolution of field of view. This sensor incorporates a RGB camera and a depth sensor, allowing a full-body 3D acquisition. Furthermore, Microsoft Software Development Kit (SDK) allows an automatic body calibration, which is an important feature for more efficient acquisitions.

Moreover, Microsoft SDK allows the development of applications in the field of markerless motion tracking system. This is possible due to its skeleton tracking algorithm that, using depth data, can determine the position of several joints on a human form [123]. The system has the possibility of detecting up to a total of 20 joints (Figure 4.1), each defined with coordinates (x,y,z) expressed in skeleton space. The origin of the referential of these coordinates is the sensor, as can be seen in Figure 4.1.

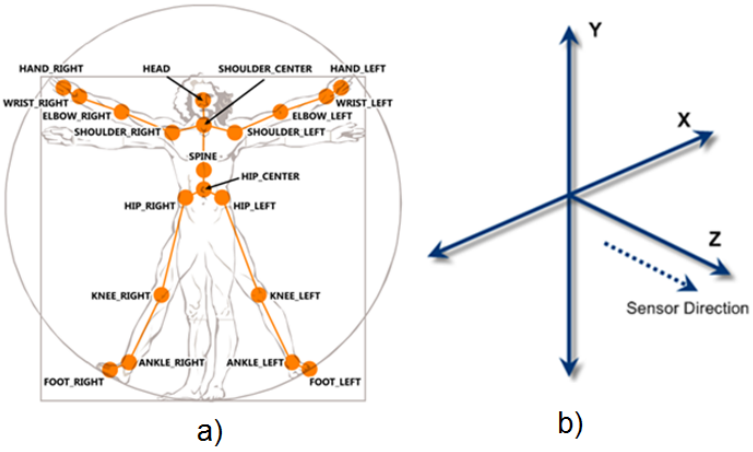

Figure 4.1: (a) Skeleton Joints tracked by the Kinect device and (b) Skeleton space axes. From [124]

4.2 Exercise Selection

Firstly, it was necessary to select the exercises to be performed by the patients in medical environment. For this purpose, some constraints were elaborated in order to allow a more precise and correct selection. It is important to mention that these rules were defined with the help of medical staff, due to their knowledge in the area. According to the defined constraints, exercises must be:

- Intuitive, to allow its execution by different people with different qualifications and ages
- Relevant, allowing the retrieval of important angles and measures to perceive upper-limb impairment
- Low time consuming
- Adaptive, allowing its performance in different conditions and places
- Independent, meaning that the exercises can be performed without any extra material
- Accepted by the medical community
- Fully captured by the device during execution

An interesting group of exercises that meets the mentioned requirements are rehabilitation exercises (examples in Figure 4.2). These are generally used in the recuperation of UBF, leading to tendon flexibility and enhancing muscular performance [43, 125, 126].

It is important to denote that the exercises depend on the phase of recuperation of the patient and the problems associated with surgery. Generally, patients are advised to start by performing simple exercises such as washing themselves, brushing their teeth, feeding themselves and brushing their hair as soon as drains and sutures are removed, being this the first step to restore normal function of the Upper Limb. Also, a regular exercise plan must be followed, with emphasis on

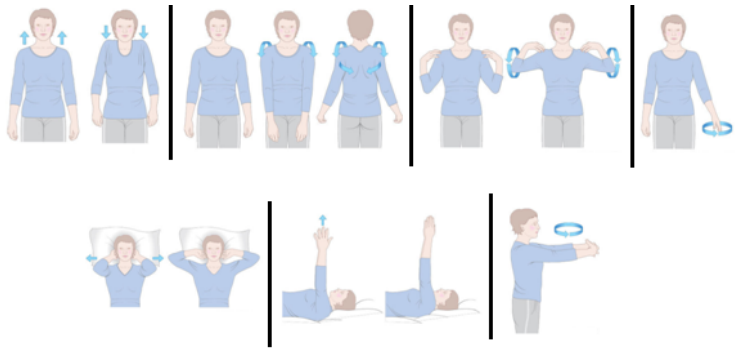

Figure 4.2: Examples of rehabilitation exercises (From [127])

stretching or reaching movements [128]. After that, exercises become more complex, mainly after the 3^{rd} week of the post-operation period.

Simple exercises do not comply with the requirements outlined previously, since they are dependent on extra material or difficult to capture with Microsoft Kinect, considering that they are small movements. Since these exercises usually have low amplitude of movement, the signal captured by the device can be very noisy.

However, exercises performed after the 3^{rd} week are interesting, since they comply with the established requirements. From these, five were selected, which allow the acquisition of relevant features. Also, it is important to obtain features that are not redundant among exercises, in order to have a better characterization of patient's state and of her problems on upper-limb mobility. Selected exercises can be found in Table 4.1, as well as the characteristics during acquisition. It is important to point out, once again, that such selection was approved by the medical staff that collaborated in this project.

Table 4.1: Selection of exercises to evaluate upper-limb problems

	Exercise 1	**Exercise 2**	**Exercise** 3	**Exercise 4**	**Exercise 5**
Name	Arm out of Side	Range of Motion	Stick	Pendulum	Walk in Walls
Left and right arm performed simultaneous	Yes	Yes	Yes	No	No
Repetitive Nature	No	No	No	Yes	No

More details of the selected exercises will presented above[1]:

- Exercise 1

  The patient starts with both arms in natural position. After that, the patient rises both arms and tries to cross them above the head, maintaining this position for two seconds (Figure 4.3).

[1] All images are adapted from [127]

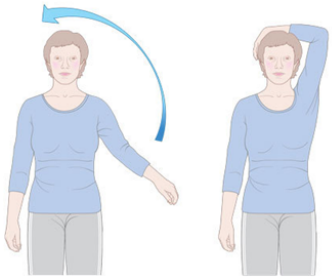

Figure 4.3: Illustrative figure of Exercise 1, Arm out of Side

- Exercise 2

  The patient starts with both arms in natural position. After that, the patient rises both arms laterally, trying to reach the highest height possible with the limbs (Figure 4.4).

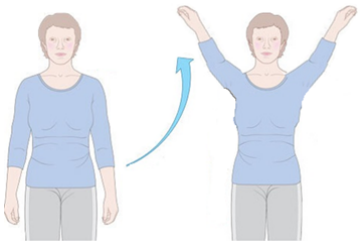

Figure 4.4: Illustrative figure of Exercise 2, Range of Motion

- Exercise 3

  The patient starts with both arms in natural position. After that, the patient rises both arms frontally, trying to reach the highest height possible with the limbs (Figure 4.5).

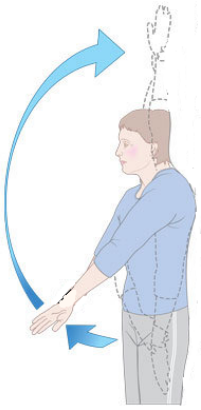

Figure 4.5: Illustrative figure of Exercise 3, Stick

- Exercise 4

  The patient is placed in a lateral position with respect to the Kinect sensor. After that, with the arm near to the sensor, the patient is asked to move the arm forward and backward. The

exercise is repeated at least 3 times. Then, the patient turns in order to use the other arm and repeats the procedure (Figure 4.6).

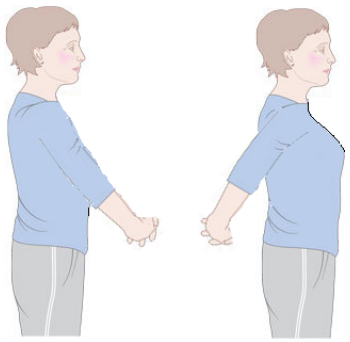

Figure 4.6: Illustrative figure of Exercise 4, Pendulum

- Exercise 5

  The patient approaches a wall and, with the arm closer to it, tries to reach the maximum height possible, taking care to keep the hand in the wall during the exercise. After that, the patient turns backwards to the camera and repeats the procedure with the other arm (Figure 4.7).

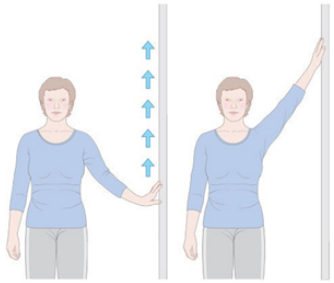

Figure 4.7: Illustrative figure of Exercise 5, Walk in Walls

Also, and since lymphedema is characterized by arm swelling, is important to access the volume of both limbs, to understand if there is or not an increased size of the affected arm. To perform this acquisition, the patient maintain the position represented in Figure 4.8 for at least 3 seconds.

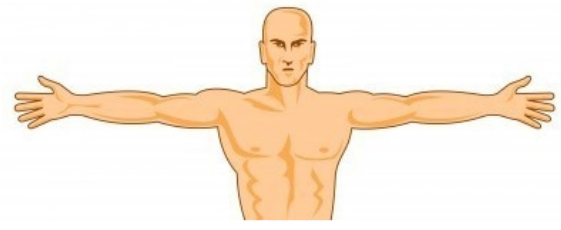

Figure 4.8: Position for Volume Data Acquisition (From [94])

4.3 Application for medical data acquisition

After the selection of the exercises, is necessary to create a software that can perform the acquisition of Skeleton Data and/or RGB-Data, and also to define the graphical interface of this application. As previously, Microsoft Kinect SDK is the best platform to perform this acquisition, since it allows the acquisition of image and data without any previous calibration, which is an important factor considering the environment that this application is targeted at, without any loss in the quality of the acquisitions. Furthermore, this device allows complete recording of the movements performed in the selected exercises.

To create the application it is vital to understand the requirements of the medical staff that will operate the system. For this purpose, inquiries were performed in order to understand the characteristics that the application needed. Those inquiries were performed orally, and were only performed to the people that will use the application, in this case a doctor and a nurse. Requirements concerning data acquisition and saving were also taken into account, despite not having input from the medical staff.

A summary of the main requirements can be seen in Table 4.2. For a better comprehension of these, they are divided in two main groups: graphic interface and software requirements.

Table 4.2: Main requirements for the application to data acquisition

Graphic Interface	Visualization of the data in real time Easy understanding of the behaviour of the application Exercise image as help Intuitive display of the constitution of the application
Software Requirements	Possibility of repeating exercise/acquisition, to rectify any error Data saving with the lowest user interference Low computational weight Prevent data losses

A quick explanation of these requirements is given below:

- Data visualization in real time

  It is important to understand if the acquisition is going on properly, thus it is necessary to have the information being acquired displayed in real time in the application.

- Easy understanding of the behaviour of the application

  The application must be intuitive, with a flow that is both easy to understand and predictable.

- Exercise image as help

  Since the application might be used by medical staff who does not have the knowledge of the exercises that are selected, an example of each exercise must be presented. This will also be helpful for medical staff who is adapted to the application, since it will work as a guide during the acquisition procedure.

- Intuitive display of the constitution of the application

  Due to the different modules that are needed in the application, it is important to have an intuitive display of all information.

- Possibility of repeating exercise/acquisition, to rectify any error

  Due to possible errors in acquisitions, it is important to have a safety mechanism that lets patients repeat exercises. For that purpose, a button was placed in the application to allow the repetition of exercises during acquisitions.

- Data saving with the lowest user interference

  Since the user of the application might have little knowledge in technology, data saving must be automatic from the moment the acquisition is started.

- Low computational weight

  Due to the high amount of data to be saved, the application must be efficient in the saving procedure. Furthermore, irrelevant data is not saved. An example of this is in Exercises 1 to 5, where RGB-D data is not saved since it is irrelevant in the characterization of the patient movement.

- Prevent data losses

  Another important aspect is to prevent data losses, since relevant information can be lost in these. With this intent, a buffer was created and, when data cannot be saved, it is kept in this buffer until such saving can be performed.

These requirements, and other aspects that can be obtained through the inquiries, allow us to understand the interactions between the system and the medical staff. These interactions are presented in Figure 4.9, in a Use Case Diagram.

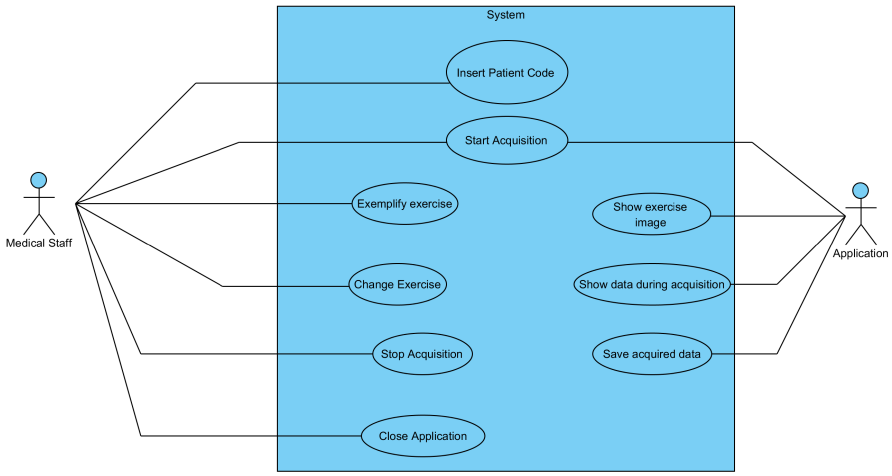

Figure 4.9: Final version of the Use Case Diagram of the application (using Visual Paradigm [2])

[2] http://www.visual-paradigm.com/

This diagram provides a better explanation of the system's behaviour as a whole. After approval by the medical staff, the application was created, as can be seen in Figure 4.10, following the defined fundamentals.

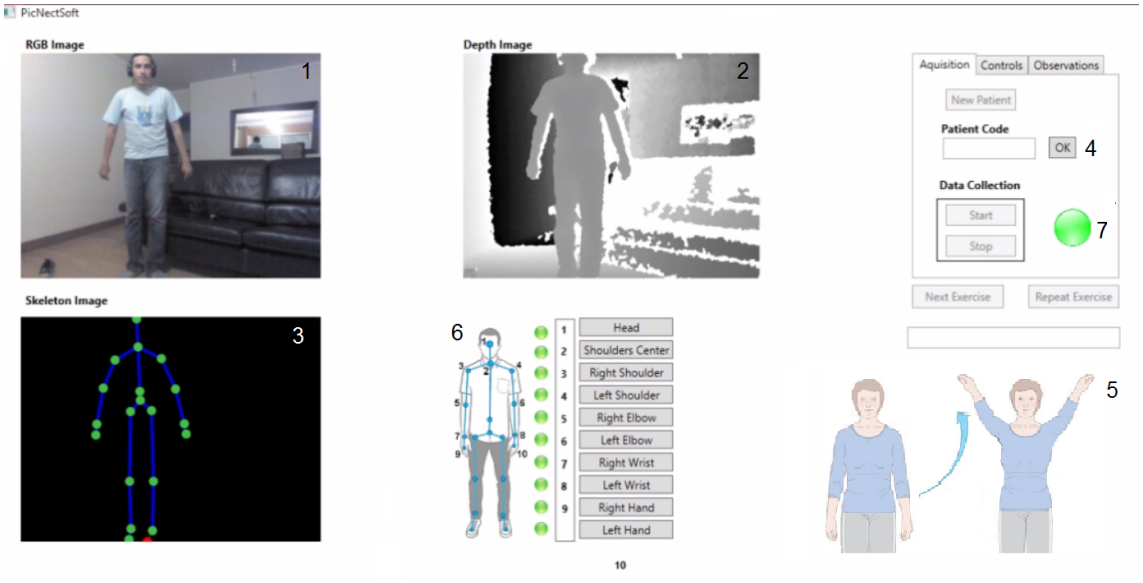

Figure 4.10: Final version of the application for data acquisition

As can be observed, the application consists in two images, one with RGB data being acquired (1 in the Figure 4.10) and the other with the depth map (2 in the Figure 4.10). The skeleton created using Kinect's algorithm is also showed (3 in the Figure 4.10), as well as which joints are being captured during the acquisition (green lights in 6 of the Figure 4.10). Furthermore, the patient's code is inserted in the box highlighted with number 4 in the Figure 4.10. The state of Kinect (online when green and offline when red) can be seen in the circle highlighted with number 7. Lastly, exercises' examples are displayed, to help medical staff during the acquisition procedure (5 in the Figure 4.10).

Some tests with the application were performed resulting in slight adjustments. The final version of the activity diagram is presented in Figure 4.11.

[3]http://www.visual-paradigm.com/

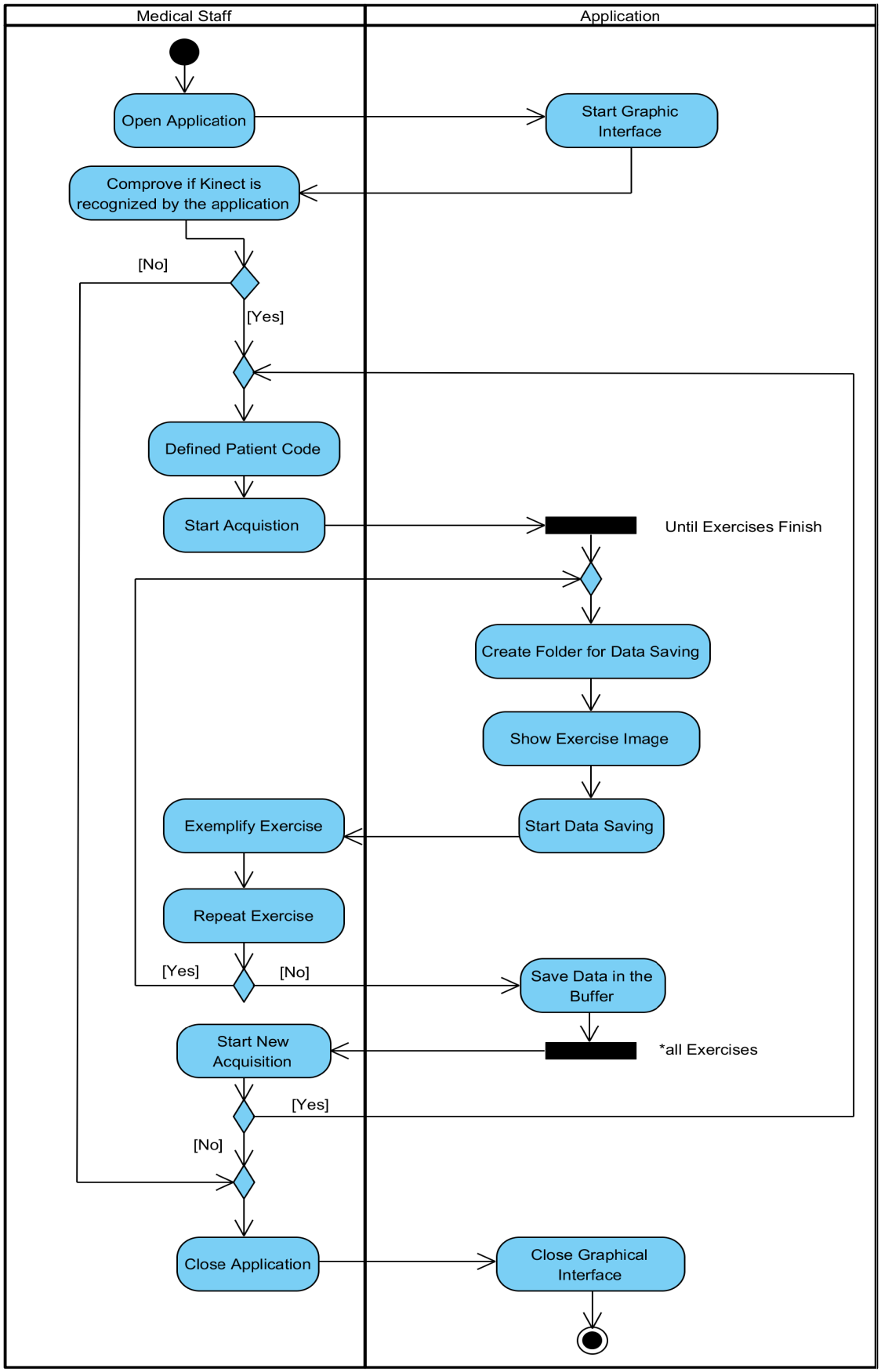

Figure 4.11: Final version of the Activity Diagram of the application (using Visual Paradigm[3])

4.4 Acquisition Environment

Data acquisitions were performed at Centro da Mama in Hospital S. João, with the environment of acquisition and placement of Kinect presented in Figure 4.12a and Figure 4.12b, respectively.

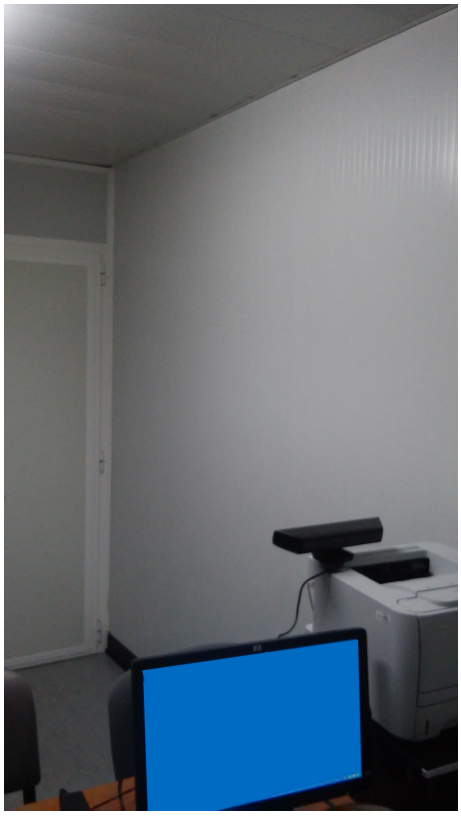

(a) Acquisition environment

(b) Positioning of Kinect

Figure 4.12: Acquisition environment and positioning of Kinect

Kinect position is not ideal, due to the difficulty to maintain parallelism between Kinect and the patient. Also, acquisitions were performed in two different spaces, which can result in some variations in the retrieved data, due to the slightly different conditions with which acquisitions were performed. Furthermore, the acquisition space had small dimensions, which led to some

difficulty in performing the exercises for some patients. Still related with the small dimensions of the space, some exercise acquisitions do not have all the joints in the gathered data. Kinect estimates the missing joints, however, this is also a source of errors.

4.5 Conclusion

In the area of RGB-D sensors, Microsoft Kinect has the best characteristics for assessing movement and volume in breast cancer patients. Its low cost and precision in the tracking system associated with its portability are important features that allow the creation of applications in the medical domain. Furthermore, it is easy to extract the data acquired by Kinect sensor for further analysis and characterization of patient condition.

After selecting the sensor, the next requirement was to select a group of physical exercises to be performed during acquisitions. Rehabilitation exercises meet the outlined requirements, thus five of these exercises were selected due to their properties and to the different features that can be extracted with them. With the selection of the sensor and exercises complete, it is possible to create an application that allows data acquisition while the patient is exercising.

Chapter 5

Database Characterization

The database includes 63 patients, from whom were acquired skeleton tracking system data, colour images and depth maps. Also, information related with the type of breast surgery that the patient was subjected, as well the year, the type of armpit surgery and the type of treatment posteriorly performed, was retrieved. These data are important, since can be related with the problems affecting the patient. Some data was impossible to retrieve, as can be seen in Table 5.1.

It is important to notice that two patients did not feel comfortable to remove the upper body clothes, which is an essential condition for volume acquisition. In these cases, this value was computed by averaging the volume ratio for all patients.

Upper-body functionality was computed for all 63 patients by performing DASH questionnaires (Appendix A) to all of them, due to its better results in breast cancer population, even when compared with inquiries specifically designed for this condition [46]. As previously explained, DASH consists of 30 questions that allow the assessment of pain, weakness and numbness, with a scale of 0-100, where a higher score reflects greater upper extremity disability. Patients were divided in two groups, 0-39 showed excellent or good upper body functionality, 40-100 showed regular or bad upper body functionality [129]. Patients were then divided in two classes, where 0 represents the first group and 1 the second.

Also, with DASH it is possible to compute if the patient has pain, weakness or stiffness. For these, patients were divided in two classes, where 1 represents the presence of this condition and 0 the absence. Lastly, it was assessed if patients had lymphedema and also divided in binary classes.

Table 5.1: Medical Information acquired from the patients: Code of Patient (Cd.), Type of Breast Surgery (B. Sg.: Mas - Mastectomy, Lum - Lumpectomy), Year of Breast Surgery (Year), Type of Armpit Surgery (A. Sg.), Chemotherapy (CT), Radiotherapy (RT), Physiotherapy (PT), Weakness (Weak.), Stiffness (SF), Functionality (FT) and Lymphedema (Lym.).

Cd.	**Age**	**B. Sg.**	**Year**	**A. Sg.**	**CT**	**RT**	**PT**	**Pain**	**Weak.**	**SF**	**FT**		**Lym.**
1	65	Lum	2004	EA	Yes	Yes	Yes	1	1	1	65.52	1	0
2	62	Mas	2010	EA	Yes	Yes	Yes	1	1	1	37.94	0	1
3	50	Mas	2011	EA	Yes	No	Yes	1	1	1	43	1	0

4	50	Mas	2011	EA	Yes	No	Yes	1	1	1	59.83	1	0
5	46	Mas	2015	EA	No	No	No	0	0	0	26.73	0	0
6	53	Mas	2014	EA	Yes	Yes	Yes	1	1	1	55.44	1	0
7	66	Mas	2013	GS	Yes	No	No	0	0	0	12.5	0	0
8	62	-	2013	GS	No	No	No	0	0	0	1.73	0	0
9	66	Lum	2010	GS	Yes	Yes	Yes	1	0	1	39.66	0	0
10	40	Mas	2011	EA	Yes	Yes	Yes	1	1	1	70.69	1	1
11	33	Mas	2012	EA	Yes	Yes	Yes	1	0	0	36.67	0	1
12	65	Lum	2002	-	No	Yes	Yes	1	1	1	65	1	1
13	79	Lum	2013	GS	No	Yes	No	0	0	0	3.45	0	0
14	62	Mas	2014	EA	No	No	No	1	1	0	58.63	1	0
15	52	Lum	2011	GS	No	Yes	Yes	1	0	0	50	1	0
16	54	Mas	2012	EA	Yes	Yes	Yes	1	1	1	51.67	1	1
17	70	Mas	2012	GS	Yes	No	No	0	1	0	11.61	0	0
18	79	Mas	2012	GS	No	No	No	1	0	0	36.21	0	0
19	44	Mas	2008	GS	No	No	No	0	0	0	0	0	0
20	48	Mas	2008	GS	No	No	No	1	1	0	35	0	0
21	68	Mas	1995	EA	Yes	Yes	Yes	0	0	0	25	0	0
22	45	Mas	-	GS	No	No	No	0	1	0	25	0	0
23	73	Mas	2009	GS	No	No	No	0	0	0	7.5	0	0
24	45	Mas	2012	GS	No	No	No	0	0	0	8.34	0	0
25	67	Lum	2010	-	No	Yes	No	1	0	0	45.38	1	0
26	48	Mas	2012	GS	Yes	No	Yes	0	1	0	25	0	1
27	49	Mas	2014	-	Yes	No	Yes	0	0	0	7.15	0	1
28	66	Mas	2011	EA	Yes	Yes	Yes	1	1	1	37.07	0	1
29	62	Mas	1995	-	Yes	Yes	Yes	1	1	1	68.11	1	1
30	72	Lum	2009	-	No	Yes	No	1	0	0	7.76	0	0
31	57	Lum	2013	GS	No	Yes	No	1	1	0	23.28	0	0
32	67	Lum	2013	GS	No	Yes	No	0	0	1	15	0	0
33	48	Mas	2013	EA	Yes	Yes	Yes	1	1	1	77.59	1	1
34	59	Lum	2014	GS	No	Yes	No	0	0	0	0	0	0
35	34	-	2014	EA	Yes	Yes	Yes	1	0	0	30.56	0	0
36	55	Mas	2015	GS	No	No	Yes	1	1	1	85	1	0
37	65	Mas	2006	EA	Yes	Yes	Yes	1	1	1	82.15	1	1
38	48	Lum	2011	EA	Yes	Yes	Yes	1	1	1	43.11	1	1
39	63	Lum	2010	GS	Yes	Yes	Yes	1	1	1	43.34	1	1
40	49	Mas	2010	EA	Yes	No	Yes	1	1	1	70	1	1
41	50	Mas	2010	EA	Yes	Yes	Yes	0	0	0	10.84	0	1

42	62	Mas	2010	EA	Yes	Yes	Yes	1	1	1	32	0	1
43	75	Mas	2011	EA	Yes	No	Yes	1	1	1	57.41	1	1
44	85	Lum	2008	EA	No	No	Yes	0	0	0	0	0	1
45	56	Lum	2013	GS	No	Yes	No	0	0	1	17.6	0	0
46	55	Mas	2009	EA	Yes	Yes	Yes	1	1	1	77.28	1	1
47	64	Lum	2009	EA	Yes	Yes	Yes	0	0	0	0	0	1
48	48	-	2009	GS	No	No	Yes	1	1	1	50	1	1
49	48	Mas	2010	EA	Yes	Yes	Yes	1	1	1	56.67	1	1
50	67	Lum	2014	GS	Yes	Yes	No	0	0	0	14.66	0	0
51	52	Lum	2014	GS	No	Yes	No	1	0	0	16.08	0	0
52	46	Lum	2014	GS	Yes	Yes	No	0	1	0	51.73	1	0
53	58	Lum	2013	GS	Yes	Yes	No	1	1	1	69.17	1	0
54	42	Mas	2013	GS	Yes	No	Yes	1	0	0	42.5	1	0
55	76	Mas	2015	GS	No	No	No	0	0	0	15.52	0	0
56	45	Mas	2011	EA	Yes	Yes	Yes	1	1	1	43.34	1	1
57	43	Mas	2011	EA	Yes	Yes	Yes	0	0	0	0	0	1
58	65	Lum	2014	EA	Yes	Yes	Yes	0	1	1	28.45	0	0
59	65	Lum	2014	GS	No	Yes	No	0	1	0	30.84	0	0
60	87	Lum	2010	EA	Yes	Yes	Yes	1	1	1	64.17	1	1
61	60	Mas	2014	EA	Yes	Yes	Yes	1	1	1	30.18	0	0
62	47	Lum	2015	GS	No	Yes	No	1	1	1	81.25	1	1
63	58	Lum	2011	EA	Yes	Yes	Yes	1	1	1	73.34	1	1

To achieve a better understanding of the data that was acquired, Table 5.2 shows the division according to the output. As can be seen, the division between all the different classes is quite balanced, which is an important aspect to consider when classification methods are applied to small databases.

Table 5.2: Physical condition of the patients

	Pain	**Weakness**	**Stiffness**	**Lymphedema**	**Functionality**
1	39	36	31	27	28
0	24	27	32	36	35

Also, it is possible to observe that most patients suffer of more than one problem. To study if the patologies are related or if any output is redundant, a correlation matrix is done (Table 5.3).

As can be seen, Lymphedema is the output that shows the lowest correlation values, with the highest value being 0.431, registered along with Stiffness. However, none of the outputs show a

Table 5.3: Correlation between Pain, Weakness, Stiffness, Lymphedema and Functionality

	Pain	**Weakness**	**Stiffness**	**Functionality**	**Lymphedema**
Pain	1	0.51	0.576	0.636	0.283
Weakness	0.51	1	0.66	0.581	0.361
Stiffness	0.576	0.66	1	0.589	0.431
Functionality	0.636	0.581	0.589	1	0.323
Lymphedema	0.283	0.361	0.431	0.323	1

very high correlation value, with the maximum being between Weakness and Stiffness. Thus, all outputs are important and not redundant for the characterization of patients' condition.

Chapter 6

Feature Extraction

Data acquisition varies according to the exercises, due to their different characteristics and goal. Therefore, and as previously mentioned, skeleton data was extracted for all exercises and RGB-D data was only acquired for Volume Measurements. These different types of data acquisition can divided the exercises in two main groups, based in what is the main data focus:

- Based on Skeleton Tracking System Data
- Based on RGB-D Data

Exercises 1 to 5 belong to the first group and their processing is similar. Only volume measurements fall in the second group. This division allows a better understanding of features' extraction from the data.

6.1 Based on Skeleton Tracking System Data

The skeleton tracking system from Microsoft Kinect was used to retrieve coordinates of joints and other important points of the human body over the exercise, allowing the characterization of the patient's movement during this period of time and shows very accurate precision [130]. However, its precision can be influenced by ambient conditions (e.g. luminosity) and movement or errors in the estimation of occluded joints [131]. Two examples of noisy signals obtained using Kinect can be seen in Figure 6.1.a and Figure 6.1.b, which represent the X coordinates of the left and right wrist, respectively, during Exercise 3. As it is noticeable, the signals have some spikes (highlighted in orange) that are not natural when compared with a smoother signal (Figure 6.2). These errors can affect some extracted features, since some features are computed using maximum/minimums, thus being a problem in this type of signals.

To solve this problem it is important to perform signal processing. In this work, 5 filters were tested to sort which was the most indicated one for these exercises. This allows the reduction of the impact of errors, enabling a more precise characterization of the movement and the extraction of features that better describe the patient's movement.

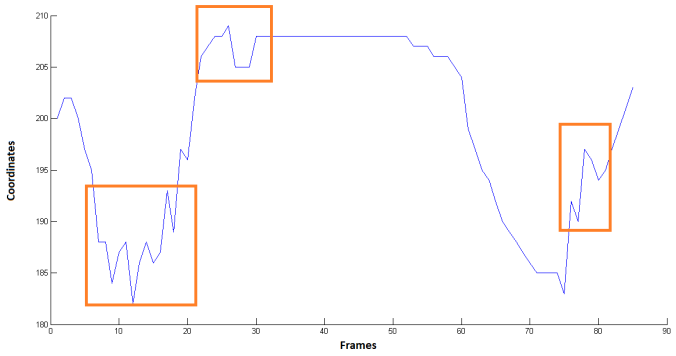

(a) X coordinates of the Left Wrist

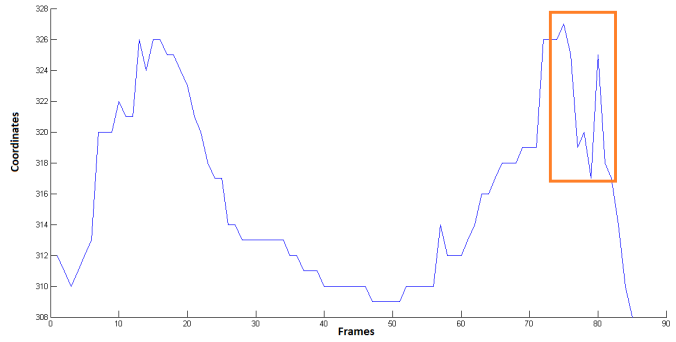

(b) X coordinates of the Right Wrist

Figure 6.1: Signals acquired using Microsoft Kinect. Noise highlighted in orange

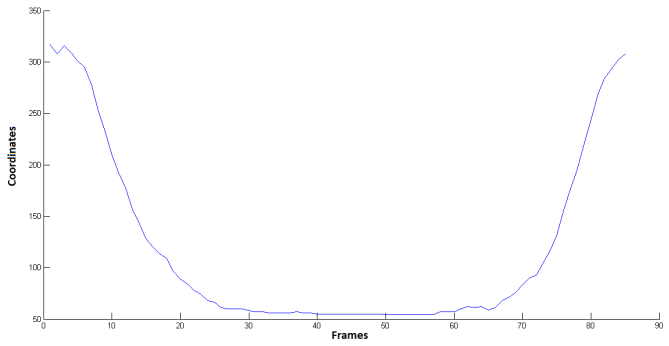

Figure 6.2: Signals with little noise acquired using Microsoft Kinect

6.1.1 Filters

In this work, several filters were considered, that will be described and tested to understand which one is better for each exercise.The chosen filters were based on how often they appear in the literature:

- Median Filter
- Moving Average Filter
- Gaussian Filter
- Low-Pass Filter
- Kalman Filter

It is important to understand their behaviour and the factors that can be modified to improve their precision and thus improve the results. After that, the filters will be tested by comparing them with a ground truth signal obtained by manual anutation.

6.1.1.1 Median Filter

A median filter is a nonlinear filter which is usually used for noise reduction, resulting in a smoother signal. This type of filter allows edge preservation and efficient noise attenuation with robustness against impulsive-type noise [132]. However, it can have unwanted effects, such as the loss of vital data from the signal.

This filter usually works in a window of an odd number of samples, which are sorted in ascending order, being the middle (median) value used as the filter output, as can be seen in Equation 6.1 [132].

$$y[n] = MED(x[n-k], ..., x[n], ...x[n+k]) \tag{6.1}$$

Window length of $2k+1$, $y[]$ is output signal, $x[]$ is the input signal and n is the index of the core sample.

6.1.1.2 Moving Average Filter

Very common in digital signal processing, the moving average filter allows noise reduction while retaining a sharp step response, however shows poor results in frequency domain encoded signals.

As the name implies, this filter operates by averaging a number of points from the input signal, resulting in the output signal. Equation 6.2 illustrates the system behaviour. To simplify this explanation, a window of length k will be considered. The averaging filter uses values from *–k/2* to *k/2*, summing the values of the input signal between these two limits. After that, the resulting value is divided by *k+1*, obtaining the averaged core value as the output signal.

$$y[n] = \frac{1}{k+1} \times \sum_{j=-k/2}^{k/2} x[n+j] \tag{6.2}$$

where $y[]$ is the output signal and $x[]$ is the input signal, k is the window length and n the index of the core sample.

6.1.1.3 Gaussian Filter

The Gaussian filter is a linear filter that is used in a wide number of fields, from signal to image processing. This is due to its nature, behaving as a weighted mean, where weight values are calculated according a Gaussian distribution (a function of probability theory) described by Equation 6.3 [133].

$$g(x) = \frac{1}{\sqrt{2\pi} \times \sigma} \times \mathrm{e}^{-\frac{x^2}{2\sigma^2}} \tag{6.3}$$

Gaussian distribution is related with standard deviation, represent by σ in the Equation 6.3. A greater sigma leads to less weight on the core value and higher weights on its neighbours, leading to a smoother signal. However, an excessively high sigma leads to loss of signal characteristics such as peaks or other important features.

Another important aspect in the definition of a Gaussian Filter is the window where the filter acts. The window in this filter is a weight window that consists in a normalized Gaussian distribution, with a weight given to each value. This weighted window is then multiplied by the elements in question, being the value of the output signal a sum of these multiplications [133].

6.1.1.4 Low Pass Filter

The low pass filter consists in a filter that has minimal effect in signals with a frequency lower that a certain cut-off frequency, and that attenuates in a certain amount frequencies which are higher than the cut-off frequency. A first order low pass filter has the following transfer function (Equation 6.4):

$$f(s) = \frac{1}{1 + \frac{s}{wc}} \tag{6.4}$$

Where *wc* is equal to *2*π*cutoff* frequency.

While there are diverse types of low pass filters, in this work a Type II Chebyshev filter was used, since it minimizes the error between the idealized filter and the actual filter, and has no ripple effect in the passband. However, this ripple effect is present in the stopband, as can be seen in Figure 6.3.

6.1.1.5 Kalman Filter

Used commonly in navigation and control of vehicles, the Kalman Filter consists in a recursive algorithm that uses a series of measurements over time, with noise associated, using them to

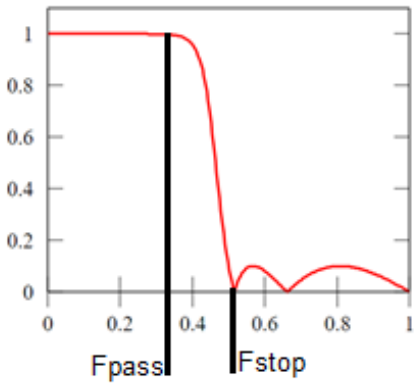

Figure 6.3: Typical responde of a Type II Chebyshev filter (Adaptation from [134])

compute estimations of unknown variables. These estimations are usually more precise than those based only in a single measurement, since the weighted average used in this filter allows a better estimation of the uncertainty associated [135, 136].

The algorithm works in a two-step process: a prediction step, where the Kalman filter produces estimates of the current state variables with associated uncertainties, and an updating step, where the next measurement is observed and the estimates are updated using a weighted average. This weighted average is done by giving more weight to estimates with higher certainty [135, 136]. An example of Kalman filtration is presented in Figure 6.4.

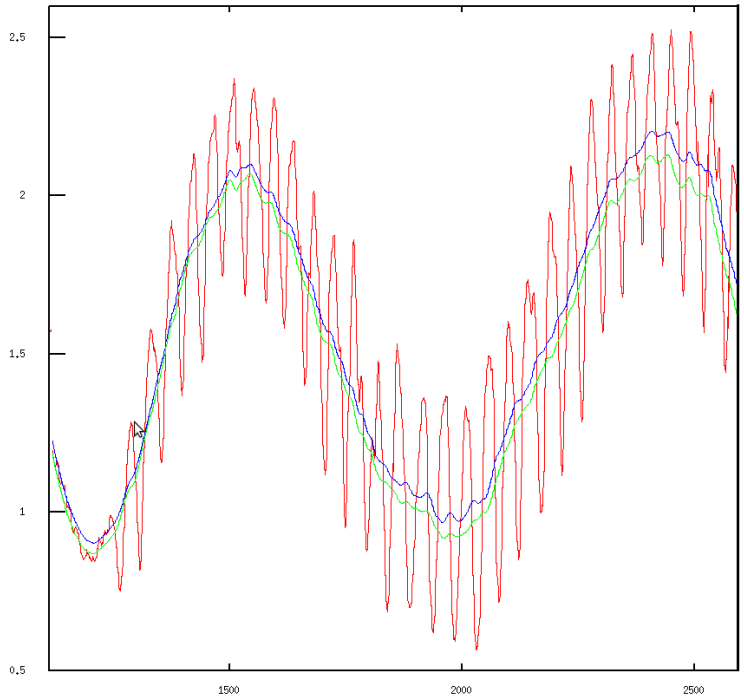

Figure 6.4: Kalman filtration of a noisy signal (in red). Result signal in blue and real signal in green (Adaptation from [137])

6.1.2 Filter Selection

In this work, filter selection was performed comparing a filtered signal with a signal obtained from color image that were manually marked. To perform a correct comparasion, the coordinates of the marked signal were converted to depth dimension. These markings were made in two joints per exercise, as can be seen in Table 6.1 according to the specificities of the exercise.

Table 6.1: Joints acquired for each exercise to filter selection

	Exercise 1	Exercise 2	Exercise 3	Exercise 4	Exercise 5
Right Elbow	Yes				
Left Elbow	Yes			Yes	Yes
Right Wrist		Yes	Yes		
Left Wrist		Yes	Yes	Yes	Yes

Raw signal was obtained using the skeleton tracking system algorithm of Microsoft Kinect in the considered joints. These signals were then filtered and compared with the signal acquired by manual tracking (ground truth). This comparison was done using a covariance matrix, since it allows the comparison between two random signals represented by two random vectors. In this case, the covariance matrix for each joint will be a 2x2 matrix, where the principal diagonal is 1 (comparison between the signal to itself) and the secondary diagonal represented is the variance obtained when comparing both signals. This value has been normalized, allowing an easy comparison.

So, for each joint two comparisons were performed: X_{filter} with X_{manual} and Y_{filter} with Y_{manual}, resulting in 4 values for each exercise. Of these, the minimum and maximum values of variance were selected, and these two values were compared with those of the other filters.

The results of the variance between skeleton data and manually tracked data can be found in Table 6.2.

Table 6.2: Values obtained using a covariance matrix between the manually marked signal and Microsoft Kinect's skeleton tracking system algorithm

Exercise 1		Exercise 2		Exercise 3		Exercise 4		Exercise 5	
Min	Max	Min	Max	Min	Max	Min	Max	Min	Max
0.9568	0.9934	0.9724	0.9914	0.7124	0.9977	0.9296	0.9926	0.9688	0.999

The obtained values show similarity between the marked signal and the signal obtained using the skeleton tracking system, except for the minimum observed in Exercise 3. This minimum value corresponds to the computation of coordinates X of the right wrist in this exercise. Furthermore, coordinates X of the left wrist also showed a low value. One explanation for this problem is the difficulty of the skeleton tracking system to measure wrist value when the wrist is perpendicular to the Kinect, leading to occlusions joints. This also explains why the other exercises do not present such low values.

These results also show that the manual tracking method is suitable to perform this comparison. After this, all the filters that were previously explained were applied to the skeleton tracking

system data, and covariance matrices were computed. Important to refer that, since some filters lead to delays in the signal, these delays were computed and fixed.

6.1.2.1 Median Filter

As explained in 6.1.1.1, the median filter is dependent on a window with a certain length. So, to test the behaviour of this filter, different windows were used in order to determine the best parameterization. After that, the signals were compared with the manual tracking signal. An initial window length of 2 was selected, and it was increased until there was a decrease in the variance. Results can be found in Table 6.3.

Table 6.3: Variance obtained between manual marked signal and skeleton tracking system algorithm of Microsoft Kinect after median filter was applied.Best values highlighted.

	Exercise 1		Exercise 2		Exercise 3		Exercise 4		Exercise 5	
Window Length	Min	Max	Min	Max	Min	Max	Min	Max	Min	Max
2	0.6347	0.9529	0.8885	0.9786	0.2006	0.9774	0.8296	0.9541	0.6558	0.9808
5	**0.9609**	**0.9932**	**0.9669**	**0.9905**	**0.7336**	**0.9974**	**0.8808**	**0.9892**	**0.9693**	**0.9989**
10	0.4327	0.8721	0.3724	0.9217	0.19	0.9698	0.3856	0.93	0.6289	0.9804

The median filter obtained better values for a window length of 5. A example of median filter processing is presented in Figure 6.5.

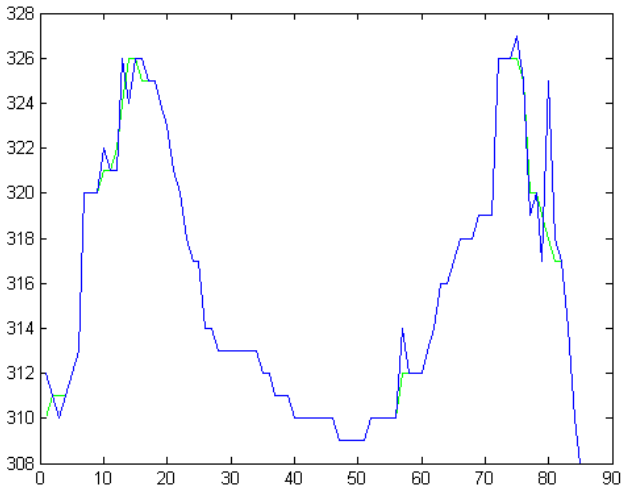

Figure 6.5: Original signal for X coordinates of the Right Wrist (in blue) and result signal after median filter processing (in green)

6.1.2.2 Moving Average Filter

Similarly to the Median Filter, the Moving Average Filter has only one parameter that has to be parametrized: the window length. An initial window length of 2 was chosen and it was increased

until there was a decrease in the variance value. Results can be found in Table 6.4.

Table 6.4: Variance obtained between manual marked signal and skeleton tracking system algorithm of Microsoft Kinect after moving average filter was applied. Best values highlighted.

	Exercise 1		Exercise 2		Exercise 3		Exercise 4		Exercise 5	
Window Length	Min	Max	Min	Max	Min	Max	Min	Max	Min	Max
2	0.884	0.9802	0.8757	0.9699	0.6596	0.972	0.2883	0.7973	0.8911	0.9871
5	**0.9489**	**0.9944**	**0.9556**	0.9884	**0.7906**	**0.9962**	**0.822**	**0.9608**	**0.9573**	**0.998**
10	0.933	0.9826	0.9146	**0.9932**	0.6635	0.9834	0.6015	0.9069	0.9337	0.9926
20	0.6785	0.8386	0.7086	0.8526	0.3533	0.7866	0.2859	0.8543	0.6067	0.9015

Better results are obtained when a window length of 5 is used, except for the maximum in Exercise 2, where the best variance value was observed for a window length of 10. Also, a example of moving average filter processing is present in Figure 6.6.

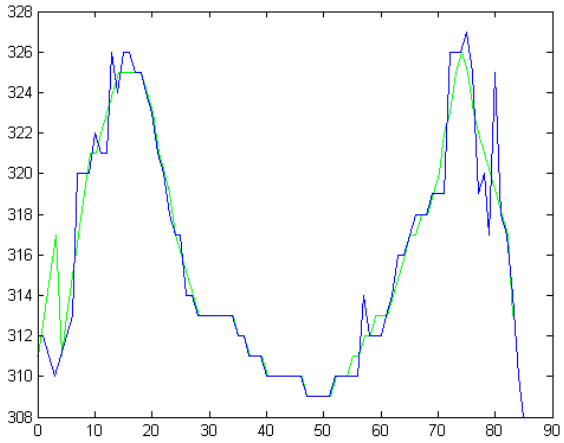

Figure 6.6: Original signal for X coordinates of the Right Wrist (in blue) and result signal after moving average filter processing (in green)

6.1.2.3 Gaussian Filter

The behaviour of a Gaussian filter is related with the following two variables: σ and window length.

Based on the results obtained with the moving average and median filters, an initial window length of 5 was initially defined. From here, one lower and two higher values (2, 7 and 15, respectively) were defined in order to have a bigger range of window lengths. Sigma values varied between 1, 2, 5, 7 and 15.

In order to test the performance of the Gaussian filter all the different windows were tested for each sigma value, with the obtained results being presented in Table 6.5.

Likewise average and median filters, the window length that presents the best results is 5, with an associated sigma of 2. A low sigma allows the maintenance of low frequency variations,

Table 6.5: Variance obtained between manual marked signal and skeleton tracking system algorithm of Microsoft Kinect after Gaussian filter was applied. Best values highlighted. Sigma as Sig and Window Length as WL

		Exercise 1		Exercise 2		Exercise 3		Exercise 4		Exercise 5	
Sig	WL	Min	Max	Min	Max	Min	Max	Min	Max	Min	Max
1	2	0.9562	0.9947	0.9711	0.9875	0.7521	0.9883	0.9072	0.9859	0.9657	0.9988
1	5	0.9487	0.9871	0.9415	0.9958	0.6705	0.993	0.8067	0.9559	0.9521	0.9957
1	7	0.9135	0.9729	0.89	0.9862	0.5903	0.9765	0.4712	0.8634	0.914	0.9876
1	15	0.6412	0.8488	0.6247	0.8282	0.1955	0.8031	0.2051	0.8713	0.6277	0.9118
2	2	0.9298	0.9911	0.9315	0.9853	0.74	0.991	0.6803	0.919	0.9417	0.9954
2	5	**0.963**	**0.9948**	**0.973**	0.992	**0.7564**	**0.9976**	**0.9313**	**0.989**	**0.9659**	**0.9989**
2	7	0.9494	0.9883	0.9424	**0.9963**	0.682	0.9926	0.8042	0.9551	0.9515	0.9954
2	15	0.7329	0.8908	0.7083	0.887	0.3007	0.8614	0.4003	0.7308	0.7271	0.9375
5	2	0.7486	0.9367	0.7466	0.903	0.4644	0.901	0.4545	0.5623	0.7733	0.9572
5	5	0.8617	0.9727	0.857	0.9586	0.623	0.9587	0.0793	0.7475	0.8801	0.9816
5	7	0.9159	0.9873	0.9162	0.9797	0.7129	0.9831	0.521	0.8816	0.9274	0.9922
5	15	0.913	0.9745	0.8909	0.9864	0.6255	0.972	0.3387	0.8668	0.9189	0.9882
7	2	0.5702	0.867	0.6235	0.7948	0.245	0.7918	0.1284	0.8485	0.5974	0.911
7	5	0.714	0.9228	0.7317	0.882	0.4183	0.8783	0.3952	0.7048	0.7395	0.9477
7	7	0.8002	0.9512	0.8077	0.9264	0.526	0.9242	0.3233	0.6157	0.8195	0.9642
7	15	0.9486	0.9947	0.932	0.9891	0.7397	0.971	0.0946	0.935	0.9505	0.9988
15	2	0.0049	0.4289	0.077	0.4524	0.1501	0.2501	0.4528	0.7056	0.2399	0.5889
15	5	0.0649	0.5257	0.1848	0.5128	0.2031	0.3325	0.6737	0.8739	0.0724	0.6641
15	7	0.1367	0.5889	0.2654	0.5532	0.1611	0.4281	0.6212	0.8137	0.0243	0.7909
15	15	0.5236	0.8141	0.6125	0.779	0.2067	0.7631	0.0248	0.4725	0.4617	0.8695

attenuating variations with a very high frequency. Also, a example of gaussian filter processing is present in Figure 6.7.

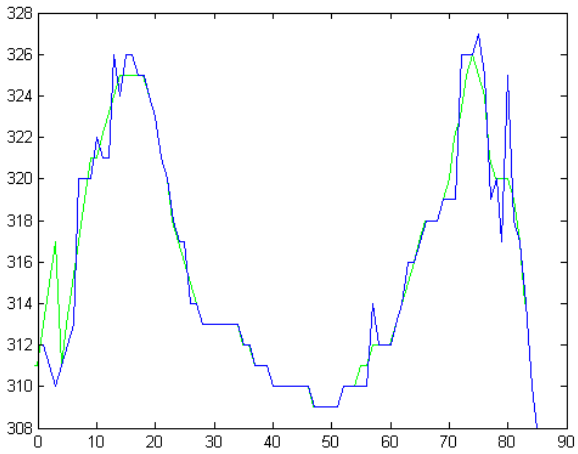

Figure 6.7: Original signal for X coordinates of the Right Wrist (in blue) and result signal after gaussian filter processing (in green)

6.1.2.4 Low Pass Filter

To perform a low pass filtering it is essential to define the frequency where the filter needs to act. In order to do that, it is necessary to define what is considered noise and calculate its frequency. In this work, noise was defined as the spikes that seem unrelated with the exercise and resemble unnatural movements (as explained in Figure 6.1). Bearing this in mind, using some of the acquired data, it was possible to estimate that the noise's average frequency was approximately 92 Hz. However, it was also noticed that the noise had a very wide-ranging frequency (higher standard deviation measured in the noisy data), also seen in Figure 6.1.

In a Chebyshev Type II filter, it is necessary to define two frequencies: a frequency where the filter starts to act (Fpass, in Figure 6.3) and the value where the stopband starts (Fstop, in Figure 6.3). So, knowing that the average frequency of the signal was approximately 90 Hz, five Fpass frequencies were used: 80, 85, 90, 95 and 100 Hz.

Another important aspect is the window of the filter. To understand its impact, the difference between Fpass and Fstop was varied, allowing a window between 40 and 60 Hz. The results are presented in Table 6.6.

Table 6.6: Variance obtained between manual marked signal and skeleton tracking system algorithm of Microsoft Kinect after Low-Pass filter was applied. Best values highlighted. Window Length, Fpass and Fstop in Hz.

		Exercise 1		Exercise 2		Exercise 3		Exercise 4		Exercise 5	
Fpass	Fstop	Min	Max	Min	Max	Min	Max	Min	Max	Min	Max
80	120	0.8438	0.9759	0.8696	0.9808	0.4299	0.9911	0.1449	0.8249	0.892	0.9971
85	125	0.8809	0.9869	0.9111	0.9794	0.594	**0.997**	0.0117	0.8714	0.9146	0.9971
90	130	0.9167	0.9937	0.9262	0.9793	0.6693	0.9951	0.1122	0.8995	0.9262	0.9962
95	135	0.931	0.9947	0.9229	**0.9856**	0.6807	0.9881	0.0074	**0.9216**	0.9249	0.9922
100	140	0.9312	0.9919	0.9133	0.9788	0.7093	0.9782	0.0067	0.9118	0.9005	0.9864
80	125	0.8755	0.9826	0.8901	0.9829	0.5172	0.9953	0.0795	0.859	0.9174	0.998
85	130	0.9054	0.991	0.9183	0.9785	0.6576	0.9966	0.0315	0.8938	0.9283	0.997
90	135	0.9361	0.9958	**0.9289**	0.9849	0.6906	0.9912	0.068	0.9169	0.9312	0.994
95	140	0.9316	0.9938	0.9187	0.9829	0.7478	0.983	0.0132	0.9186	0.9206	0.9893
100	145	0.9278	0.99	0.9088	0.9731	0.6832	0.9713	0.0271	0.8909	0.8906	0.9834
80	130	0.8983	0.987	0.8999	0.9835	0.567	0.9964	0.0678	0.8809	0.9294	**0.9984**
85	135	0.9328	0.9954	0.9288	0.9823	0.7113	0.9941	0.1147	0.9115	0.933	0.9952
90	140	0.9383	**0.9959**	0.9269	0.9842	0.7477	0.988	0.0614	0.9146	0.9313	0.992
95	145	0.9296	0.9928	0.916	0.9794	0.7258	0.9782	0.0068	0.909	0.9162	0.9871
100	150	0.9123	0.9846	0.8974	0.9601	0.6395	0.9567	**0.2055**	0.8319	0.8669	0.9772
80	140	0.9347	0.994	0.9233	0.9833	0.6916	0.9955	0.0273	0.9175	**0.9431**	0.9967
85	145	**0.9416**	0.9954	0.9252	0.9825	**0.7604**	0.9854	0.0839	0.9106	0.9286	0.9904
90	150	0.93	0.992	0.914	0.9765	0.7156	0.9744	0.0026	0.8984	0.911	0.9854
95	155	0.9163	0.9866	0.8992	0.9653	0.6621	0.9611	0.0301	0.8589	0.8869	0.979
100	160	0.9019	0.9802	0.8829	0.9531	0.6019	0.945	0.0023	0.7992	0.8573	0.9724

The best variance values for this filter are very uncertain, with different window lengths, Fpass

and Fstop between exercises. This is due to noises with higher standard deviation. Noise can also be related to the patient and to how she does the exercise, with a varied frequency, so a low pass filter is not the optimal solution.

6.1.2.5 Kalman Filter

When defining a Kalman filter, it is necessary to calculate the initial state variables and, after that, the filter acts by itself, predicting and updating its estimations. So, unlike the other filters, in Kalman filter no values were varied. Values of variance for this filter are presented in Table 6.7.

Table 6.7: Variance obtained between manual marked signal and skeleton tracking system algorithm of Microsoft Kinect after Kalman Filter was applied.

Exercise 1		Exercise 2		Exercise 3		Exercise 4		Exercise 5	
Min	Max	Min	Max	Min	Max	Min	Max	Min	Max
0.9609	0.9941	0.9733	0.9916	0.7269	0.9978	0.9315	0.9908	0.967	0.9991

As expected, the Kalman filter presents good variance results in almost all results considered. Also, a example of Kalman filter processing is present in Figure 6.8.

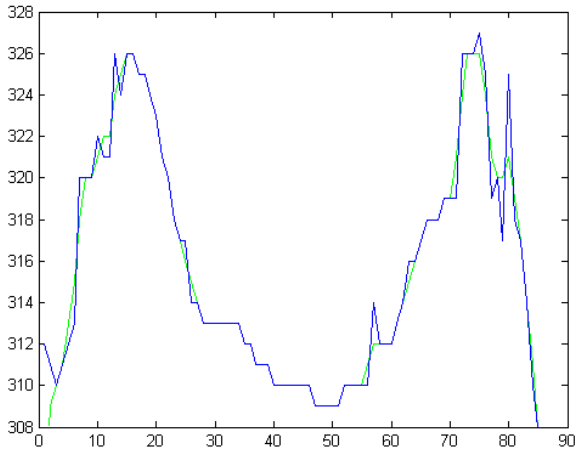

Figure 6.8: Original signal for X coordinates of the Right Wrist (in blue) and result signal after Kalman filter processing (in green)

6.1.2.6 Comparing filters

In order to compare the filters, the best results in the five exercises were selected for each filter (maximum of minimum and maximum of maximum for each). Results are compared in Table 6.8.

As expected, the minimum for Exercise 3 is very poor in all filters, due to the difficulty of the skeleton tracking system to measure the X coordinates of the wrist during this exercise. However, the application of the filters mitigates the difference, something that was expected, since the dif-

Table 6.8: Best variance results from all filters. Best values highlighted

	Exercise 1		Exercise 2		Exercise 3		Exercise 4		Exercise 5	
Filter	Min	Max	Min	Max	Min	Max	Min	Max	Min	Max
Median	0.9609	0.9932	0.9669	0.9905	0.7336	0.9974	0.8808	0.9892	**0.9693**	0.9989
Moving Average	0.9489	0.9944	0.9556	0.9932	**0.7906**	0.9962	0.822	0.9608	0.9573	0.998
Gaussian	**0.963**	0.9948	0.973	**0.9963**	0.7564	0.9976	0.9313	0.989	0.9659	0.9989
Low-Pass	0.9416	**0.9959**	0.9289	0.9856	0.7604	0.997	0.2055	0.9216	0.9431	0.9984
Kalman	0.9609	0.9941	**0.9733**	0.9916	0.7269	**0.9978**	**0.9315**	**0.9908**	0.967	**0.9991**

ficulty of measuring coordinates X leads to values with a higher frequency, which are reduced by the filters.

To minimize errors, it was decided that the same filter would be applied in all five exercises, since different filters could lead to different artefacts, which could lead to incorrect conclusions. Likewise, to perform this selection, the best results for each exercise (maximum and minimum) were selected, as can be seen in Table 6.8. In these results, Kalman filter presents a higher variance in 5 of the 10 values. Furthermore, in those Exercises where Kalman Filter does not have the best variance, this filter still presents similar values to those of the best filter.

It is also important to compare the results of the signal after processing by the Kalman filter with the skeleton tracking system data, as presented in Table 6.9.

Table 6.9: Comparison between Skeleton Tracking System and Kalman Filter

	Ex.1		Ex.2		Ex.3		Ex.4		Ex.5	
	Min	Max	Min	Max	Min	Max	Min	Max	Min	Max
Skeleton Tracking System	0.9568	0.9934	0.9724	0.9914	0.7124	0.9977	0.9296	0.9926	0.9688	0.999
Kalman Filter	0.9609	0.9941	0.9733	0.9916	0.7269	0.9978	0.9315	0.9908	0.967	0.9991

These results show that the Kalman filter results in a more accurate data when compared with manual tracking data using color images, as intended, since it had 8 of 10 values with higher variance when compared to the Skeleton Tracking System Algorithm. These results allows to conclude that Kalman Filter is a possible solution filter to apply in the acquired medical data.

To verify these results, other methods of comparing the signals were performed. Initially, in each signal of an exercise, only the filters with the best parameters combination were applied. For instance, in Exercise 1, the signal was filtered with a median filter with a window length of 5, a moving average filter with also a window length of 5, a Gaussian filter with a window length of 5 and a sigma of 2 and a Low-Pass Filter with F_{pass} of 90 Hz and F_{stop} of 140 Hz. After that, the distance in each frame between the manual marked signal and the processed signals was computed. This distance was calculated through Equation 6.5.

$$d = \sqrt{(x2^2 - x1^2) + (y2^2 - y1^2)} \tag{6.5}$$

For each exercise, two vectors with the distances were obtained. After that, the average and standard deviation of the distances for each vector was computed. Finally, the average of these two previously calculated average distances and standard deviations were computed, obtaining the final average distance and standard deviation. Obtained results are presented in Table 6.10.

Table 6.10: Average and standard deviation of the distances between manual marked signal and the remaining signals (distance in pixels).

	Exercise 1		Exercise 2		Exercise 3		Exercise 4		Exercise 5	
Skeleton System	20.34	2.43	20.25	1.79	65.71	5.57	17.01	1.33	23.95	2.31
Moving Average	20.33	1.12	20.33	1.32	65.86	4.56	17.00	1.22	23.94	2.22
Median	20.34	1.23	20.44	1.46	90.24	4.75	16.74	1.15	24.09	2.14
Gaussian	20.29	1.31	20.31	1.22	90.13	4.82	17.03	1.37	24.03	2.11
Low-Pass	19.33	1.43	21.16	1.39	108.54	4.69	17.03	1.44	29.76	2.19
Kalman	19.37	1.10	19.32	1.05	64.32	4.23	16.59	1.21	23.72	2.11

As expected, Kalman filter showed better results in almost all exercises. It is also interesting to see the values for Exercise 3, where there is a very high standard deviation. This helps supporting the explanation that was previously given. It is also important to notice that Skeleton Tracking System exhibited higher standard deviation. This can be explained due to the presence of noise in this signal, increasing this value. Kalman filter, on the other hand, presented a low standard deviation, as expected, since it smooths the signal and approximates the resultant signal to the marked signal.

However, the difference obtained is not very significant in terms of distance, which could render this step discardable. To verify if signal filtering had the expected results, the initial signals (Figures 6.1 and 6.2) were again observed, and the impact of filtering was analysed. A complete signal of Exercise 3 can be found in Figure 6.9.

As it is possible to observe in Figure 6.9, Kalman filter led to a substantial reduction of the noise present in the original signal, as expected. This leads to a better feature acquisition, since movement characterization is improved. Also, it is important to notice if Kalman filter has unwanted effects in signals with reduced noise. For that, the signal present in Figure 6.2, where pre and post processed versions of the signal are presented (Figure 6.10), was analysed.

As can be seen, Kalman filter had little effect in this signal, even improving the reduced noise that the signal had (highlighted in orange). These observations, along with the results obtained using the covariance matrix and distance calculations, allows us to conclude that Kalman filter is the most suitable solution to filter the acquired data obtained from Microsoft Kinect's skeleton tracking system.

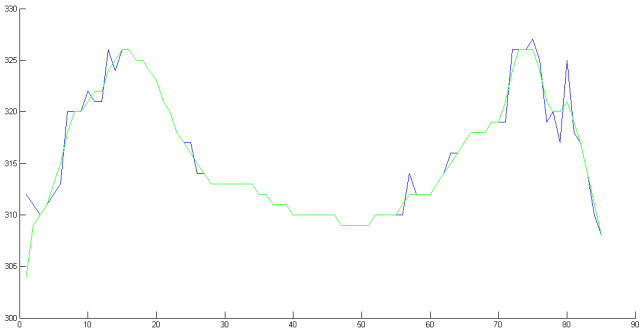

(a) X coordinates of the Left Wrist for original signal (blue) and signal after Kalman filter processing (green)

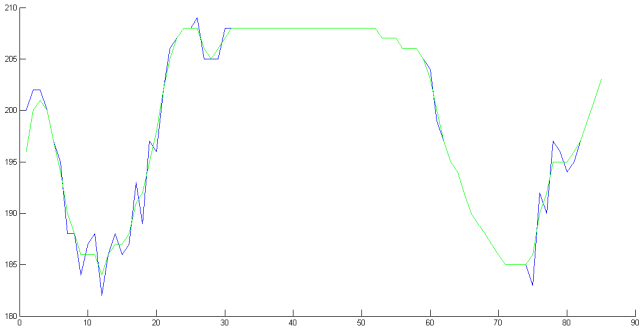

(b) X coordinates of the Right Wrist for original signal (blue) and signal after Kalman filter processing (green)

Figure 6.9: Original signals acquired using Skeleton Tracking System of Kinect and subsequently processed with a Kalman filter

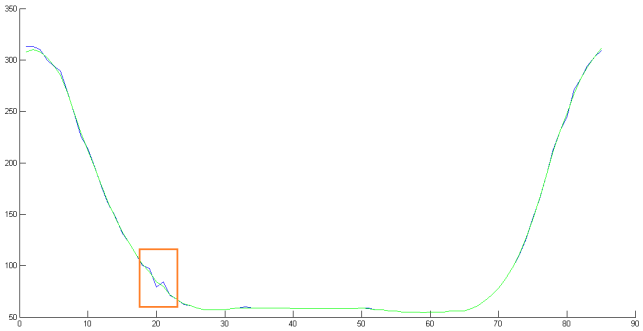

Figure 6.10: Signals with reduced noise acquired using Microsoft Kinect (blue) and subsequently processed with a Kalman filter (green)

6.1.3 Features extraction based in Skeleton data

After the selection of the filter, it was necessary to define the features that were acquired. As seen in Table 4.1, Exercise 4 has different characteristics from the remaining exercises, since it is a repetitious exercise and can be clearly divided in two phases. However, this is only possible by performing further processing for this Exercise, as explained below. After that, it is possible to apply similar algorithms to extract the features, as explained in the remaining chapter[1]. In order to normalize the features, a ratio between the two arms is performed for each feature. These ratios will be then used to classified the patient condition (Chapter 7).

Processing methodology in Exercise 4

Exercise 4 can be divided in two clear phases: a first one when the arm is ahead of the body (In red/dashed in Figure 6.11), and a second one when the arm is behind (in Green/Solid in Figure 6.11). These two phases are independent and have different characteristics that can be extracted.

Figure 6.11: Exercise 4 and the two independent phases present

The first step consists in differentiating the two phases in the exercise. These phases can be divided when the arm is parallel to the body, i.e., when the coordinate Y of the wrist reaches its minimum. Initially, the local minimums for all exercises are obtained (Section of the green/dashed signal highlighted in red in Figure 6.12), as well as the absolute minimum for the wrist in the Y-axis. After that, local minimums are compared with the absolute minimum and are selected using a nearest criteria.

[1] All images are adapted from http://hippie.nu/ unicorn/tut/img/basics/humananatomy/human-proportion2.jpeg

The second step consists in classifying the two phases of the exercise. This is possible using the values of the X-axis also in the wrist. So, if between the previously defined peaks, the coordinate X of the wrist reaches a local minimum (Phase 1 and 3 in Figure 6.12), the arm is placed ahead of the rest of the body. On the contrary, if there is a local maximum between the minimum peaks of coordinate Y (Phase 2 and 4 in Figure 6.12), the arm is behind the rest of the body.

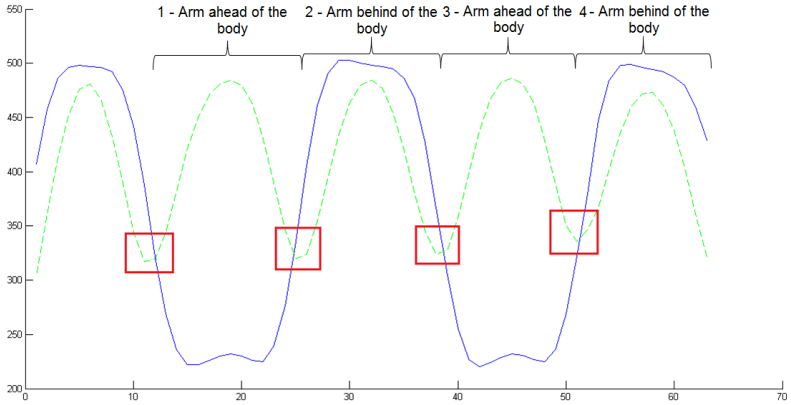

Figure 6.12: Division of Exercise 4 in the two phases. Coordinate Y of the wrist in green/dashed signal and coordinate X of the wrist in blue/solid signal

This differentiation allows calculate different features for each phase. So, and since the exercise was a repetitive nature, for each phase is computed the mean. A diagram representing the method can be found in Figure 6.13.

6.1.3.1 Elbow Height

An important factor to detect reduced mobility is the detection of the height that the shoulder reaches during the movement. This can be obtained by using the Y coordinates of the elbow during the movement, and then computing the maximum reached by each elbow (Red/dashed line in Figure 6.14a).

6.1.3.2 Wrist Height

Similarly to shoulder height, the maximum of each wrist during the exercise is computed. This feature may seem redundant, however, due to the nature of the exercises, it can be relevant since it enables a different characterization of the movement (Green/solid line in Figure 6.14a).

6.1.3.3 Elbow Width

This feature is only computed in Exercise 4, and is calculated using the values of the X coordinates. With this feature, it is possible to understand the arm's range. If the arm is ahead of the body, the minimum of the coordinates X is calculated, whereas if the arm is behind the body, the maximum is computed (Green/solid line in Figure 6.14b).

[2]http://www.visual-paradigm.com/

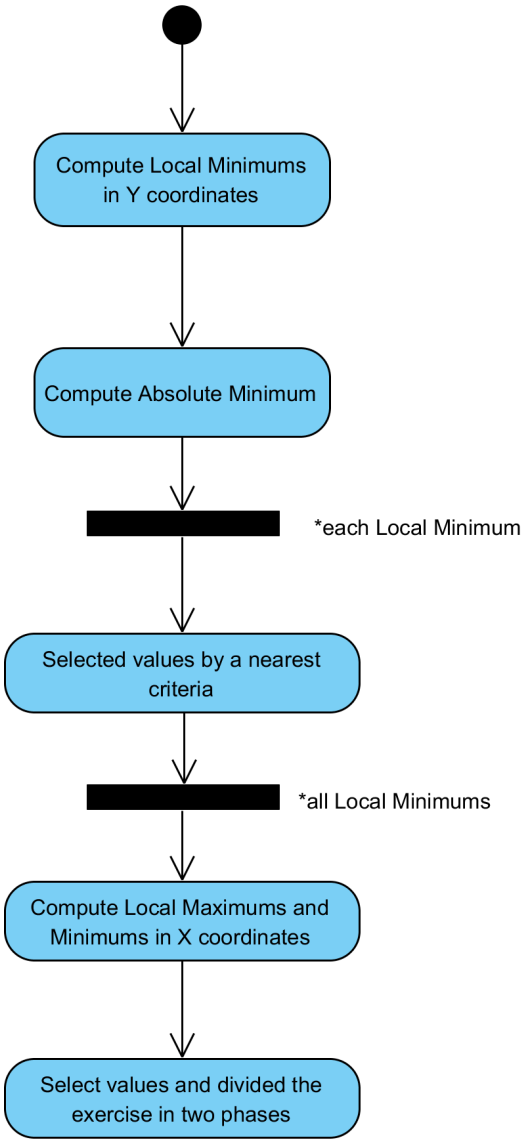

Figure 6.13: Flowchart of processing in Exercise 4 (using Visual Paradigm [2])

6.1.3.4 Wrist Width

This feature is also computed only for Exercise 4 and has a similar purpose to that of shoulder width (Red/dashed line in 6.14b).

6.1.3.5 Range of Motion

Decreased shoulder range of motion is a common consequence observed in patients with problems on upper-limb mobility. This can be calculated by the angle between the shoulder and the elbow (Angle represented in green in Figure 6.14c). To compute this feature, the X and Y coordinates must be obtained both for the shoulder and elbow during the exercise. After that, the angle between

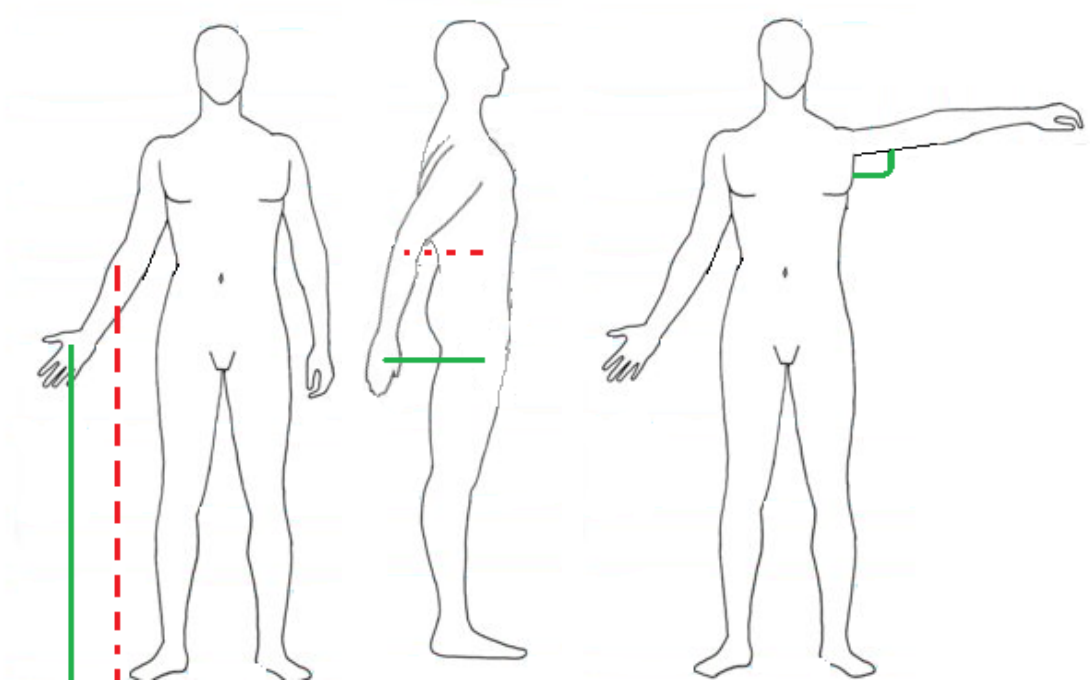

(a) Elbow (red/dashed line) and wrist (green/solid line) height

(b) Elbow (red/-dashed) and wrist (green/solid) width

(c) Range of Motion in green

Figure 6.14: Exemplification of features acquired

these two points is computed for each frame, finishing with the determination of the maximum for each arm (Equations 6.6-6.8).

This is a very important feature in Exercise 2, since it can be related with abduction measurements obtained in medical environment using a goniometer.

$$X_{\Delta coor} = X_{shoulder} - X_{elbow} \tag{6.6}$$

$$Y_{\Delta coor} = Y_{shoulder} - Y_{elbow} \tag{6.7}$$

$$RoM = max(\arctan({}^{Y_{\Delta coor}}/_{X_{\Delta coor}})) \tag{6.8}$$

6.1.3.6 Elbow Flexion

Elbow flexion is a relevant feature as it lets us understand how the patient tries to compensate some difficulty in the movement during the exercise. Furthermore, it is even more relevant in Exercise 1, since that exercise is designed to reach the minimum angle possible.

Using X and Y coordinates for each arm's shoulder, elbow and wrist, the angle can be computed. After that, the minimum is selected for each arm (Angle in Green in Figure 6.15a), using Equations 6.9-6.15 .

$$X_{\Delta coor1} = X_{shoulder} - X_{elbow} \tag{6.9}$$

$$Y_{\Delta coor1} = Y_{shoulder} - Y_{elbow} \tag{6.10}$$

$$ang_1 = (\arctan(Y_{\Delta coor1}/X_{\Delta coor1})) \tag{6.11}$$

$$X_{\Delta coor2} = X_{elbow} - X_{wrist} \tag{6.12}$$

$$Y_{\Delta coor2} = Y_{elbow} - Y_{wrist} \tag{6.13}$$

$$ang_2 = (\arctan(Y_{\Delta coor2}/X_{\Delta coor2})) \tag{6.14}$$

$$ElbFlex = min(180 - ang_1 - ang_2) \tag{6.15}$$

6.1.3.7 Duration of the Exercise

Another important feature to take into account is how much time the patient takes to perform the different exercises. Firstly, the end of the exercise is determined using other features (for instance, in Exercise 1, this can be done by detecting when elbow flexion reaches its minimum). Then, the samples between this point and the nearest starting point (defined as the nearest local minimum) is calculated.

In order to reject local minimums during the exercise, whose cause is due to sudden movements or other artefacts, a Gaussian filter is used to filter data in this feature.

6.1.3.8 Velocity of the movement

An important factor that can indicate motion problems is the velocity at which the exercise is performed. To compute this feature, the coordinates of the wrist are considered, since they have the biggest variation during movement execution. Using X and Y coordinates, the variation of the position between each frames is measured, using Equation 6.16.

$$v[n] = \sqrt{(x[n]^2 - x[n-1]^2) + (y[n]^2 - y[n-1]^2)} \tag{6.16}$$

To reduce noise generated from the environment and small body movements, a low-pass filter is used with a cut-off frequency of 2 Hz. After that, maximum velocity is determined during the Time of Exercise previously calculated.

6.1.3.9 Accelaration of the movement

Using velocity's results, it is possible to obtain the instantaneous acceleration throughout the exercise, by applying Equation 6.17. After that, there is a selection of the maximum acceleration of movement during the time of exercise.

$$a[n] = Vinst[n] - Vinst[n-1] \tag{6.17}$$

6.1.3.10 Compensatory Movement

During exercise execution, some patients tend to compensate some problems in the performance by inclining their body. To understand if this is due to problems in arm mobility, it is necessary to compute some compensatory movements that the patient may perform during the exercise.

Using the X coordinates of the hip and shoulders' centre (Green/solid line in Figure 6.15b) it is possible to understand if the patient performs some compensatory movement during the exercise. For that, a ratio between these two values is computed during the exercise, and the maximum is obtained.

6.1.3.11 Inclination

Due to its specific characteristics, Exercise 4 is performed with some inclination between hip and shoulder (in red in Figure 6.15c). This inclination is determined for each phase by computing the difference of the X coordinate between Shoulder and Hip, since it is related with the inclination.

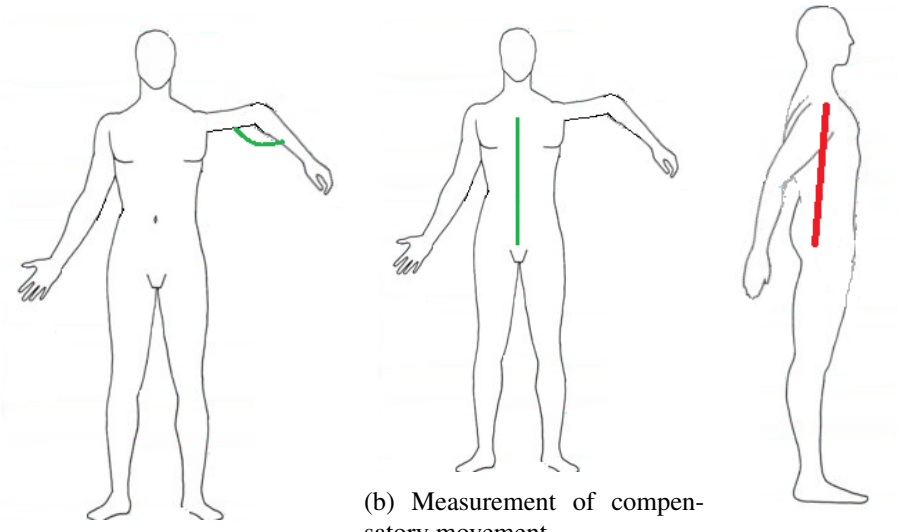

(a) Elbow Flexion in green

(b) Measurement of compensatory movement

(c) Inclination

Figure 6.15: Representation of features acquired

6.1.3.12 Angle Hip-Shoulder-Wrist

This feature is also specific to Exercise 4. For each phase of the exercise, the angle between the hip, shoulder and wrist is calculated for each frame, using X and Y coordinates of these joints. After that, the maximum angle of each phase of the exercise is computed (Line green in Figure 6.16).

These two angles are very important, since they are determined in medical conditions using a goniometer and can be related with these (flexion when the arm is ahead of the body and extension when the arm is behind).

Figure 6.16: Representation of the angle between hip-shoulder-wrist

6.1.4 Summary

Table 6.11 summarizes feature acquisition for each exercise and numbers that are attribute. Important to notice that Exercise 4 has two phases.

Table 6.11: Summary of features extracted using Skeleton Tracking System Data

	Exercise 1	Exercise 2	Exercise 3	Exercise 4	Exercise 5
Elbow Height	1	8	15		37
Wrist Height	2	9	16		38
Elbow Width				24 & 25	
Wrist Width				26 & 27	
Range of Motion	3	10	17		39
Elbow Flexion	4		18	30 & 31	40
Duration of the Exercise	5	11	19	32 & 33	41
Velocity	6	12	20	34 & 35	42
Acceleration	7	13	21	36	43
Compensatory Movement Hip-Shoulder		14	22		44
Inclination				23	
Angle Hip-Shoulder-Wrist				28 & 29	

6.2 Based on RGB-D Data

Volume is an important feature, since lymphedema is characterized by an arm swelling that can be perceived using volume measurements. Therefore, in addition to the features extracted using the exercises which have already been described, an exercise was performed to estimate volume of both arms (Figure 4.8). For that, depth and colour images were used, complemented with data from the skeleton tracking system.

Volume estimation from this data can be performed using different methodologies. In this work, three methodologies were used:

- Based in depth map data (Method 1)
- Segmentation using Skeleton based mask applied in colour images (Method 2)
- Segmentation based in depth map mask applied in colour images (Method 3)

6.2.1 Based in depth map data

This methodology leads to the creation of a region where the volume will be calculated. Also, this mask is used further used to perform segmentation in colour images, as will be further explained. This methodology can be divided in 4 phases:

- Depth-map noise reduction
- Kinect Rotation Compensation
- Patient Segmentation
- Arm Segmentation

6.2.1.1 Depth-map noise reduction

Using its IR projector and camera sensor, Kinect is able to capture depth maps of the surrounding environment. However, this data has noise-related issues, due to the limited working distance of the camera, occlusions, multiple reflections, transparent objects or scattering in particular surfaces. This leads to regions were data is undefined. To solve this problem, it is necessary to understand where these unresolved points are and how to correct them.

One possible approach is the depth hole filling strategy, described in the work of Yang *et al.* [138]. Firstly, depth holes are recognized, allowing the construction of a binary image with the position of these holes (Figure 6.17a). After that, these regions are labelled by 8-connectivity, and the resulting blobs are dilated using a 5x5 diamond structural element (Figure 6.17b). The initial labelled image is then subtracted from the dilated image, calculating the boundary of the bold, as can be seen in Figure 6.17c.

Thereon, the boundary's histogram is computed, and the dominant peaks are detected (peaks are considered dominant peaks if they have more than 5% of the pixels of the considered region).

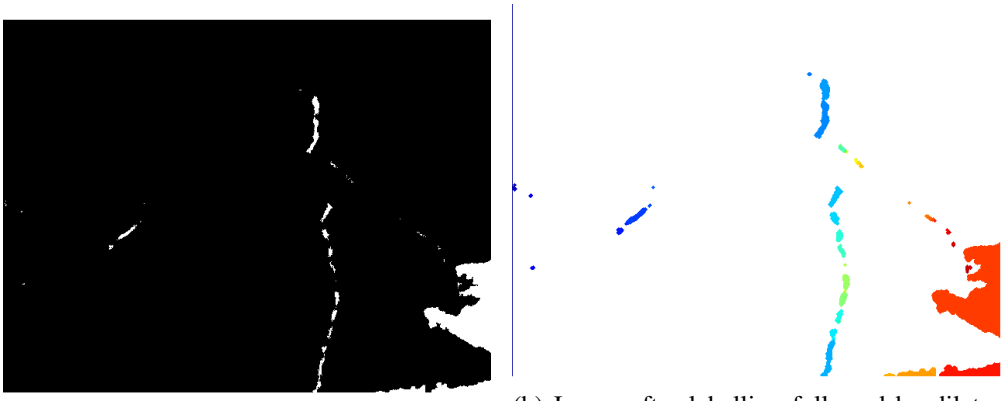

(a) Image after depth holes recognition

(b) Image after labelling followed by dilatation

(c) Resulting image with the boundary's of depth holes

Figure 6.17: Methodology to detect the boundary's of depth holes in Patient 33

Then, a threshold is defined as the average of these dominant peaks, and the unresolved regions are filled with a median of the values greater than the calculated threshold. This is possible since it can be assumed that the neighbours of depth holes' regions have valid information for the filling purpose [138].

However, noise problems in depth images, mainly in boundary regions, are not resolved. A possible solution for this problem is using a bilateral filter (Figure 6.18), since it is a non-iterative, local, and relatively simple method. This filter combines a domain kernel (σ_d), that gives higher weight to pixels closer to the target pixel, and a range kernel (σ_r), that gives higher weight to pixels similar to the target pixel [139]. Hence, in smooth regions, since the target pixel is similar to its neighbourhood, bilateral filter acts as standard domain filter and averages away the small, weakly correlated differences between pixel values caused by noise. However, if a boundary between two regions with very different intensities is considered, and the bilateral filter is centred in the brighter region, the target pixel will be substituted by an average of the bright pixels in its vicinity, disregarding the darker region. To understand the best parameterization of the bilateral filter, the three parameters were varied, achieving the best result for σ_r = 5, σ_d = 15 and with a 15x15 window.

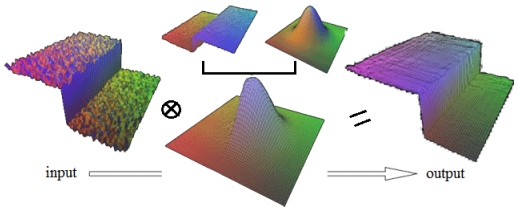

Figure 6.18: Bilateral filter: the shape of the Gaussian kernel is dynamic based on difference of pixel intensity. Adapted from [140]

6.2.1.2 Kinect Rotation Compensation

To ensure correct volume determination, it is important to have the patient parallel to the Kinect sensor when performing the acquisition. Nonetheless, this parallelism can be difficult to obtain in medical environment. As previously explained (Chapter 4.4), this problem was noticeable during the acquisitions. On the other hand, it is easier to ensure that the patient is parallel to the wall.

It is also important to ensure this positioning, as the angle between the Kinect sensor and the patient can be compensated by the rotation of the depth map during processing. For this purpose, the distance between the Kinect sensor and the wall above the hands must be calculated. Since the wall is at the same distance in these two points (X_1 and X_2), and knowing the distance that the depth data has, it is possible to obtain the angle of rotation (θ in Figure 6.19).

Knowing the width between these two points, it is possible to calculate a central point where the image has to be rotated. Depth data for each point between the two hands can then be updated, using for that purpose equation 6.18

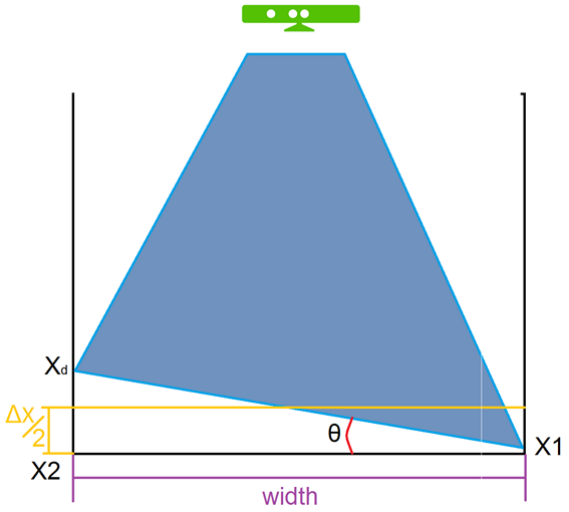

Figure 6.19: Method used to compensate the Kinect rotation

$$I_{Fin}(y,x) = I_{Ini}(y,x) - \frac{depth_{dif}}{2} + x \times \tan(\theta) \tag{6.18}$$

6.2.1.3 Patient Segmentation

The image captured by Kinect is usually composed of background and patient. However, this data can have other non-desirable objects present. These objects can influence patient segmentation, since traditional thresholding methods are affected by its presence. Accordingly, to perform patient segmentation, it is necessary to obtain, initially, the depth information for the joints present in the image, that are defined using the skeleton tracking system, since with this information it is possible to understand the body's depth value.

After this assessing, a double threshold is defined using the maximum and minimum intensity values of these points. However, some points of the body can be considered background when using such a rigid threshold. To solve this problem, a margin of 5% is considered for the maximum and the minimum, defining the final threshold to segment the patient.

To ensure that no small holes are present in the segmented image, a fill holes filter is applied. Finally, to obtain a smoothed body shape, a median filter with a window size of 11x11 is used. This method can be seen in Figure 6.20

(a) Image after thresholding (b) Image after fill holes filter (c) Image after median filter

Figure 6.20: Patient Segmentation method for patient 26

6.2.1.4 Arm Segmentation

To perform a correct volume assessment it is important to define the region of interest - the upper-arm - that is defined superiorly by the shoulder, inferiorly by the elbow and communicates medially with the axilla [13]. Therefore, there are five points that define the region: the armpit (A1), the medial (E1) and lateral (E2) elbow point, and the medial (S2) and lateral shoulder point (S1) (Figure 6.22).

To compute these points, a dilatation is firstly performed using a morphological dilation of the segmented portion of the image, using a 3x3 structuring element. After that, an exclusive disjunction between the dilated image and the segmented image is performed to obtain the silhouette (Figure 6.21).

Armpit detection

To detect the A1 point, the algorithm searches for the points below the shoulder that are obtained using the skeleton tracking system, since the A1 point will always be beneath Kinect's shoulder

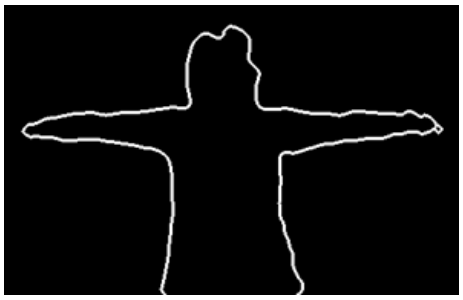

Figure 6.21: Silhouette obtained for Patient 26

joint. After that, the point of the silhouette that is the closest to this point is selected and considered the armpit.

Medial elbow detection

E1 is calculated by searching for the points obtained by the skeleton tracking system that are in close proximity to the elbow. However, some restrictions are applied to guarantee a correct selection of E1, such as considering points valid only if the line segment $\overline{A1E1}$ does not intersect $\overline{SE}$.

Lateral elbow detection

Firstly, the line between $\overline{SE}$ and its slope is computed. After that, a line perpendicular to this segment that contains E1 is computed. Finally, the point of the silhouette that contains this line and is situated above E1 is determined. In order to choose a valid E2 it must be guaranteed that $\overline{SE}$ intersects $\overline{A1E2}$.

Lateral shoulder detection

The algorithm starts off by computing the line that contains E1 and E2. After that, a parallel line is drawn that must pass the shoulder's point obtained by the skeleton tracking system. The point of the silhouette that contains this line is selected. To ensure that this point is correct, $\overline{S2E1}$ and $\overline{SE}$ must intersect.

Medial Shoulder Detection

In order to determine S2, the point of intersection between $\overline{E1A1}$ and $\overline{S2S}$ must be computed.

This process is repeated for each image in both arms. Example of this method is present in Figure 6.22. After that, the obtained masks are compared with the marked mask (Chapter 6.2.5).

6.2.2 Segmentation using Skeleton based mask applied in colour images

As explained previously, the depth map has several noise problems that can affect results. Even with methodologies specifically drawn to reduce its impact, this problem can still interfere with

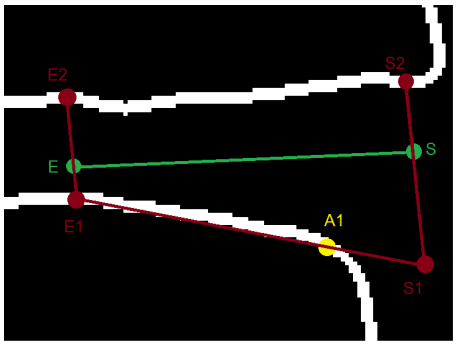

Figure 6.22: Arm segmentation

boundary detection. In colour data these problems are minimized, since the acquisition does not have unresolved points. Nevertheless, segmentation in this dimension can be challenging, even more in environments where there is little control of background and possible objects' colours.

Grab Cut is an interesting approach to solve this problem, since it combines texture information and edge information to obtain the segmented imagem [141]. This method was created by a team from Microsoft Research Cambridge and needs a mask to be initialized by the user. This mask can have 4 values: 0 for certain foreground, 1 for certain background, 2 for possible foreground and 3 for possible background. After that, the algorithm estimates colour distribution on the foreground and background using a Gaussian mixture model. This allows the construction of a Markov random field over the pixel labels, being the remaining pixels classified using an energy function. These two steps are repeated until convergence.

In this method, the mask to use in GrabCut is computed using information from Skeleton Tracking System and has two values: possible foreground and possible background. The segment between the elbow and shoulder is labelled as possible foreground and the rest of the image as possible background (Figure 6.23a)). The resultant mask is then converted and applied to colour image (Figure 6.23b)). Then, segmentation in colour dimention is performed, resulting in a binary image with foreground and background (Figure 6.23c)).

(a) Mask used (b) RGB image to segment (c) Segmentation result

Figure 6.23: Methodology of Method 2 for Patient 1

After that, the segmented image is converted to depth dimension and arm segmentation is performed using the method explained in 6.2.1.4.

6.2.3 Segmentation based in depth map mask applied in colour images

This methodology is similar to the previous explained, since segmentation is also done in colour images using GrabCut. However, in this segmentation the mask used was not from Skeleton data but is the final mask computed by methodology only based in depth map data, with values of segmented arm being labelled as possible foreground and the rest of the image as possible background (Figure 6.24a)). This mask is then converted to colour dimension and was used a Grab Cut algorithm to segment the colour image (Figure 6.24b)), which results in a binary image with the segmentation of the patient (Figure 6.24c)).

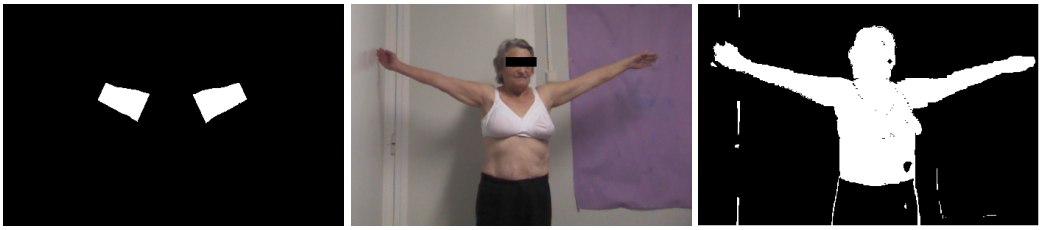

(a) Mask used (b) RGB image to segment (c) Segmentation result

Figure 6.24: Methodology of Method 3 for Patient 17

After that, the segmented image is converted to depth dimension and arm segmentation is performed using the method explained in 6.2.1.4.

Summary

Segmentation methods are resumed in Figure 6.25.

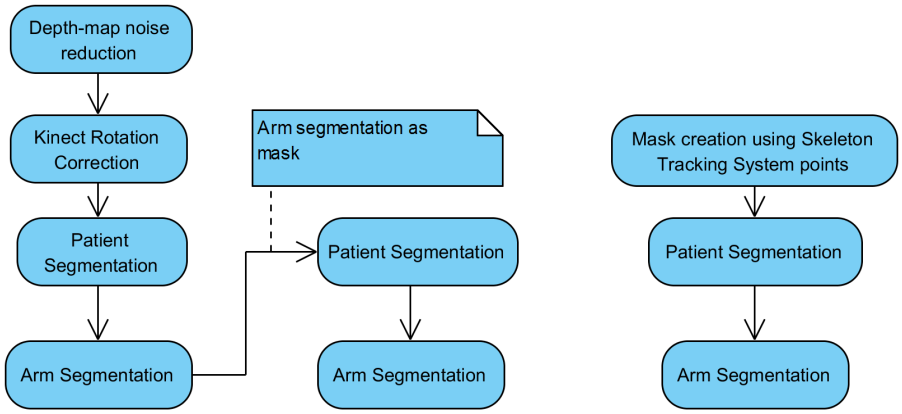

Figure 6.25: Flowchart of arm segmentation for all 3 methods

6.2.4 Comparison of segmentation methods

To study the best segmentation method, a subset of 20 patients was arbitrarily selected and, on these, manual masks of the upper-arm were constructed. Dice coefficient and Jaccard Index were

then computed between manual masks and masks obtained through the three methods, enabling the evaluation of the segmentation methods. Manual masks were created in colour dimension and then convert to depth dimension, to ensure a more precise annotation.

Dice coefficient measures the extent of spatial overlap between two binary images, giving a higher weight to instances where the two images agree. Its values range between 0 (no overlap) and 1 (perfect agreement), and it is calculated using Equation 6.19.

$$D = \frac{2|A \cap B|}{|A| + |B|} \tag{6.19}$$

Jaccard Index measures similarity between finite sample sets, and is computed by the number of shared attributes, divided by the total number of attributes present in either of the sample sets. Its values range between 0 (no similarity) and 1 (equal) and it is calculated using Equation 6.20].

$$J = \frac{|A \cap B|}{|A \cup B|} \tag{6.20}$$

Results can be found in Table 6.12.

Table 6.12: Dice coefficient and Jaccard Index results of arm segmentation for three methods

	Method 1	Method 2	Method 3
Dice coefficient (D)	0.794	0.721	0.724
Jaccard Index (J)	0.672	0.635	0.642

Considering the results presented in Table 6.12, the best segmentation process is that which uses only depth data, showing a good overlapping between ground truth and the detected arm. Also, the lower results for segmentation when using Colour data are due to problems in segmentation by using GrabCut, as can be seen in Figure 6.26.

Figure 6.26: Problems in patient segmentation using GrabCut method for Patient 47

Furthermore, it is important to refer that manual segmentation is harder to control and is operator-dependent. To minimize this error, only one operator was used to correct the manual segmentation that was performed. A comparative analysis between manual segmentation and segmentation using the three methods can be found in Figure 6.27.

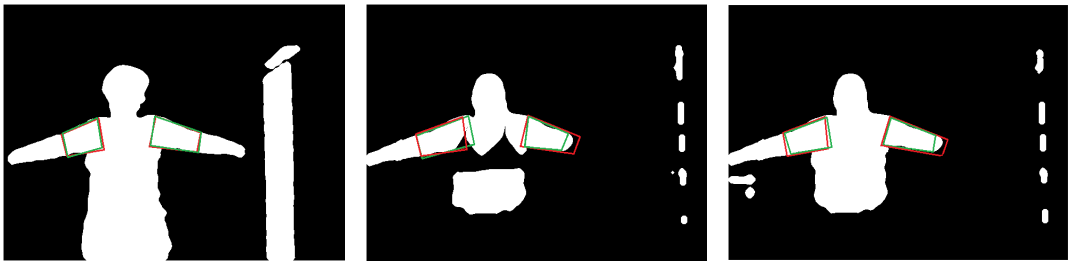

(a) Method 1 (b) Method 2 (c) Method 3

Figure 6.27: Arm contour detection examples for the three methods. Detected contour (red) and ground truth (green)

Therefore, in order to estimate the volume of each patient, the depth methodology was chosen.

6.2.5 Volume Estimation

After performing the arm segmentation, it is necessary to calculate the volume of the arm. For this approach colour and depth data is used, and applying the mask that was previously created, it is possible to compute the point cloud of each arm. Then, a convex hull algorithm is used on the set of computed points. Convex hull tries to find the smallest convex set that contains all the points, allowing the creation of a solid containing all the points of the arm (Figure 6.28).

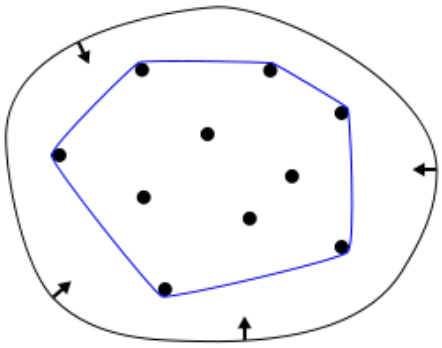

Figure 6.28: Demonstration Convex Hull algorithm behaviour[3]

To validate this approach, two acquisitions of objects with known volume were performed, and the real volumes were compared with the values obtained through this approach. Since we are working with arms, the two selected objects were a truncated cone and a cylinder, since its geometry is similar. The volume of these two solids was calculated by placing them in a container full of water and then measuring the volume of water that overflowed. Then, acquisitions with

[3]https://upload.wikimedia.org/wikipedia/commons/thumb/d/de/ConvexHull.svg/258px-ConvexHull.svg.png

Kinect were performed, and a methodology similar to the one that was previously explained was performed to improve and correct depth data. Next, object segmentation was performed manually in colour images which were transformed to the depth dimension. Results are presented in the Table 6.13.

Table 6.13: Volume validation for known objects

	Cylinder	Truncated Cone
Real Volume	1.92	0.103
Algorithm Calculation	1.79	0.085
Ratio	0.895	0.825

Firstly, it is important to refer that the algorithm's calculation only computes half of the object's volume, which can be a source of errors in the calculation, since it was considered that the other half was symmetric. Furthermore, depth data used in the segmentation procedure has some unresolved points that were estimated using information from their vicinity. This can also be a source of problems, since it leads to an incorrect estimation. Also, the conditions where the acquisitions were performed were not the most correct ones, in order to simulate the conditions where medical acquisitions were performed. Finally, segmentation of the object is subjected to errors, since it was performed manually.

Results showed some difference between the real value and the calculated one, which was expected. However, the differences were similar between the two objects, and should be minimized when the ratio between the volumes of both arms is computed.

Volume estimation methodology

To volume estimation, 40 images were selected for each patient (20 of depth data and 20 of colour data). The methodology of arm segmentation using method 1, followed by volume calculation, was performed in these images. Only values within a range of 40% of the median of each patient were considered, in order to discard possible outliers. Then, the mean value of the remaining values for each arm was obtained, and their ratio was computed. Volume ratio between the two arms was the 45^{th} feature extracted. An example of a point cloud created using this methodology is present in Figure 6.29

Figure 6.29: Example of point cloud created using the methodology for volume estimation

6.3 Conclusion

Feature extraction can be based in two sources: skeleton tracking system data and RGB-D data. Processing of these two types of data is distinct. Regarding the skeleton tracking system, filter processing is a must due to the presence of noise in the signal. With that in mind, a method for filter selection was created and tested, with results leading to the selection of Kalman filter. The following step was to define, for each exercise, a selection of features to be extracted that could characterize patient's movement.

RGB-D data was used for volume estimation. For that purpose, three methods were tested to understand which one resulted in a more accurate arm segmentation. Of the three tested methods, the method using only depth information was the one that showed better results. After selecting the method, volume estimation was performed. To understand if volume estimation was susceptible to errors, the method was used in known objects, with good results being obtained.

Chapter 7

Classification Models

Classification can be described as the problem of assigning an observation one from a set of classes, using a set of features from this new observation. This can be achieved by using classification models, which are a very important method to create an objective procedure to evaluate upper-body function, since it enables the creation of a gold standard with which future measures can be compared with.

In this work, patients were divided in several classes, as explained in Chapter 5, and machine learning techniques are applied to create predictive classifications models. In this work we used the following supervised learning classifiers:

- Fisher Linear Discriminant Analysis (LDA)
- Naïve Bayes Classifier
- Support Vector Machines (SVM)

Furthermore, due to the high number of extracted features, feature selection is tested.

7.1 Classification Models tested

7.1.1 Fisher Linear Discriminant Analysis

Using linear combination of the variables, LDA tries to find which combination best separates two or more classes. In order to do that, data is projected on a line and classification occurs in this one-dimensional space. The best projection is the one that maximizes the distance between the classes' means and minimizes variance within each class [142].

For instance, there are two classes with n_1 samples and n_1 samples, respectively. LDA finds the projection that maximize J_w, which is the ratio of between-class S_B and within-class scatter matrices S_w. Sample mean is defined by Equation 7.4.

$$J_w = \frac{w^T S_B w}{w^T S_W w} \tag{7.1}$$

$$S_B = (m_1 - m_2)(m_1 - m_2)^T \tag{7.2}$$

$$S_w = \sum_{i=1,2} \sum_{x \in C_i} (x - m_i)(x - m_i)^T \tag{7.3}$$

$$m_i = \frac{1}{n_i} \sum_{x \in C_i} x \tag{7.4}$$

So, assuming that S_w is a non-singular matrix, Equation 7.5 describes an analytical expression for w which maximizes J_W. This allows the calculation of the optimal projection direction w that results in the best separation between two classes as possible.

$$w = S_w^{-1}(m_1 - m_2) \tag{7.5}$$

7.1.2 Naïve Bayes Classifier

This classifier is based on Bayes' theorem, assuming that the pair of features is conditionally independent. This classifier can be described as a simple probabilistic classifier that, given a class variable y with two classes y_1 and y_2 and a dependent feature vector, these two can be related by Equation 7.6:

$$p(y|E) = \frac{p(y)p(E|y)}{p(E)} \tag{7.6}$$

E is then classified as from class y_1 if:

$$f_b(E) = \frac{p(y = y_1|E)}{p(y = y_2|E)} \geq 1 \tag{7.7}$$

Also, and since its classification is based on a naïve independence approach, the end result is calculated by:

$$f_b(E) = \frac{p(y = y_1)}{p(y = y_2)} \prod_{i=1}^{n} \frac{p(x_i|y = y_1)}{p(x_i|y = y_2)} \tag{7.8}$$

7.1.3 Support Vector Machines

SVM are based in decision planes that define decision boundaries, corresponding to hyperplanes in the feature space which separate the classes. The best hyperplane is the one that separates data of two different classes with the largest margin. SVM has its name due to the support vectors,

which are the data points closest to the separating hyperplane. This method only uses these points since they are the most difficult samples to classify (Figure 7.1).

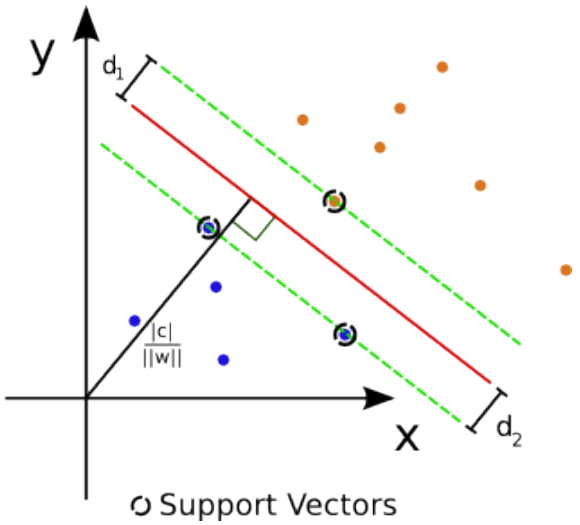

Figure 7.1: Separating hyperplane and margins for an SVM trained with two classes samples. Samples on the margin are called the support vectors (From [143])

SVM also works in nonlinear conditions. In these, and since it is not possible to find a hyperplane that separates perfectly the two classes' points, the method calculates the hyperplane that separates the most data points, seeking to obtain the largest margin while maintaining data misclassification to a minimum [144]. In order to accomplish that, a penalty for misclassifying is added to the objective function through a weight identified as C. In this case, we are in the presence of a C-SVM classifier that, given a higher C, tries to avoid misclassification.

The computation of large margin decision boundaries allows a classification less prone to overfitting, which occurs when a model performs well on the training dataset, but fails to generalize its performance in non-trained data.

7.2 Feature Selection

Due to the high number of features being extracted, feature selection must be performed. Three feature selection methods were tested, in order to understand which jeopardized less the classification results. It is important to note that classification results will probably still be harmed, since feature selection can lead to local minimums, which is not the best classification result (absolute minimum).

The three used methods are further explained and consist in:

- Mutual information
- Sequential Floating Forward Selection (SFFS)
- Foward Selection

A pre-feature selection for all three methods was also tested, in order to understand if it was possible to obtain better results when compared with results for all 45 features extracted. To do this, for each exercise, a correlation matrix was computed with all features. Then, the pairs of features with dependence higher than 0.5 were selected (values in yellow in example Table 7.1). For each feature encompassed in these pairs, its average variance with the remaining features (values in green in example Table 7.2) was computed (values in blue in example Table 7.2), being the feature with the lowest average variance selected. When computing a given feature's average variance, its value in the main diagonal was discarded, as well as the variance value of the feature with its pair. The remaining variances, which relate the given feature with the remaining features, were considered in the computation of the average value. Eliminated features are highlighted in red in Table 7.3.

Table 7.1: Selection the pairs of features with variance higher than 0.5 (Example)

	X1	X2	X3	X4
X1	1	0.3	0.35	0.45
X2	0.3	1	0.2	0.7
X3	0.35	0.2	1	0.15
X4	0.45	0.7	0.15	1

Table 7.2: Selection of the best feature using lowest avarage variance (Example)

	X1	X2	X3	X4	
X1	1	0.3	0.35	0.45	
X2	0.3	1	0.2	0.7	0.25
X3	0.35	0.2	1	0.15	
X4	0.45	0.7	0.15	1	
				0.3	

Table 7.3: Eliminated feature (Example)

	X1	X2	X3	X4
X1	1	0.3	0.35	0.45
X2	0.3	1	0.2	0.7
X3	0.35	0.2	1	0.15
X4	0.45	0.7	0.15	1

Afterwards, the same methodology was performed inter-exercise for the remaining features, leading to a final set.

7.2.1 Mutual Information

This method is based on Perez et al. [145], method, based in Naïve Bayes classifier (Chapter 7.1.2), maintaining the strong conditional independence assumption and searching in the space of possible structures guided by estimated accuracy.

Mutual information can be computed using Equation 7.9, where C is a multinomial random variable with r possible values and a probability distribution given by $P(C = c) = P(c)$. X is a random variable with a normal density function of parameters μ and σ^2. Assuming that X conditioned to $C = c$ follows a normal density with parameters μc and $\sigma^2 * c$, the mutual information between variables X and C is given by [145]:

$$I(X;C) = \frac{1}{2}[\log(\sigma^2) - \sum_{c=1}^{r} P(c)\log((\sigma_c))^2] \tag{7.9}$$

After computing mutual information, variables (features) are sorted from highest to lowest and are inserted, one at a time, in the classifier.

7.2.2 Sequential Floating Forward Selection

Being considered an extension of Sequential Forward Selection (SFS), the algorithm starts with an empty feature subset and adds features to the subset until the desired size is reached. For that, in each iteration, the subset is evaluated using a criterion function that leads to the maximum improvement in performance. Nonetheless, SFFS differs from SFS, as it allows the removal of features included in the subset, using for that intent a conditional exclusion that only acts when the resulting subset performs better using the criterion function after the removal of a particular feature [146, 147].

Initially, the algorithm starts with an empty subset of features so that $k = 0$ (where k is the size of the final subset) and Y is the set of initial features:

$$Y = y_1, y_2, ..., y_d \tag{7.10}$$

After that, features are included in the subset using a criterion function.

$$x^+ = arg\ max\ J(x_k + x)\ with\ x \in Y - X_k \tag{7.11}$$

$$X_k + 1 = X_k + x^+ \tag{7.12}$$

$$k = k + 1 \tag{7.13}$$

$$x^- = arg\ max\ J(x_k - x)\ where\ x \in X_k \tag{7.14}$$

$$if\ J(x_k - x) > J(x_k - x):$$

$$X_k - 1 = X_k - x^-$$

$$k = k - 1$$

$$end$$

These two steps are repeated until k reaches the value of the intended final subset.

7.2.3 Foward Selection

Foward Selection is a simple algorithm used to perform feature selection. Firstly, the error associated with the classification of one feature is computed. This feature (Feature A) is then kept and a new subset of features is formed by the combination of Feature A with the remaining ones. The error of all these combinations is computed, and the best combination is fixed. The process continues until maximum subset size is reached.

7.2.4 Summary

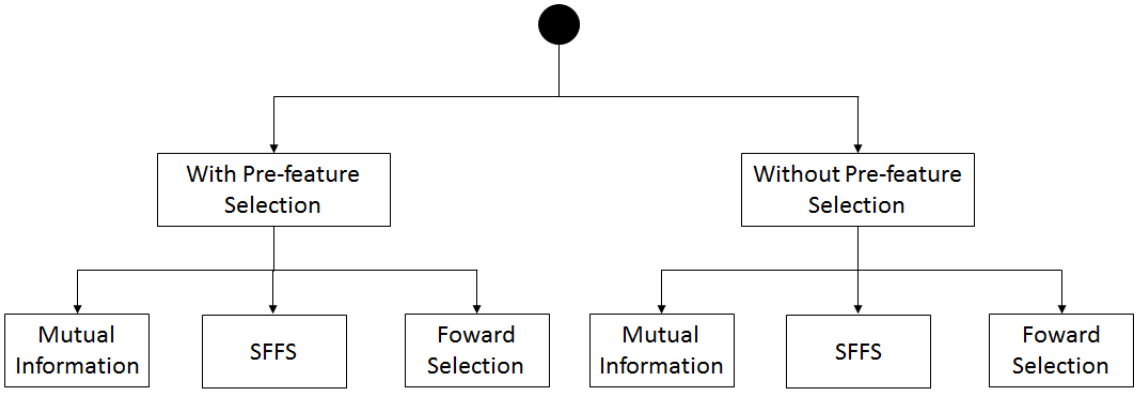

Figure 7.2: Feature Selection methodology

7.3 Classification Results

Classification models were designed for the subsets obtained through feature selection, using a Leave One-Out scheme [148]. All outputs were trained using the three previously described classifiers. SVMs' training can have different parameterizations, as explained below:

- Kernels: Linear, polynomial (with order varying from 2 to 6) and radial basis function (rbf) (varying y with the following values: 0.25, 0.5, 0.75 and 1).
- Exponential growing sequences of C, from C=2^{-2} to C=2^{6}

For each type of classifier that was described, the number of features that led to the lowest misclassification in each output is presented. In the cases where more than one subset of features obtained minimum misclassification, the model with less complexity was chosen.

Features and classifiers' parameters that led to the selection of the best classifier for each output are presented. Moreover, chosen classifiers had their confusion matrix, precision 7.15 and

recall 7.16 computed using the following equations, where TP are the true positive values, FP the false positive and FN the false negative.

$$Precision = \frac{TP}{TP+FP} \tag{7.15}$$

$$Recall = \frac{TP}{TP+FN} \tag{7.16}$$

It is important to refer that, for Functionality classification, only results using Forward Selection were obtained, due to the low time available to perform this classification. Results achieved using Forward Selection to classify the remaining outputs do support this decision, since they have proven to be much better than those obtained with other feature selection methodologies.

7.3.1 Pain Classification

Pain classification results are present in Table 7.4.

Table 7.4: Pain Classification Results

		With Pre-Feature Selection		Without Pre-Feature Selection	
		MER	**Number of Features used**	**MER**	**Number of Features used**
MI	**LDA**	0.429	5	0.444	6
	NB	0.302	16	0.397	4
	SVM	0.302	6	0.317	9
SFFS	**LDA**	0.333	12	0.333	12
	NB	0.429	11	0.429	11
	SVM	0.27	5	0.27	5
Forward Selection	**LDA**	0.254	13	0.238	18
	NB	0.238	9	0.222	16
	SVM	0.222	5	0.19	4

Firstly, it is important to notice that SFFS with and without pre-feature selection had the same results. This occurred not only in Pain classification but also in all the other outputs where SFFS was tested, which allows us to conclude that calculating classification models without pre-feature selection, when using SFFS, is a redundant phase. This also shows that filter selection using correlation matrix is valid.

It is also interesting to notice that Forward Selection methodology worked better without pre-feature selection, which also occurred in all other outputs. This is due to the loss of information that occurs when pre-feature selection is used, and supports the fact that these results are possibly not the best ones that can be computed, since not all combinations were tested. However, and as was previously explained, Feature Selection is necessary due to the high number of features being tested, since it is unfeasible to test all combinations.

Furthermore, it is important to notice that Forward Selection is the method that had better results. This can be explained since both Mutual Information and SFFS are feature selection methods that try to predict which is the best subset of features without using any classification information. In spite of requiring much more computational power, Forward Selection uses classification information to perform this selection, which can explain the better results achieved.

On the contrary, Mutual Information had better results when pre-selection was performed. This can be explained by the methodology behind Mutual Information, which works best with a lower number of features. However, not only is this reduction not desired in normal feature selection methodologies, but also Mutual Information with pre-selection was not the best approach for all outputs, hence an abusive use of feature selection can lead to incorrect results.

The best classifier and its associated characteristics are presented in Table 7.5. Confusion Matrix for this classifier is presented in Table 7.6, as well as Recall and Precision.

Table 7.5: Parameters of best classifier for pain classification

Classifier	**Pre-Feature Selection**	**Feature Selection Methodology**	**Kernel**	**C**	**Order**	**y**	**MER**	**Feature Set**
SVM	No	Forward Selection	rbf	1	-	0.25	0.19	[15 22 24 33]

Table 7.6: Confusion Matrix, Precision and Recall results for pain classification

Predict / **True**	**With Pain**	**Without Pain**
With Pain	38	1
Without Pain	11	13

Recall	0.974
Precision	0.776

As expected, results obtained for SVMs were very good, since it proved to be a good option when there is a limited amount of data available, as in this case. Also, it is relevant to notice that the feature set is composed by features from Exercise 3 (Shoulder Height and Compensatory Movement Hip-Shoulder) and Exercise 4 (Shoulder Width and Duration of the Exercise). Furthermore, pain classification showed a high recall result due to the low error in classification of patients with pain. Precision results were lower. However, these results, as well as the associated error, are very promising for the performance of pain classification in breast cancer patients.

7.3.2 Stiffness Classification

Stiffness classification results are present in Table 7.7.

The best classifier and its associated characteristics are presented in Table 7.8. Confusion Matrix for this classifier is presented in Table 7.9, as well as Recall and Precision.

Table 7.7: Stiffness Classification Results

		With Pre-Feature Selection		Without Pre-Feature Selection	
		MER	**Number of Features used**	**MER**	**Number of Features used**
MI	**LDA**	0.349	3	0.349	3
	NB	0.413	1	0.397	4
	SVM	0.317	10	0.302	8
SFFS	**LDA**	0.397	2	0.397	2
	NB	0.365	9	0.365	9
	SVM	0.270	6	0.270	6
Forward Selection	**LDA**	0.286	8	0.254	10
	NB	0.286	7	0.270	8
	SVM	0.159	3	0.127	7

Table 7.8: Parameters of best classifier for stiffness classification

Classifier	**Pre-Feature Selection**	**Feature Selection Methodology**	**Kernel**	**C**	**Order**	**y**	**MER**	**Feature Set**
SVM	No	Forward Selection	rbf	8	-	0.75	0.127	[21 28 36 38 39 42 45]

Table 7.9: Confusion Matrix, Precision and Recall results for stiffness classification

Predict / **True**	**With Stiffness**	**Without Stiffness**
With Stiffness	39	6
Without Stiffness	2	25

Recall	0.833
Precision	0.939

As expected, SVM was the best classifier, with the best results being obtained using forward selection without feature selection and using correlation matrix. The feature set is composed by features obtained from Exercise 3, Exercise 4, Exercise 5 and Volume. Furthermore, stiffness classification shows high recall and precision, and low error in classification. These results are very promising and allow us to conclude that this methodology is a suitable solution for stiffness classification.

7.3.3 Weakness Classification

Weakness classification results are present in Table 7.10.

The best classifier and its associated characteristics are presented in Table 7.11. Confusion Matrix for this classifier is presented in Table 7.12, as well as Recall and Precision.

Table 7.10: Weakness Classification Results

		With Pre-Feature Selection		Without Pre-Feature Selection	
		MER	**Number of Features used**	**MER**	**Number of Features used**
MI	**LDA**	0.317	12	0.381	17
	NB	0.397	4	0.397	5
	SVM	0.286	7	0.27	4
SFFS	**LDA**	0.365	2	0.365	2
	NB	0.365	8	0.365	8
	SVM	0.286	6	0.286	6
Forward Selection	**LDA**	0.349	6	0.286	12
	NB	0.317	8	0.286	5
	SVM	0.19	5	0.111	7

Table 7.11: Parameters of best classifier for weakness classification

Classifier	**Pre-Feature Selection**	**Feature Selection Methodology**	**Kernel**	**C**	**Order**	**y**	**MER**	**Feature Set**
SVM	No	Forward Selection	rbf	8	-	1	0.111	[4 10 15 16 28 35 43]

Table 7.12: Confusion Matrix, Precision and Recall results for weakness classification

Predict / True	**With Weakness**	**Without Weakness**
With Weakness	26	5
Without Weakness	2	30

Recall	0.839
Precision	0.929

Once more, and as expected, SVM was the best classifier, using forward selection without feature selection and using correlation matrix. The feature set is composed by features obtained from all exercises. Furthermore, weakness classification shows high recall and precision, and also a low error in classification. These results are very promising and allow us to conclude that this methodology is a suitable solution for weakness classification.

7.3.4 Lymphedema Classification

Lymphedema classification results are present in Table 7.13.

The best classifier and its associated characteristics are presented in Table 7.14. Confusion Matrix for this classifier is presented in Table 7.15, as well as Recall and Precision.

As expected, SVM is the better classifier, using forward selection without feature selection using correlation matrix. The feature set is composed by features obtained from Exercise 3, Ex-

Table 7.13: Lymphedema Classification Results

		With Pre-Feature Selection		Without Pre-Feature Selection	
		MER	**Number of Features used**	**MER**	**Number of Features used**
MI	**LDA**	0.349	7	0.381	15
	NB	0.413	7	0.46	3
	SVM	0.27	14	0.286	1
SFFS	**LDA**	0.397	1	0.397	1
	NB	0.381	2	0.381	2
	SVM	0.286	10	0.286	10
Forward Selection	**LDA**	0.397	10	0.317	22
	NB	0.333	7	0.317	3
	SVM	0.19	6	0.159	8

Table 7.14: Parameters of best classifier for lymphedema classification

Classifier	**Pre-Feature Selection**	**Feature Selection Methodology**	**Kernel**	**C**	**Order**	**y**	**MER**	**Feature Set**
SVM	No	Forward Selection	rbf	2	-	0.75	0.159	[16 21 24 26 28 29 38 43]

Table 7.15: Confusion Matrix, Precision and Recall results for lymphedema classification

Predict / **True**	**With Lymphedema**	**Without Lymphedema**
With Lymphedema	20	7
Without Lymphedema	3	33

Recall	0.741
Precision	0.87

ercise 4 and Exercise 5. It is important to compare these results with those obtained by Moreira [7], since in this work lymphedema is also classified. Results obtained in this work shows better precision and error (0.87 vs. 0.86 obtained by Moreira and 0.159 vs. 0.19 obtained by Moreira, respectively), with similar results for recall (0.741 vs. 0.75 obtained by Moreira). This can be explained by the higher number of exercises used and also by the higher number of patients from whom data was acquired.

Furthermore, these results are very promising and allow us to conclude that this methodology is a suitable solution for lymphedema classification.

7.3.5 Functionality Classification

Functionality was the last output tested in the classification models. Due to limitations in terms of time, only Forward Selection was tested as a feature selection method for this output. Results can

be found in Table 7.16.

Table 7.16: Functionality Classification Results

		With Pre-Feature Selection		Without Pre-Feature Selection	
		MER	**Number of Features used**	**MER**	**Number of Features used**
Forward Selection	**LDA**	0.286	6	0.286	4
	NB	0.269	4	0.238	4
	SVM	0.206	9	0.127	8

The best classifier and its associated characteristics are presented in Table 7.17. Confusion Matrix for this classifier is presented in Table 7.18, as well as Recall and Precision.

Table 7.17: Parameters of best classifier for functionality classification

Classifier	**Pre-Feature Selection**	**Feature Selection Methodology**	**Kernel**	**C**	**Order**	**y**	**MER**	**Feature Set**
SVM	No	Forward Selection	rbf	8	-	0.55	0.127	[2 3 8 11 15 27 33 36]

Table 7.18: Confusion Matrix, Precision and Recall results for functionality classification

Predict / True	**Low Functionality**	**High Functionality**
Low Functionality	24	4
High Functionality	4	31

Recall	0.857
Precision	0.857

As expected, SVM is the better classifier, using forward selection without feature selection and using correlation matrix. The feature set is composed by features obtained from Exercise 1, Exercise 2, Exercise 3 and Exercise 4. Moreira [7] also performed a functionality evaluation, but using UEFI inquiries instead of the DASH inquiries that were used in this work. Although it is possible to compare results, with this work showing better results in the two evaluated parameters (error and recall), this comparison needs to be performed conservatively due to the different methodology used in both works.

Results obtained (high recall and precision with low associated error) are very promising and allow us to conclude that this methodology is a suitable solution for functionality classification.

7.4 Conclusion

Initially, and due to the high number of features extracted, feature selection was performed using six different methods for four of the outputs, with only two methods being used for the remaining output, which was Functionality. After that, and for the obtained subsets, different supervised classification algorithms (LDA, Naive Bayes and SVMs) were trained and tested in a LOO scheme.

The best results were verified with SVMs with RBF kernels, with a misclassification error of 0.19 for pain, 0.127 for stiffness, 0.111 for weakness, 0.159 for lymphedema and 0.127 for functionality classification. These results are very promising, and are better when compared to results from existing literature. In the future it is important to create a global model, instead of using five separate models for each state.

Therefore, the proposed methodology appears to be suitable for the evaluation of upper-body functional status in breast cancer patients.

Chapter 8

Conclusion

The use of surgery procedures and, posteriorly, radiation therapy for breast cancer treatment brings side-effects such as a reduction of QOL in women. This can be due to lowered UBF, usually caused by the presence of lymphedema, or other aspects, from pain to muscle stiffness. Although there currently are methods to assess these problems, the most used are subjective (such as water displacement and self-reports inquiries), having limited capabilities, being necessary to use in parallel to better assessment of patient condition.

In recent years, several research groups have tried to use objective technologies to solve this problem. However, costs associated with this are high, which has been proved to be a problem in its adoption. Furthermore, most methods are complex and require a professional to be performed. One of the most promising technologies is the application of 3D Human Tracking System to extract features. However, due to the associated costs, most recent studies are focusing in the application of RGB-D sensors. An example is Microsoft Kinect. Despite existing some research in this field, there does not exist yet a system which allows for both an exhaustive diagnosis of upper body functional impairments, and for an assessment of patient condition (for instance, pain and muscle stiffness).

This work consisted in applying Microsoft Kinect and its capabilities (RGB-D sensor and skeleton tracking algorithm), to acquired features and assess patients' condition and parameters associated with their UBF. Due to its ability to disrupt patients QOL, functional parameters should be considered in any breast cancer treatment evaluation. Also, an important factor in these systems is the need of an early detection of lymphedema, since it is a major factor on UBF.

All the research depends on training and testing examples used in the development of the models. Therefore, the project had a phase for data collection, where patients carried out a protocol in order to collect important features in a real environment, as if it were made in a normal day of their daily life. With this in mind, the first step of this work was to improve the software for data acquisition proposed by Moreira [7]. Using Kinect for Windows SDK, RGB, depth frames and skeleton data were collected over time. After that, data was processed to acquire the intended features. Methodology used for data processing can be divided in two main groups: Skeleton tracking data methodology and RGB-D data methodology.

Data from skeleton tracking system had noise that can influence the outputs. To reduce its effect, several filters were tested to understand which one worked better in this environment. After this selection, several features were extracted from the processed signal to understand which can more accurately characterize patient condition.

Using RGB-D data, it is possible to estimate patients' upper limb volume. For this, it was necessary to process data using several methods for arm segmentation. These methods were compared, with the most accurate one for volume estimation being chosen. It is important to refer that, despite having some problems associated, segmentation using just depth maps was the most accurate approach, which shows that the problems are minimized by processing data. Also, colour processing had problems an incorrect segmentation in some images.

Extracted features were used to test the behaviour of several supervised learning algorithms (LDA, Naive Bayes and SVMs), in order to build a predictive classification model to assess the presence of pain, lymphedema, stiffness, weakness and patients' functionality.Obtained results showed that the proposed methodology can be used to classify patients' condition. Also, when compared with results obtained from other works, the created methodology herein described obtained better results in the detection of lymphedema and in functionality analysis.

8.1 Future Work

Although the results obtained by this work were satisfactory, an improvement of these will lead to a more robust methodology and classification. In order to do that, it is important to understand the medical needs, increasing the number of medical staff that participates in the study. This will allow the creation of a more diverse and adaptable application.

Furthermore, it is important to add more exercises to the application in order to understand if there is any impact in the classification. Also, the application must be capable of detecting which exercise the patient is performing. This will enhance the efficiency of the application, and make it less prone to errors.

This work can also be enriched by evolving the existing database into a more diverse one, and by applying other methods of classification. This way, it will be possible to test the viability of the proposed method in all kinds of patients.

Regarding filter selection, other types of filters must be tested to have a better understanding of the behaviour of the filtering process of this data. As explained before, the data filtering step is of utmost importance to retrieve more accurate features, and a broader filter selection can lead to better results. Also, the existing methodology for filter selection can be improved, using more than two joints for this selection.

An important aspect was found in the classification of lymphedema, where volume estimations were expected to be relevant. However, the feature set for this type of classification did not include volume estimations. Also, colour segmentation showed lower results, which was not expected. A more complete methodology in this type of segmentation, using not only GrabCut but more methodologies for patient segmentation, can reveal to be more efficient.

Furthermore, arm segmentation can be evaluated using measures from the arm, enabling a better methodology for the selection of the best arm segmentation method.

Concerning the supervised classification models, it is important to use not only binary outputs but also multi-class outputs. Pain levels and functionality can be two of these multi-class outputs. However, this will require a more diverse and complete database. Additionally, the creation of a single model to evaluate lymphedema, pain, stiffness, weakness and functionality is an important step forward in this work.

It is also important to understand how other variables, such as physiotherapy or the type of surgery, affect patients' conditions. An analysis of patient condition over time will also be an interesting and relevant aspect to include in this study.

Lastly, an important aspect to test is the impact of feature selection. In order to assess that, a comparison between feature selection results and results obtained using all possible combinations can be performed. Additionally, other feature selection methods can be tested to understand their impact.

References

[1] A. Jemal, F. Bray, M. M. Center, J. Ferlay, E. Ward, and D. Forman, "Global cancer statistics," *CA: a cancer journal for clinicians*, vol. 61, no. 2, pp. 69–90, 2011.

[2] T. Tarver, "Cancer facts & figures 2015. american cancer society (acs) atlanta, ga: American cancer society, 2015." *Journal of Consumer Health on the Internet*, vol. 16, no. 3, pp. 366–367, 2015.

[3] A. Jemal, M. M. Center, C. DeSantis, and E. M. Ward, "Global patterns of cancer incidence and mortality rates and trends," *Cancer Epidemiology Biomarkers & Prevention*, vol. 19, no. 8, pp. 1893–1907, 2010.

[4] M. Vahdaninia, S. Omidvari, and A. Montazeri, "What do predict anxiety and depression in breast cancer patients? a follow-up study," *Social psychiatry and psychiatric epidemiology*, vol. 45, no. 3, pp. 355–361, 2010.

[5] S. S. Fong, S. S. Ng, W. Luk, J. W. Chung, L. M. Chung, W. W. Tsang, and L. P. Chow, "Shoulder mobility, muscular strength, and quality of life in breast cancer survivors with and without tai chi qigong training," *Evidence-Based Complementary and Alternative Medicine*, vol. 2013, 2013.

[6] R. Gärtner, M.-B. Jensen, L. Kronborg, M. Ewertz, H. Kehlet, and N. Kroman, "Self-reported arm-lymphedema and functional impairment after breast cancer treatment–a nationwide study of prevalence and associated factors," *The Breast*, vol. 19, no. 6, pp. 506–515, 2010.

[7] R. Moreira, "Dynamic analysis of upper limbs movements after breast cancer surgery," *FEUP*, 2014.

[8] N. C. Institute, "What is cancer?" 2014. [Online]. Available: http://www.cancer.gov/cancertopics/cancerlibrary/what-is-cancer

[9] A. G. Knudson, "Two genetic hits (more or less) to cancer," *Nature Reviews Cancer*, vol. 1, no. 2, pp. 157–162, 2001.

[10] Cancer.org, "What is cancer?" 2014. [Online]. Available: http://www.cancer.org/cancer/cancerbasics/what-is-cancer

[11] Who.int, "Cancer - who," 2015. [Online]. Available: http://www.who.int/mediacentre/factsheets/fs297/en/

[12] D. H. Roukos, "Genome-wide association studies: how predictable is a person's cancer risk?" 2009.

[13] R. Seeley, P. Tate, and T. Stephens, *Anatomy & Physiology*. McGraw-Hill, 2007.

[14] F. Netter, *Netter - Atlas de Anatomia Humana*. ELSEVIER (MEDICINA), 2008.

[15] C. R. UK, "The breasts and lymphatic system," 2014. [Online]. Available: http://www.cancerresearchuk.org/about-cancer/type/breast-cancer/about/the-breasts-and-lymphatic-system

[16] C. C. Society, "Anatomy and physiology of the breast." [Online]. Available: http://www.cancer.ca/en/cancer-information/cancer-type/breast/anatomy-and-physiology/?region=nl

[17] M. Garcia, Jemal, E. Ward, M. Center, Y. Hao, R. Siegel, and M. Thun, "Global cancer facts & figures 2007," *Atlanta, GA: American cancer society*, vol. 1, no. 3, p. 52, 2007.

[18] L. Wilkins, *Interpreting Signs and Symptoms*, ser. LWW medical book collection. Lippincott Williams & Wilkins, 2007.

[19] C. Staging, "Ajcc - american joint committee on cancer." [Online]. Available: https://cancerstaging.org/Pages/default.aspx

[20] BreastCancer.org, "What is mastectomy?" 2013. [Online]. Available: http://www.breastcancer.org/treatment/surgery/mastectomy/what_is

[21] C. C. Society, "Surgery for breast cancer." [Online]. Available: http://www.cancer.ca/en/cancer-information/cancer-type/breast/treatment/surgery/?region=nl

[22] Breastcancer.org, "Mastectomy vs. lumpectomy," 2015. [Online]. Available: http://www.breastcancer.org/treatment/surgery/mast_vs_lump

[23] J. M. G. Arroyo and M. L. D. López, "Psychological problems derived from mastectomy: a qualitative study," *International journal of surgical oncology*, vol. 2011, 2011.

[24] V. Pikler and C. Winterowd, "Racial and body image differences in coping for women diagnosed with breast cancer." *Health Psychology*, vol. 22, no. 6, p. 632, 2003.

[25] M. J. Wexler, "Role of axillary lymph-node dissection in the management of breast cancer," *Canadian journal of surgery*, vol. 46, no. 4, p. 247, 2003.

[26] C. R. UK, "Statistics and outlook for breast cancer," 2015. [Online]. Available: http://www.cancerresearchuk.org/about-cancer/type/breast-cancer/treatment/statistics-and-outlook-for-breast-cancer

[27] S. F. Shaitelman, K. D. Cromwell, J. C. Rasmussen, N. L. Stout, J. M. Armer, B. B. Lasinski, and J. N. Cormier, "Recent progress in the treatment and prevention of cancer-related lymphedema," *CA: a cancer journal for clinicians*, vol. 65, no. 1, pp. 55–81, 2015.

[28] "The diagnosis and treatment of peripheral lymphedema: 2013 consensus document of the international society of lymphology," *Lymphology*, vol. 46, no. 1, pp. 1–11.

[29] M. J. Taylor, A. Hoerauf, and M. Bockarie, "Lymphatic filariasis and onchocerciasis," *The Lancet*, vol. 376, no. 9747, pp. 1175–1185, 2010.

[30] A. Stanton, C. Badger, J. Sitzia *et al.*, "Non-invasive assessment of the lymphedematous limb," *Lymphology*, vol. 33, no. 3, pp. 122–135, 2000.

[31] S. Ridner, L. Montgomery, J. Hepworth, B. Stewart, and J. Armer, "Comparison of upper limb volume measurement techniques and arm symptoms between healthy volunteers and individuals with known lymphedema," *Lymphology*, vol. 40, no. 1, pp. 35–46, 2007.

[32] S. C. Hayes, M. Janda, B. Cornish, D. Battistutta, and B. Newman, "Lymphedema after breast cancer: incidence, risk factors, and effect on upper body function," *Journal of clinical oncology*, vol. 26, no. 21, pp. 3536–3542, 2008.

[33] S. D. Passik and M. V. McDonald, "Psychosocial aspects of upper extremity lymphedema in women treated for breast carcinoma," *Cancer*, vol. 83, no. S12B, pp. 2817–2820, 1998.

[34] C. Miaskowski, M. Dodd, S. M. Paul, C. West, D. Hamolsky, G. Abrams, B. A. Cooper, C. Elboim, J. Neuhaus, B. L. Schmidt *et al.*, "Lymphatic and angiogenic candidate genes predict the development of secondary lymphedema following breast cancer surgery," *PloS one*, vol. 8, no. 4, p. e60164, 2013.

[35] D. N. Finegold, V. Schacht, M. A. Kimak, E. C. Lawrence, E. Foeldi, J. M. Karlsson, C. J. Baty, and R. E. Ferrell, "Hgf and met mutations in primary and secondary lymphedema," *Lymphatic research and biology*, vol. 6, no. 2, pp. 65–68, 2008.

[36] M. B. Tobin, H. J. Lacey, L. Meyer, and P. S. Mortimer, "The psychological morbidity of breast cancer–related arm swelling. psychological morbidity of lymphoedema," *Cancer*, vol. 72, no. 11, pp. 3248–3252, 1993.

[37] A. M. Megens, S. R. Harris, C. Kim-Sing, and D. C. McKenzie, "Measurement of upper extremity volume in women after axillary dissection for breast cancer," *Archives of physical medicine and rehabilitation*, vol. 82, no. 12, pp. 1639–1644, 2001.

[38] J. A. Petrek, P. I. Pressman, and R. A. Smith, "Lymphedema: current issues in research and management," *CA: A Cancer Journal for Clinicians*, vol. 50, no. 5, pp. 292–307, 2000.

[39] M. L. McNeely, K. L. Campbell, B. H. Rowe, T. P. Klassen, J. R. Mackey, and K. S. Courneya, "Effects of exercise on breast cancer patients and survivors: a systematic review and meta-analysis," *Canadian Medical Association Journal*, vol. 175, no. 1, pp. 34–41, 2006.

[40] M. D. Holmes, W. Y. Chen, D. Feskanich, C. H. Kroenke, and G. A. Colditz, "Physical activity and survival after breast cancer diagnosis," *Jama*, vol. 293, no. 20, pp. 2479–2486, 2005.

[41] K. Matthews and J. Smith, "Effectiveness of modified complex physical therapy for lymphoedema treatment," *Australian Journal of Physiotherapy*, vol. 42, no. 4, pp. 323–328, 1996.

[42] S. R. Harris and S. L. Niesen-Vertommen, "Challenging the myth of exercise-induced lymphedema following breast cancer: a series of case reports," *Journal of Surgical Oncology*, vol. 74, no. 2, pp. 95–98, 2000.

[43] D. C. McKenzie and A. L. Kalda, "Effect of upper extremity exercise on secondary lymphedema in breast cancer patients: a pilot study," *Journal of Clinical Oncology*, vol. 21, no. 3, pp. 463–466, 2003.

[44] K. H. Schmitz, A. B. Troxel, A. Cheville, L. L. Grant, C. J. Bryan, C. R. Gross, L. A. Lytle, and R. L. Ahmed, "Physical activity and lymphedema (the pal trial): assessing the safety of progressive strength training in breast cancer survivors," *Contemporary clinical trials*, vol. 30, no. 3, pp. 233–245, 2009.

[45] N. M. A. Committee, "Position statement of the national lymphedema network," 2013.

[46] S. Harrington, L. A. Michener, T. Kendig, S. Miale, and S. Z. George, "Patient-reported upper extremity outcome measures used in breast cancer survivors: A systematic review," *Archives of Physical Medicine and Rehabilitation*, vol. 95, no. 1, pp. 153 – 162, 2014. [Online]. Available: http://www.sciencedirect.com/science/article/pii/S000399931300590X

[47] A. Szuba and S. G. Rockson, "Lymphedema: classification, diagnosis and therapy," *Vascular Medicine*, vol. 3, no. 2, pp. 145–156, 1998.

[48] C. Bulley, S. Gaal, F. Coutts, C. Blyth, W. Jack, U. Chetty, M. Barber, and C.-W. Tan, "Comparison of breast cancer-related lymphedema (upper limb swelling) prevalence estimated using objective and subjective criteria and relationship with quality of life," *BioMed research international*, vol. 2013, 2013.

[49] R. Taylor, U. W. Jayasinghe, L. Koelmeyer, O. Ung, and J. Boyages, "Reliability and validity of arm volume measurements for assessment of lymphedema," *Physical Therapy*, vol. 86, no. 2, pp. 205–214, 2006.

[50] I. Swedborg, "Voluminometric estimation of the degree of lymphedema and its therapy by pneumatic compression." *Scandinavian journal of rehabilitation medicine*, vol. 9, no. 3, pp. 131–135, 1976.

[51] D. K. Sukul, P. T. den Hoed, E. Johannes, R. Van Dolder, and E. Benda, "Direct and indirect methods for the quantification of leg volume: comparison between water displacement volumetry, the disk model method and the frustum sign model method, using the correlation coefficient and the limits of agreement," *Journal of biomedical engineering*, vol. 15, no. 6, pp. 477–480, 1993.

[52] A. P. Sander, N. M. Hajer, K. Hemenway, and A. C. Miller, "Upper-extremity volume measurements in women with lymphedema: a comparison of measurements obtained via water displacement with geometrically determined volume," *Physical therapy*, vol. 82, no. 12, pp. 1201–1212, 2002.

[53] J. Zuther, "Measuring for compression arm sleeves," 2011. [Online]. Available: http://www.lymphedemablog.com/2011/08/23/measuring-for-compression-arm-sleeves/

[54] A. Stanton, J. Northfield, B. Holroyd, P. Mortimer, and J. Levick, "Validation of an optoelectronic limb volumeter (perometer®)," *Lymphology*, vol. 30, no. 2, pp. 77–97, 1997.

[55] D. Bates, J. Levick, and P. Mortimer, "Quantification of rate and depth of pitting in human edema using an electronic tonometer," *Lymphology*, vol. 27, no. 4, pp. 159–172, 1994.

[56] G. Lu, G. DeSouza, J. Armer, B. Anderson, and C.-R. Shyu, "A system for limb-volume measurement using 3d models from an infrared depth sensor," in *Computational Intelligence in Healthcare and e-health (CICARE), 2013 IEEE Symposium on*. IEEE, 2013, pp. 64–69.

[57] R. (ACR), "Lymphoscintigraphy," 2014. [Online]. Available: http://www.radiologyinfo.org/en/info.cfm?pg=lympho

[58] Emedicine.medscape.com, "Lymphoscintigraphy," 2013. [Online]. Available: http://emedicine.medscape.com/article/1890647-overview

[59] E. M. Sevick-Muraca, S. Kwon, J. C. Rasmussen *et al.*, "Emerging lymphatic imaging technologies for mouse and man," *J Clin Invest*, vol. 124, no. 3, pp. 905–914, 2014.

[60] N. Unno, K. Inuzuka, M. Suzuki, N. Yamamoto, D. Sagara, M. Nishiyama, and H. Konno, "Preliminary experience with a novel fluorescence lymphography using indocyanine green in patients with secondary lymphedema," *Journal of vascular surgery*, vol. 45, no. 5, pp. 1016–1021, 2007.

[61] A. Tiwari, K.-S. Cheng, M. Button, F. Myint, and G. Hamilton, "Differential diagnosis, investigation, and current treatment of lower limb lymphedema," *Archives of surgery*, vol. 138, no. 2, pp. 152–161, 2003.

[62] A. L. Cheville, D. H. Brinkmann, S. B. Ward, J. Durski, N. N. Laack, E. Yan, P. J. Schomberg, Y. I. Garces, V. J. Suman, and I. A. Petersen, "The addition of spect/ct lymphoscintigraphy to breast cancer radiation planning spares lymph nodes critical for arm drainage," *International Journal of Radiation Oncology* Biology* Physics*, vol. 85, no. 4, pp. 971–977, 2013.

[63] R. B. Mazess, H. S. Barden, J. P. Bisek, and J. Hanson, "Dual-energy x-ray absorptiometry for total-body and regional bone-mineral and soft-tissue composition." *The American journal of clinical nutrition*, vol. 51, no. 6, pp. 1106–1112, 1990.

[64] C. Gjorup, B. Zerahn, and H. W. Hendel, "Assessment of volume measurement of breast cancer-related lymphedema by three methods: circumference measurement, water displacement, and dual energy x-ray absorptiometry," *Lymphatic research and biology*, vol. 8, no. 2, pp. 111–119, 2010.

[65] C. Trombetta, P. Abundo, A. Felici, C. Ljoka, S. Di Cori, N. Rosato, and C. Foti, "Computer aided measurement laser (caml): technique to quantify post-mastectomy lymphoedema," in *Journal of Physics: Conference Series*, vol. 383, no. 1. IOP Publishing, 2012, p. 012018.

[66] J. G. McKinnon, V. Wong, W. J. Temple, C. Galbraith, P. Ferry, G. S. Clynch, and C. Clynch, "Measurement of limb volume: laser scanning versus volume displacement," *Journal of surgical oncology*, vol. 96, no. 5, pp. 381–388, 2007.

[67] D. Edgar, R. Day, N. K. Briffa, J. Cole, and F. Wood, "Volume measurement using the polhemus fastscan 3d laser scanning: a novel application for burns clinical research," *Journal of burn care & research*, vol. 29, no. 6, pp. 994–1000, 2008.

[68] C. Vukotich, M. Geyer, and F. Erdeljac, "Use of a laser scanning system to measure limb volume in chronic edema," *ehabilitation Engineering & Assistive Technology Society of North America (RESNA)*, 2011.

[69] H. Zhou and H. Hu, "Human motion tracking for rehabilitation—a survey," *Biomedical Signal Processing and Control*, vol. 3, no. 1, pp. 1–18, 2008.

[70] A. J. Salazar, A. S. Silva, C. Silva, C. M. Borges, M. V. Correia, R. S. Santos, and J. P. Vilas-Boas, "Low-cost wearable data acquisition for stroke rehabilitation: A proof-of-concept study on accelerometry for functional task assessment," *Topics in stroke rehabilitation*, vol. 21, no. 1, pp. 12–22, 2014.

[71] X. Zhang and C. Xu, "Real-time endpoint detection of upper limb movement based on energy threshold and residual methods," in *Biomedical Engineering and Informatics (BMEI), 2012 5th International Conference on*. IEEE, 2012, pp. 334–338.

[72] T. B. Moeslund, A. Hilton, and V. Krüger, "A survey of advances in vision-based human motion capture and analysis," *Computer vision and image understanding*, vol. 104, no. 2, pp. 90–126, 2006.

[73] A. Kolahi, M. Hoviattalab, T. Rezaeian, M. Alizadeh, M. Bostan, and H. Mokhtarzadeh, "Design of a marker-based human motion tracking system," *Biomedical Signal Processing and Control*, vol. 2, no. 1, pp. 59–67, 2007.

[74] VICON, "Vicon motion systems ltd." [Online]. Available: http://www.vicon.com/

[75] Codamotion, "[charnwood dynamics ltd." [Online]. Available: http://www.charndyn.com/

[76] R. Schmidt, C. Disselhorst-Klug, J. Silny, and G. Rau, "A marker-based measurement procedure for unconstrained wrist and elbow motions," *Journal of Biomechanics*, vol. 32, no. 6, pp. 615–621, 1999.

[77] Y. Tao and H. Hu, "Building a visual tracking system for home-based rehabilitation," in *Proc. of the 9th Chinese Automation and Computing Society Conf. In the UK*, 2003.

[78] G. C. Burdea, D. Cioi, J. Martin, D. Fensterheim, and M. Holenski, "The rutgers arm ii rehabilitation system—a feasibility study," *Neural Systems and Rehabilitation Engineering, IEEE Transactions on*, vol. 18, no. 5, pp. 505–514, 2010.

[79] M. K. Leung and Y.-H. Yang, "First sight: A human body outline labeling system," *Pattern Analysis and Machine Intelligence, IEEE Transactions on*, vol. 17, no. 4, pp. 359–377, 1995.

[80] S. X. Ju, M. J. Black, and Y. Yacoob, "Cardboard people: A parameterized model of articulated image motion," in *Automatic Face and Gesture Recognition, 1996., Proceedings of the Second International Conference on*. IEEE, 1996, pp. 38–44.

[81] L. S. Hooi, G. Sainarayanan, and L. C. Fan, "Human pose modelling and body tracking from monocular video sequences," in *Intelligent and Advanced Systems, 2007. ICIAS 2007. International Conference on*. IEEE, 2007, pp. 571–576.

[82] S. M. Seitz, B. Curless, J. Diebel, D. Scharstein, and R. Szeliski, "A comparison and evaluation of multi-view stereo reconstruction algorithms," in *Computer vision and pattern recognition, 2006 IEEE Computer Society Conference on*, vol. 1. IEEE, 2006, pp. 519–528.

[83] Y. Furukawa and J. Ponce, "Accurate, dense, and robust multiview stereopsis," *Pattern Analysis and Machine Intelligence, IEEE Transactions on*, vol. 32, no. 8, pp. 1362–1376, 2010.

[84] D. Lam, R. Z. Hong, and G. N. DeSouza, "3d human modeling using virtual multi-view stereopsis and object-camera motion estimation," in *Intelligent Robots and Systems, 2009. IROS 2009. IEEE/RSJ International Conference on*. IEEE, 2009, pp. 4294–4299.

[85] F. Caillette and T. Howard, "Real-time markerless human body tracking using colored voxels and 3d blobs," in *Mixed and Augmented Reality, 2004. ISMAR 2004. Third IEEE and ACM International Symposium on*. IEEE, 2004, pp. 266–267.

[86] L. Goncalves, E. Di Bernardo, E. Ursella, and P. Perona, "Monocular tracking of the human arm in 3d," in *Computer Vision, 1995. Proceedings., Fifth International Conference on*. IEEE, 1995, pp. 764–770.

[87] C. A. S. Haddad, M. Saad, M. d. C. J. Perez, and F. Miranda Júnior, "Assessment of posture and joint movements of the upper limbs of patients after mastectomy and lymphadenectomy," *Einstein (São Paulo)*, vol. 11, no. 4, pp. 426–434, 2013.

[88] F. Öhberg, A. Zachrisson, and Å. Holmner-Rocklöv, "Three-dimensional camera system for measuring arm volume in women with lymphedema following breast cancer treatment," *Lymphatic research and biology*, vol. 12, no. 4, pp. 267–274, 2014.

[89] P. Henry, M. Krainin, E. Herbst, X. Ren, and D. Fox, "Rgb-d mapping: Using depth cameras for dense 3d modeling of indoor environments," in *In the 12th International Symposium on Experimental Robotics (ISER*. Citeseer, 2010.

[90] J. Garcia and Z. Zalevsky, "Range mapping using speckle decorrelation," Oct. 7 2008, uS Patent 7,433,024. [Online]. Available: http://www.google.com.ar/patents/US7433024

[91] K. Litomisky, "Consumer rgb-d cameras and their applications," *University of California, Riverside. Ano*, 2012.

[92] Asus.com, "Xtion pro live - descrição." [Online]. Available: http://www.asus.com/pt/Multimedia/Xtion_PRO_LIVE/

[93] J. Han, L. Shao, D. Xu, and J. Shotton, "Enhanced computer vision with microsoft kinect sensor: A review," *Cybernetics, IEEE Transactions on*, vol. 43, no. 5, pp. 1318–1334, 2013.

[94] Codeproject.com, "Codeproject - for those who code." [Online]. Available: http://www.codeproject.com/

[95] OpenNI, "Openni." [Online]. Available: http://www.openni.org/

[96] M. K. SDK, "Microsoft kinect sdk." [Online]. Available: http://www.microsoft.com/en-us/kinectforwindows/

[97] OpenKinect, "Openkinect (libfreenect)." [Online]. Available: https://github.com/OpenKinect/libfreenect/

[98] J. Smisek, M. Jancosek, and T. Pajdla, "3d with kinect," in *Consumer Depth Cameras for Computer Vision*. Springer, 2013, pp. 3–25.

[99] K. Khoshelham and S. O. Elberink, "Accuracy and resolution of kinect depth data for indoor mapping applications," *Sensors*, vol. 12, no. 2, pp. 1437–1454, 2012.

[100] T. Dutta, "Evaluation of the kinect^{TM} sensor for 3-d kinematic measurement in the workplace," *Applied ergonomics*, vol. 43, no. 4, pp. 645–649, 2012.

[101] S. Obdrzalek, G. Kurillo, F. Ofli, R. Bajcsy, E. Seto, H. Jimison, and M. Pavel, "Accuracy and robustness of kinect pose estimation in the context of coaching of elderly population," in *Engineering in medicine and biology society (EMBC), 2012 annual international conference of the IEEE*. IEEE, 2012, pp. 1188–1193.

[102] J. Tong, J. Zhou, L. Liu, Z. Pan, and H. Yan, "Scanning 3d full human bodies using kinects," *Visualization and Computer Graphics, IEEE Transactions on*, vol. 18, no. 4, pp. 643–650, 2012.

[103] M. Zeng, L. Cao, H. Dong, K. Lin, M. Wang, and J. Tong, "Estimation of human body shape and cloth field in front of a kinect," *Neurocomputing*, vol. 151, pp. 626–631, 2015.

[104] I. Pastor, H. A. Hayes, and S. J. Bamberg, "A feasibility study of an upper limb rehabilitation system using kinect and computer games," in *Engineering in Medicine and Biology Society (EMBC), 2012 Annual International Conference of the IEEE*. IEEE, 2012, pp. 1286–1289.

[105] Y.-J. Chang, S.-F. Chen, and J.-D. Huang, "A kinect-based system for physical rehabilitation: A pilot study for young adults with motor disabilities," *Research in developmental disabilities*, vol. 32, no. 6, pp. 2566–2570, 2011.

[106] G. Kurillo, J. J. Han, S. Obdrzálek, P. Yan, R. T. Abresch, A. Nicorici, and R. Bajcsy, "Upper extremity reachable workspace evaluation with kinect." in *MMVR*, 2013, pp. 247–253.

[107] J. Engel, J. Kerr, A. Schlesinger-Raab, H. Sauer, and D. Hölzel, "Axilla surgery severely affects quality of life: results of a 5-year prospective study in breast cancer patients," *Breast cancer research and treatment*, vol. 79, no. 1, pp. 47–57, 2003.

[108] J. M. Armer, M. E. Radina, D. Porock, and S. D. Culbertson, "Predicting breast cancer-related lymphedema using self-reported symptoms," *Nursing research*, vol. 52, no. 6, pp. 370–379, 2003.

[109] V. Velanovich and W. Szymanski, "Quality of life of breast cancer patients with lymphedema," *The American journal of surgery*, vol. 177, no. 3, pp. 184–188, 1999.

[110] S. Mak, K. Mo, J. Suen, S. Chan, W. Ma, and W. Yeo, "Lymphedema and quality of life in chinese women after treatment for breast cancer," *European Journal of Oncology Nursing*, vol. 13, no. 2, pp. 110–115, 2009.

[111] C. P. Gabel, M. Yelland, M. Melloh, and B. Burkett, "A modified quickdash-9 provides a valid outcome instrument for upper limb function," *BMC musculoskeletal disorders*, vol. 10, no. 1, p. 161, 2009.

[112] S. Solway, A. A. of Orthopaedic Surgeons *et al.*, *The DASH outcome measure user's manual*. Institute for Work & Health, 2002.

[113] D. E. Beaton, J. N. Katz, A. H. Fossel, J. G. Wright, V. Tarasuk, and C. Bombardier, "Measuring the wole or the parts?: Validity, reliability, and responsiveness of the disabilities of the arm, shoulder and hand outcome measure in different regions of the upper extremity," *Journal of Hand Therapy*, vol. 14, no. 2, pp. 128–142, 2001.

[114] I.-L. Nesvold, S. D. Fosså, B. Naume, and A. A. Dahl, "Kwan's arm problem scale: psychometric examination in a sample of stage ii breast cancer survivors," *Breast cancer research and treatment*, vol. 117, no. 2, pp. 281–288, 2009.

[115] P. W. Stratford, J. M. Binkley, and D. M. Stratford, "Development and initial validation of the upper extremity functional index," *Physiotherapy Canada*, vol. 53, no. 4, pp. 259–267, 2001.

[116] P. Stratford, "Assessing disability and change on individual patients: a report of a patient specific measure," *Physiotherapy canada*, vol. 47, no. 4, pp. 258–263, 1995.

[117] S. Coster, K. Poole, and L. J. Fallowfield, "The validation of a quality of life scale to assess the impact of arm morbidity in breast cancer patients post-operatively," *Breast cancer research and treatment*, vol. 68, no. 3, pp. 273–282, 2001.

[118] S. Ahn, B. Park, D. Noh, S. Nam, E. Lee, M. Lee, S. Kim, K. Lee, S. Park, and Y. Yun, "Health-related quality of life in disease-free survivors of breast cancer with the general population," *Annals of Oncology*, vol. 18, no. 1, pp. 173–182, 2007.

[119] C. M. Chen, S. J. Cano, A. F. Klassen, T. King, C. McCarthy, P. G. Cordeiro, M. Morrow, and A. L. Pusic, "Measuring quality of life in oncologic breast surgery: A systematic review of patient-reported outcome measures," *The breast journal*, vol. 16, no. 6, pp. 587–597, 2010.

[120] K. L. Campbell, A. L. Pusic, D. S. Zucker, M. L. McNeely, J. M. Binkley, A. L. Cheville, and K. J. Harwood, "A prospective model of care for breast cancer rehabilitation: function," *Cancer*, vol. 118, no. S8, pp. 2300–2311, 2012.

[121] R. Freitas-Silva, D. M. Conde, R. d. Freitas-Júnior, and E. Z. Martinez, "Comparison of quality of life, satisfaction with surgery and shoulder-arm morbidity in breast cancer survivors submitted to breast-conserving therapy or mastectomy followed by immediate breast reconstruction," *Clinics*, vol. 65, no. 8, pp. 781–787, 2010.

[122] S. C. Hayes, S. Rye, D. Battistutta, T. DiSipio, and B. Newman, "Upper-body morbidity following breast cancer treatment is common, may persist longer-term and adversely influences quality of life," *Health Qual Life Outcomes*, vol. 8, no. 1, p. 92, 2010.

[123] J. Webb and J. Ashley, *Beginning Kinect Programming with the Microsoft Kinect SDK*. Apress, 2012.

[124] R. Dumont, "Kinect sdk 1.0 - 3 - track bodies with the skeletonstream." [Online]. Available: http://archive.renauddumont.be/post/2012/04/19/Kinect-SDK-10-3-Track-bodies-with-the-SkeletonStream

[125] M. L. McNeely, K. Campbell, M. Ospina, B. H. Rowe, K. Dabbs, T. P. Klassen, J. Mackey, and K. Courneya, "Exercise interventions for upper-limb dysfunction due to breast cancer treatment," *The Cochrane Library*, 2010.

[126] B. Cheema, C. A. Gaul, K. Lane, and M. A. F. Singh, "Progressive resistance training in breast cancer: a systematic review of clinical trials," *Breast cancer research and treatment*, vol. 109, no. 1, pp. 9–26, 2008.

[127] "Exercises after breast reconstruction surgery using muscle from your back | cancer research uk," 2014. [Online]. Available: http://www.cancerresearchuk.org/about-cancer/type/breast-cancer/treatment/surgery/reconstruction/exercises-after-breast-reconstruction-using-back-muscle

[128] D. Burdick, "Rehabilitation of the breast cancer patient," *Cancer*, vol. 36, no. S2, pp. 645–648, 1975.

[129] P. G. V. Clé, L. E. Tasso, R. I. Barbosa, M. d. C. R. Fonseca, V. M. C. Elui, F. B. Roncaglia, N. Mazzer, and C. H. Barbieri, "Estudo retrospectivo do estado funcional de pacientes com fratura do rádio distal submetidos à osteossíntese com placa lcp," *Acta fisiátrica*, vol. 18, no. 4, 2011.

[130] B. Galna, G. Barry, D. Jackson, D. Mhiripiri, P. Olivier, and L. Rochester, "Accuracy of the microsoft kinect sensor for measuring movement in people with parkinson's disease," *Gait & posture*, vol. 39, no. 4, pp. 1062–1068, 2014.

[131] M. Huber, A. Seitz, M. Leeser, and D. Sternad, "Validity and reliability of kinect skeleton for measuring shoulder joint angles: a feasibility study," *Physiotherapy*, 2015.

[132] L. Yin, R. Yang, M. Gabbouj, and Y. Neuvo, "Weighted median filters: a tutorial," *Circuits and Systems II: Analog and Digital Signal Processing, IEEE Transactions on*, vol. 43, no. 3, pp. 157–192, 1996.

[133] D. Marr and E. Hildreth, "Theory of edge detection," *Proceedings of the Royal Society of London B: Biological Sciences*, vol. 207, no. 1167, pp. 187–217, 1980.

[134] T. Agarwal, "Chebyshev filter - diffferent types of chebyshev filters." [Online]. Available: http://www.elprocus.com/types-of-chebyshev-filters/

[135] J. L. Anderson, "An ensemble adjustment kalman filter for data assimilation," *Monthly weather review*, vol. 129, no. 12, pp. 2884–2903, 2001.

[136] P. L. Houtekamer and H. L. Mitchell, "Data assimilation using an ensemble kalman filter technique," *Monthly Weather Review*, vol. 126, no. 3, pp. 796–811, 1998.

[137] P. Quadcopter, "Data logging and kalman filtering," 2009. [Online]. Available: https://quadcopter.wordpress.com/2009/11/11/data-logging-and-kalman-filtering/

[138] N.-E. Yang, Y.-G. Kim, and R.-H. Park, "Depth hole filling using the depth distribution of neighboring regions of depth holes in the kinect sensor," in *Signal Processing, Communication and Computing (ICSPCC), 2012 IEEE International Conference on*. IEEE, 2012, pp. 658–661.

[139] C. Tomasi and R. Manduchi, "Bilateral filtering for gray and color images," in *Computer Vision, 1998. Sixth International Conference on*. IEEE, 1998, pp. 839–846.

[140] Graphics, "Realtime bilateral filter on gpu," 2015. [Online]. Available: http://graphics.im.ntu.edu.tw/~zho/Bilateral/index.html

[141] C. Rother, V. Kolmogorov, and A. Blake, "Grabcut: Interactive foreground extraction using iterated graph cuts," *ACM Transactions on Graphics (TOG)*, vol. 23, no. 3, pp. 309–314, 2004.

[142] E. Alexandre-Cortizo, M. Rosa-Zurera, and F. Lopez-Ferreras, "Application of fisher linear discriminant analysis to speech/music classification," in *Computer as a Tool, 2005. EUROCON 2005. The International Conference on*, vol. 2. IEEE, 2005, pp. 1666–1669.

[143] Kostyuk, "Numb3rs 219: Dark matter." [Online]. Available: http://www.math.cornell.edu/~numb3rs/kostyuk/num219.htm

[144] J. S. Cardoso and M. J. Cardoso, "Towards an intelligent medical system for the aesthetic evaluation of breast cancer conservative treatment," *Artificial Intelligence in Medicine*, vol. 40, no. 2, pp. 115–126, 2007.

[145] A. Perez, P. Larranaga, and I. Inza, "Supervised classification with conditional gaussian networks: Increasing the structure complexity from naive bayes," *International Journal of Approximate Reasoning*, vol. 43, no. 1, pp. 1–25, 2006.

[146] P. Somol, P. Pudil, J. Novovičová, and P. Paclık, "Adaptive floating search methods in feature selection," *Pattern recognition letters*, vol. 20, no. 11, pp. 1157–1163, 1999.

[147] S. Raschka, "Sequential feature selection algorithms in python," 2013. [Online]. Available: http://sebastianraschka.com/Articles/2014_sequential_sel_algos.html#sffs

[148] R. O. Duda, P. E. Hart, and D. G. Stork, *Pattern classification*. John Wiley & Sons, 2012.

Appendix A

DASH Questionnaire - Institute for Work and Health (in Portuguese)

DISABILITIES OF THE ARM, SHOULDER AND HAND

DASH

Portugal

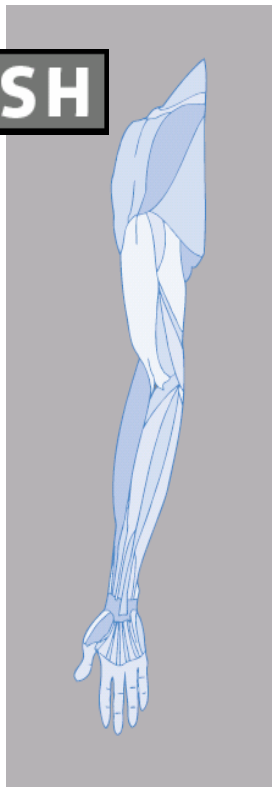

INSTRUÇÕES

Com este questionário pretendemos conhecer os seus sintomas, bem como a sua capacidade para desempenhar determinadas actividades.

Responda, por favor, a *todas* as perguntas e, com base na sua condição física na última semana, faça um círculo à volta do número que considere mais adequado.

Se, na última semana, não teve oportunidade de desempenhar uma determinada actividade, por favor seleccione a resposta com *maior probabilidade* de ser a mais adequada.

Não importa qual a mão ou braço que utiliza para desempenhar a actividade ou o modo como a realiza. Por favor, responda apenas com base na sua capacidade para realizar a tarefa.

DISABILITIES OF THE ARM, SHOULDER AND HAND

Por favor, classifique a sua capacidade para desempenhar as actividades seguintes na última semana, fazendo um círculo à volta do número à frente da resposta adequada.

		NENHUMA DIFICULDADE	POUCA DIFICULDADE	ALGUMA DIFICULDADE	MUITA DIFICULDADE	INCAPAZ
1.	Abrir um frasco novo ou com tampa bem fechada.	1	2	3	4	5
2.	Escrever.	1	2	3	4	5
3.	Rodar uma chave na fechadura.	1	2	3	4	5
4.	Preparar uma refeição.	1	2	3	4	5
5.	Abrir e empurrar uma porta pesada.	1	2	3	4	5
6.	Colocar um objecto numa prateleira acima da cabeça.	1	2	3	4	5
7.	Realizar tarefas domésticas pesadas (por exemplo: lavar paredes, lavar o chão).	1	2	3	4	5
8.	Fazer jardinagem ou trabalhar no quintal.	1	2	3	4	5
9.	Fazer a cama.	1	2	3	4	5
10.	Carregar um saco de compras ou uma pasta.	1	2	3	4	5
11.	Carregar um objecto pesado (mais de 5 kg).	1	2	3	4	5
12.	Trocar uma lâmpada acima da cabeça.	1	2	3	4	5
13.	Lavar a cabeça ou secar o cabelo.	1	2	3	4	5
14.	Lavar as costas.	1	2	3	4	5
15.	Vestir uma camisola.	1	2	3	4	5
16.	Usar uma faca para cortar alimentos.	1	2	3	4	5
17.	Actividades de lazer que requerem pouco esforço (por exemplo: jogar às cartas, fazer tricô, etc.).	1	2	3	4	5
18.	Actividades de lazer que exijam alguma força ou provoquem algum impacto no braço, ombro ou mão (por exemplo: golfe, martelar, ténis, etc.).	1	2	3	4	5
19.	Actividades de lazer, nas quais movimenta o braço livremente (por exemplo: jogar ao disco, jogar badminton, etc.).	1	2	3	4	5
20.	Utilizar meios de transporte para se deslocar (de um lugar para o outro).	1	2	3	4	5
21.	Actividades sexuais.	1	2	3	4	5

DISABILITIES OF THE ARM, SHOULDER AND HAND

		NÃO AFECTOU NADA	AFECTOU POUCO	AFECTOU	AFECTOU MUITO	INCAPACITOU
22.	Em que medida é que, na última semana, o seu problema no braço, ombro ou mão afectou as suas actividades sociais habituais com a família, os amigos, os vizinhos ou outras pessoas? (Faça um círculo à volta do número)	1	2	3	4	5

		NÃO LIMITOU NADA	LIMITOU POUCO	LIMITOU	LIMITOU MUITO	INCAPACITOU
23.	Em que medida é que, na última semana, o seu problema no braço, ombro ou mão o limitou no trabalho ou noutras actividades diárias? (Faça um círculo à volta do número)	1	2	3	4	5

Por favor, classifique a gravidade dos sintomas seguintes na <u>última semana</u>. (Faça um círculo à volta do número)

	NENHUMA	POUCA	ALGUMA	MUITA	EXTREMA
24. Dor no braço, ombro ou mão.	1	2	3	4	5
25. Dor no braço, ombro ou mão ao executar uma actividade específica.	1	2	3	4	5
26. Dormência (formigueiro) no braço, ombro ou mão.	1	2	3	4	5
27. Fraqueza no braço, ombro ou mão.	1	2	3	4	5
28. Rigidez no braço, ombro ou mão.	1	2	3	4	5

	NENHUMA DIFICULDADE	POUCA DIFICULDADE	ALGUMA DIFICULDADE	MUITA DIFICULDADE	TANTA DIFICUL-DADE QUE NÃO CONSIGO DORMIR
29. Na última semana, teve dificuldade em dormir, por causa da dor no braço, ombro ou mão? (Faça um círculo à volta do número)	1	2	3	4	5

	DISCORDO TOTALMENTE	DISCORDO	NEM CONCORDO NEM DISCORDO	CONCORDO	CONCORDO TOTALMENTE
30. Sinto-me menos capaz, menos confiante ou menos útil por causa do meu problema no braço, ombro ou mão. (Faça um círculo à volta do número)	1	2	3	4	5

PONTUAÇÃO DASH INCAPACIDADES/SINTOMAS = $\left[\frac{(\text{soma de n respostas})}{n} - 1\right] \times 25$, onde n é igual ao número de respostas válidas.

Não se pode calcular uma pontuação DASH se existirem mais de 3 itens não válidos.

DISABILITIES OF THE ARM SHOULDER AND HAND

MÓDULO RELATIVO AO TRABALHO (OPCIONAL)

As perguntas que se seguem são relativas ao impacto que o seu problema no braço, ombro ou mão tem na sua capacidade para trabalhar (incluindo as tarefas domésticas, se estas forem a sua actividade principal).

Por favor indique qual a sua profissão / actividade : _____

□ Não trabalho. (Pode saltar esta secção).

Faça um círculo à volta do número que melhor descreve a sua capacidade física na última semana. Teve alguma dificuldade em:

	NENHUMA DIFICULDADE	POUCA DIFICULDADE	ALGUMA DIFICULDADE	MUITA DIFICULDADE	INCAPAZ
1. fazer os movimentos que normalmente utiliza no seu trabalho?	1	2	3	4	5
2. fazer o seu trabalho habitual devido a dores no braço, ombro ou mão?	1	2	3	4	5
3. fazer o seu trabalho tão bem como gostaria?	1	2	3	4	5
4. fazer o seu trabalho no tempo habitual?	1	2	3	4	5

MÓDULO RELATIVO A DESPORTO / MÚSICA (OPCIONAL)

As perguntas que se seguem são relativas ao impacto que tem o seu problema no braço, ombro ou mão, quando toca *um instrumento musical*, pratica *desporto* ou *ambos*. Se pratica mais do que um desporto ou toca mais do que um instrumento musical (ou ambos), responda em função da actividade que é mais importante para si.

Por favor indique qual o desporto ou instrumento musical mais importante para si:_____

□ Não pratico desporto, nem toco um instrumento musical. (Pode saltar esta secção.)

Faça um círculo à volta do número que melhor descreve a sua capacidade física na última semana. Teve alguma dificuldade em:

	NENHUMA DIFICULDADE	POUCA DIFICULDADE	ALGUMA DIFICULDADE	MUITA DIFICULDADE	INCAPAZ
1. usar a técnica habitual para tocar o instrumento musical ou praticar desporto?	1	2	3	4	5
2. tocar o instrumento musical ou praticar desporto devido a dores no braço, ombro ou mão?	1	2	3	4	5
3. tocar o instrumento musical ou praticar desporto tão bem como gostaria?	1	2	3	4	5
4. estar o tempo habitual a tocar o instrumento musical ou a praticar desporto?	1	2	3	4	5

PONTUAR OS MÓDULOS OPCIONAIS: Somar os valores atribuídos a cada resposta; dividir por 4 (número de itens); subtrair 1; multiplicar por 25.
A pontuação de um módulo opcional pode não ser calculada no caso de algum dos itens não ter sido respondido.

DASH Portugal

Appendix B

Acquisition Protocol

1. Place Microsoft Kinect in a stable platform and connect to a PC through a USB connection
2. Open the application
3. Verify if in (1) can be read “Application is ready!!! Please insert the patient code!!”.

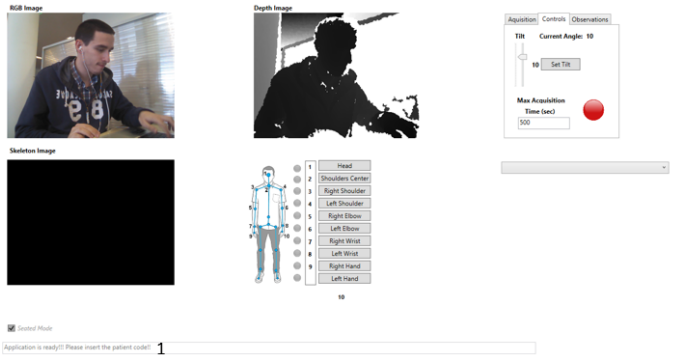

   (a) If is shown “Kinect Not Ready!!”, reconnect the Kinect to USB. If does not work, reboot PC.

4. Observe if the skeleton image is detected (2) and if the green light close to Data Collection box is green (3).

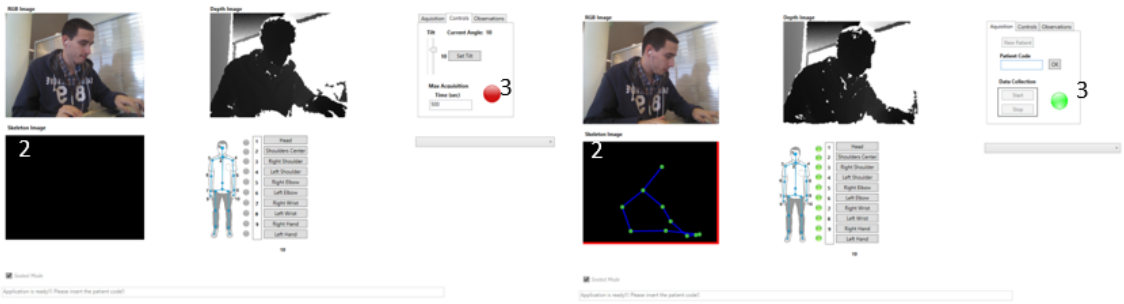

5. Insert Patient Code. Select OK (4).

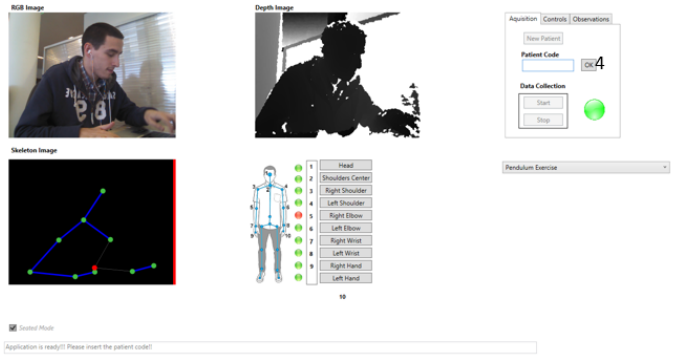

6. Select Start in Data Collection (5)

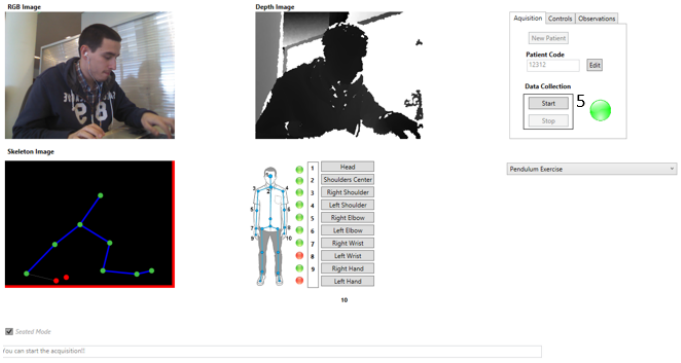

7. Ask the patient to perform the exercises in the images

8. Select Stop (7) in Data Collector.

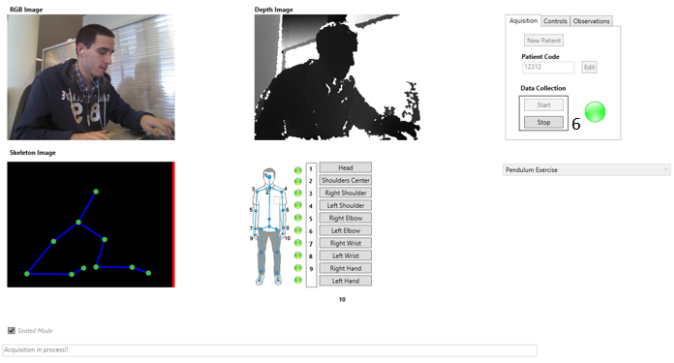

9. Insert new Patient Code or, if not needed, close application.

Appendix C

Acquisition Requirements

C.1 Kinect System

Kinect has an RGB camera and a infrared depth sensors formed by a projector and an infrared camera on the same band. The resolution of RGB video 8-bit VGA is 640x480 pixels, but the hardware is capable of resolutions up to 1280x1024 (at a lower frame rate). Depth sensor has a resolution of 640x480 pixels with 11-bit depth that allows 2.048 sensibility levels. Both video outputs work at 30 frames per second (fps).

C.1.1 Hardware requirements

The sensor should be connect to a computer with the following minimum requirements:

- Windows 7, Windows 8, Windows Embedded Standard 7, Windows Embedded POSReady 7 or Windows 10
- 32 bit (x86) or 64 bit (x64) processor
- Dual-core 2.66-GHz or faster processor
- USB 2.0
- 2 GB RAM
- Microsoft Kinect Software Development Kit (SDK) or Kinect Runtime

C.1.2 Limits

The sensor has some limitations, but it works well under the following ranges (all from the center of the Kinect):

- Horizontal viewing angle: 57○
- Vertical viewing angle: 43○

- User distance for best results: 1.2m (down to 0.4m in near mode) to 4m (down to 3m in near mode)
- Depth range: 400mm (in near mode) to 8000mm (in standard mode)
- Temperature: 5 to 35 degrees Celsius
- Elevation angle of the tilt motor in the sensor: –27○ to +27○.

C.1.3 Skeleton Joints

- A skeleton contains 20 positions, one for each "joint" of human body;
- The 3D position of each of the skeleton joints (if active tracking is enabled) are stored as (x, y, z) coordinates.
- Each x, y and z coordinate represents the distance in meters from the Kinect sensor, which is consider the origin, looking in the direction of the positive z-axis.
- In the default full skeleton mode, Kinect track the skeleton with 20 joints.
- In the seated mode, Kinect track the skeleton only with the 10 upper joints.

C.1.4 Position

- The sensor should be localized 1 – 1.8 m away from the patient and at 0.6 – 1.8 m off the floor (depending on patients height), with nothing between the patient and the sensor.
- Only the patient should be in the detection's range of the sensor.
- The sensor shouldn't be placed on or in front of a speaker or on a surface that vibrates or makes noise.

C.1.5 Room environment

- The room should have enough light so that the patient's face is clearly visible and evenly lit. The side or back lighting, especially from a window, should be avoided.

C.2 Patient

- Patients need to be at least 1 m tall and
- Patient should maintain the upper limbs in the coronal plane.

C.3 Saving Data

- The Kinect is used in order to gather the information about the patient in RGB images and depth maps and of a .csv file which is composed by the tridimensional coordinates of each joint.
- Color images are stored in a file with 32 bits per pixel with a resolution of 640x480 at 15 frames/sec.
- Depth images are stored in a file with 16 bits per pixel with a resolution of 640x480 at 30 frames/sec.

C.3.1 Files Organization

- Data is saved in a folder with the name $PatientXX_code_yyyy_m m_d d_h h_m m_s s_E xerciseYY$, where XX represents the patient's number, $code$ the patient's code, $yyyy_m m_d d_h h_m m_s s$ represents respectively the year, month, day, hour, minutes and seconds and YY the Exercise Number.
- RGB images file names are in the format: $PatientXX_code_Color000000N_yyyy_m m_d d_h h_m m_s s_m s.png$, where XX represents the patient's number, $code$ the patient's code, N the RGB picture number and $yyyy_m m_d d_h h_m m_s s_m s$ represents respectively the year, month, day, hour, minutes, seconds and milliseconds when the frame is acquired.
- Depth images file names are in the format: $PatientXX_code_Depth000000N_yyyy_m m_d d_h h_m m_s s_m s.png$, where XX represents the patient's number, $code$ the patient's code, N the RGB picture number and $yyyy_m m_d d_h h_m m_s s_m s$ represents respectively the year, month, day, hour, minutes, seconds and milliseconds when the frame is acquired.
- The .csv file name is in the format: $PatientXX_code_SkeletonPositionData_ExerciseYY.csv$, where XX represents the patient's number, $code$ the patient's code and YY the Exercise Number.